



The synthesis of an array of stapled  
polyproline peptides

**Dominic Brightwell**

This dissertation is submitted for the degree of  
*Master of Science*

Supervisor: Dr Aniello Palma

October 15<sup>th</sup>, 2019

School of Physical Sciences

## **Declaration**

I hereby declare that except where specific reference is made to the work of others, the contents of this dissertation are original and have not been submitted in whole or in part for consideration for any other degree or qualification in this, or any other university. This dissertation is the result of my own work and includes nothing which is the out come of work done in collaboration except where specifically indicated in the text and Acknowledgements.

**Abbreviations:**

PPI / PolPro1 – Polyproline type 1

PPII / PolPro2 – Polyproline type 2

DCM – Dichloromethane

MeOH – Methanol

EtOAc – Ethyl Acetate

THF – Tetrahydrofuran

DMSO – Dimethyl-sulfoxide

DMF - Dimethylformamide

FCC – Flash Column Chromatography

CD – Circular Dichroism

FT-IR – Fourier-transform infrared (spectroscopy)

NMR – Nuclear-magnetic resonance (spectroscopy)

TLC – Thin-layer chromatography

HPLC – High-performance liquid chromatography

LCMS – Liquid Chromatography Mass spectrometry

IM-MS – Ion-mobility mass spectrometry

ESI – Electro-spray ionisation

RCM – Ring-closing Metathesis

PLE – Pig-liver esterase

DPBS – Dulbecco's phosphate-buffered saline

TFA – Trifluoroacetic acid

DIPEA- Diisopropylethylamine

DMAP – 4-Dimethylaminopyridine

Boc<sub>2</sub>O – Boc-anhydride

DEAD – Diethyl azodicarboxylate

PyBOP - benzotriazol-1-yl-oxytripyrrolidinophosphonium hexafluorophosphate

SPPS – Solid-phase peptide synthesis

## Contents

1. Introduction .....	1
2. Results and Discussion .....	9
2.1 Functionalised Monomer Synthesis Results and Analysis .....	10
2.1.1 Synthesis of 4-position functionalised trans-proline monomer: .....	10
2.1.2 Synthesis of 4-position functionalised cis-proline monomer: .....	12
2.2 Peptide Synthesis Results and Analysis: .....	13
2.2.1 RCM Reactions .....	15
2.2.2 HPLC Analysis .....	15
2.2.3 CD Spectroscopy Results .....	20
2.2.4 FT-IR Spectroscopy Analysis of Peptides .....	23
2.4 Mimetic-peptide Monomer Synthesis Results and Analysis .....	26
2.4.1 Synthesis of trans-phenol proline monomer: .....	28
2.4.2 Synthesis of tert-butyl ethylcarbamate proline monomer: .....	29
2.5 5-position functionalised monomer synthesis .....	30
3. Conclusion .....	32
4. Future Plan .....	32
5. Experimental .....	33
5.1 Synthesis of 5-position functionalised proline-monomer .....	34
5.2 Synthesis of <i>trans</i> -4-position functionalised proline monomer .....	36
5.3 Synthesis of <i>cis</i> -4-position functionalised proline monomer .....	39
5.4 Synthesis of polyproline peptides .....	41
5.4.1 General Solid Phase Peptide Synthesis Protocol: .....	41
5.4.2 Ring-closing Metathesis Reactions: .....	43
5.5 Mimetic-peptide specific monomers synthesis .....	45
6. Acknowledgements .....	48
References .....	48
Appendices .....	51
Appendix – A – NMR Spectra .....	52
Appendix – B – Mass Spec and prep-HPLC data .....	79
Appendix – C – CD Spectra .....	86
Appendix – D – FT-IR Spectra .....	94

## Abstract

The purpose of this investigation was to determine if a short all hydrocarbon linker can be used to staple a polyproline chain and therein favour an alternative conformation to the typical type exhibited in an aqueous environment. An array of functionalised P(Pro)<sub>7</sub> peptides were synthesised with olefin containing sidechains present at the 4C position on the 4<sup>th</sup> and 7<sup>th</sup> monomer units. Ruthenium-catalysed olefin metathesis was then used to form an all hydrocarbon *i-i+3* linker between the two sidechains, effectively ‘stapling’ the peptide at the C-terminal. The conformation of the subsequent ‘stapled’ peptides was then investigated using, FT-IR and circular dichroism (CD), to determine the polyproline type I or type II character. The stapling of the peptides proved to alter the conformation from the typical PolPro2 character exhibited in an aqueous environment.

## 1. Introduction

Polyproline is known to form two different helical structures; the right-handed helix PolPro1 and the left-handed helix PolPro2 (*Figure 1*). The PolPro1 conformation has a more condensed helix with 3.3 residues per turn and all its peptide bonds in the *cis* conformation with 5.6 Å per turn. PolPro2 has 3.0 residues per turn with every third residue stacked on top of each other 9.4 Å apart and bonds all in the *trans* conformation. <sup>[1]</sup> Interconversion can occur between these two types with a theorised intermediate of discontinuous *trans* and *cis* amide proline bonds. <sup>[2]</sup>

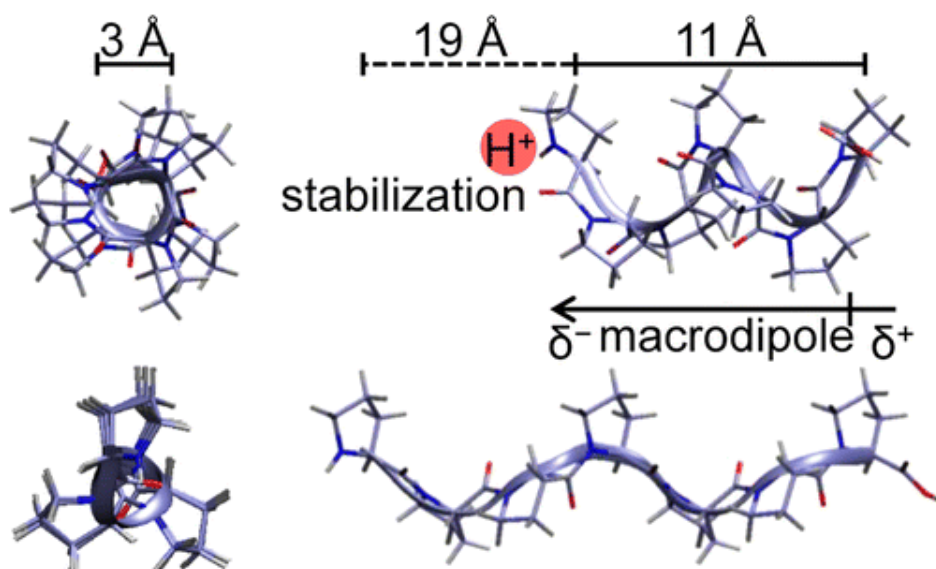


*Figure 1* – Two Views of All-*cis* PolPro1 (*top*) and All-*trans* PolPro2 (*bottom*) helices of Pro<sub>7</sub>. Length and width dimensions and charge stabilization of the macrodipole of PolPro1 is also shown. <sup>[5]</sup>

PolPro2 is the more common conformation occurring in natural proteins and involved in many biological processes as it is generally more stable. Due to the lack of N-H amide groups along the backbone resulting in a lack of intramolecular hydrogen bonds present in a typical alpha-helix (*figure 2*), proline does not just favour trans-peptide bonds and is free to adopt both the *cis* and *trans* isomers of proline with N-C atoms from pyrrolidine rings forming part of the backbone. The PolPro2 *trans* configuration is favoured in water, TFE, organic acids and benzyl alcohol while PolPro1 *cis* is usually only favoured in aliphatic alcohols such as propanol.<sup>[3]</sup> In nonpolar solvents such as propanol the formation of the more condensed right-handed helix shields the peptide backbone, while in more polar solvents the flipping of all the amide bonds to the *trans* configuration results in the more extended helix, which is stabilised by interactions of the exposed carbonyl groups with the polar solvent.<sup>[4]</sup> Interconversion between PolPro1  $\rightarrow$  PolPro2 occurs via two mechanism; via an exothermic proton transfer process (*reaction 1*) and an entropically driven endothermic conformational change resulting from *reaction 2*. These two processes, observable through kinetic investigations using IM-MS data, together, produce an extremely slow proton transfer process leading to slow conversion.<sup>[5]</sup> Maximum conversion (96 %) to PolPro1 occurs in propanol after six days in long chain polyprolines.<sup>[6]</sup> This is due to the former transition being caused by cis-trans isomerisation while the latter transition is due to hydrogen bond breakage/formation.<sup>[3]</sup> Several methods can be used to limit the interconversion of the two polyproline types and favour one over the other.

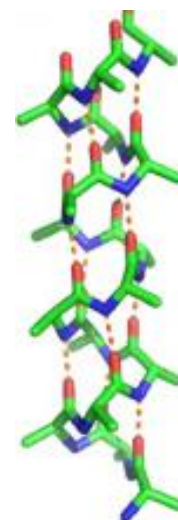
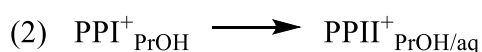


*Figure 2* - Molecular view of an  $\alpha$ -helix with intramolecular hydrogen bonds in orange<sup>[37]</sup>



The alpha-helix is the most commonly occurring motif in the secondary structure of proteins and plays an important role in various biological processes such as protein-protein interactions. The  $\alpha$ -helix is a right-handed helical structure with each residue corresponding to a  $100^\circ$  turn (3.6 residues per turn). Protein-protein interactions that are mediated by an alpha-helical peptide are

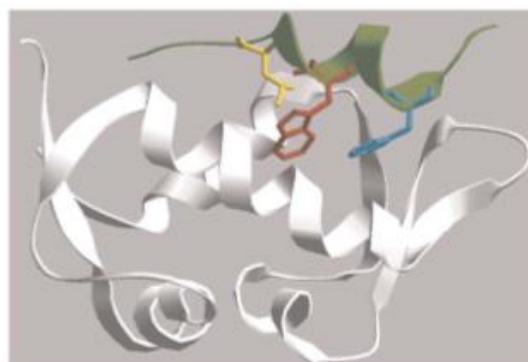


*Figure 3* – binding site p53 residues 15-19 (colour) binding to MDM2 (white)<sup>[10]</sup>

potential therapeutic targets and there is increasing interest in finding ways to mimic or induce the conformation of a helical peptide in an attempt to increase bioavailability, cell penetration, stability or binding affinity. <sup>[7]</sup> Alpha-helix mimetics act to induce or stabilize the  $\alpha$ -helical structure of a natural or synthetic peptide chain. This is done by using several different methods to favour the  $\alpha$ -helix conformation in peptides, such as “hydrogen bond surrogate” helices, or mimic the structure using synthetic non-natural structures. However, peptides that are representative of a fraction of a protein often show reduced conformational stability outside the folded environment of the protein giving poor binding affinity and cell impermeability and as such rarely have high biological activity when removed from the protein and used as a therapeutic molecule. <sup>[8]</sup> Stapled peptides, where hydrophobic linkers between appropriate residues along the peptide chain are joined by ring-closing metathesis, are an important potential strategy to form conformationally constrained peptides. Significant progress has been made in recent years in the development of potent cell permeable alpha-helical stapled peptides especially in the field of cancer treatment such as; targeting p53 antagonists to reactive the tumour suppressors pathway in cells and, outside the field of cancer, in the inhibition of HIV-1 infection by both intracellular and extracellular effects, for example. <sup>[9]</sup> Significantly, the interaction of the E3 ubiquitin ligase MDM2 with p53, where MDM2 binds to a short stretch of the tumour-suppressing protein p-53 (*Figure 3*), has seen significant investigation with a small molecule peptide shown to bind more strongly to MDM2, out-competing the p53 peptide limiting inhibition of p53 activity. <sup>[10]</sup> As such further recent work investigating the use of stapled peptides in place of the small molecule inhibitor, with the target of developing a dual inhibitor of MDMX and MDM2, where small molecule inhibitors have only proven to target MDM2 and therefore have a limited therapeutic scope due to MDMX being highly overexpressed in over 70% of p53-positive patient samples. <sup>[11]</sup> This research has shown that a stapled peptide can more effectively inhibit p53-MDM2/MDMX interactions showing promising tumour suppression models in humans. <sup>[12]</sup> This highlights the importance of the development of potential new mimetics to target alpha-helical protein-protein interactions, with the hydrocarbon staple presenting an effective method for stabilisation of peptide mimetics showing increasing success as more stapled peptides with promising therapeutic effects are synthesised.

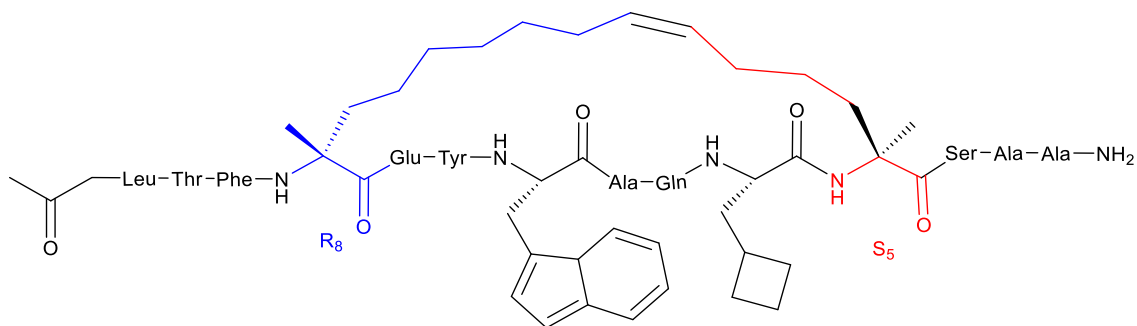


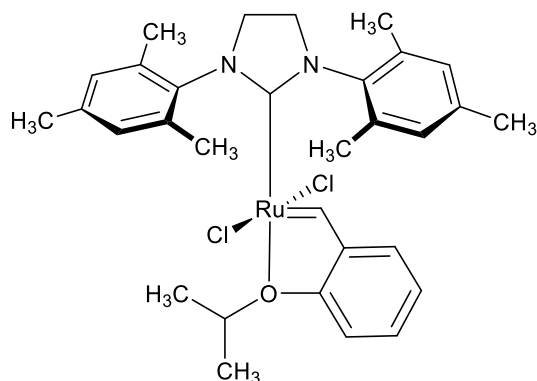
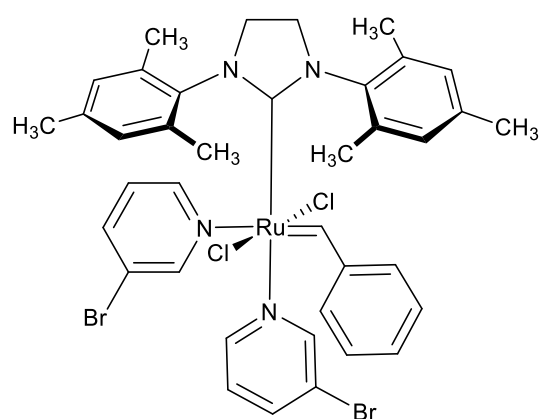
*Figure 2* – Chemical structure of **ATSP-7041**, a stapled-peptide dual-inhibitor of both MDM2 and MDMX, that exhibits a more durable effect on p53 signalling than small-molecule MDM2-selective inhibitors<sup>[12]</sup>

Previously many approaches to helix stabilisation involved the use of polar and pharmacologically labile cross-links such as disulfides and lactam bridges. Hydrocarbon cross-links present a more stable alternative and increase the likelihood of cell penetration, due to increased hydrophobicity from the introduction olefinic sidechains<sup>[13]</sup>, give greater resistance to proteolysis and increased biological activity.<sup>[14][15]</sup> Cell penetration is a key component of drug development with the cell membrane presenting a significant impediment to the delivery of therapeutic molecules into the target cell. As such the addition of an all-hydrocarbon staple not only acts to stabilize helicity but is an effective method to facilitate the penetration of a peptide through the cell membrane, with stapled peptides having improved cell penetration compared their wild type counterparts (10-20 times more penetrating).<sup>[16]</sup> The amphipathic surface provided by a staple acts to facilitate the translocation of a peptide through the phospholipid bilayer which penetrates the membrane through an energy dependent endocytosis pathway.<sup>[17]</sup>

The progress of Grubbs and co-workers in the development of olefin cross-linking of helices between residues on adjacent turns using ruthenium-catalysed ring-closing metathesis has improved the accessibility of the incorporation of an all hydrocarbon cross-linker into a peptide. studies have shown that hydrocarbon cross-links can show a significant propensity to influence helical stability. However, the position of attachment, linker length, and stereochemistry determine the effect of the cross-link on the stability and can act to stabilize or destabilize the helix. These factors also affect the success of the RCM reaction, with minimal cross-linking occurring between linkers too short to favourably form cross-links with distant or unfavourably positioned residues.<sup>[18]</sup>

The use of ring-closing olefin metathesis to form a hydrocarbon bridge between side chains of constituent amino acids has been shown to be an effective and facile method to form a cross-link between residues, with side-chains one turn apart ( $i \rightarrow i+3$ ) on the same side of the peptide backbone. Therefore, the desired location for the staple at the C-terminal separated by two

residues theoretically presents an appropriate site for non-natural amino acids used to form the cross-link. Also, the synthesis of a set of stapled peptides allows identification of the optimal stapling setup therefore, the synthesis of various peptide isomers as well as varying cross-linker lengths and locations is desirable in designing an optimal stapled peptide given.<sup>[19]</sup> It has also been shown that a conformational shift of the peptide helix occurs when cross-linking between peptide side-chains is introduced into a peptide potentially due to the constraint imposed by the linkage.<sup>[20]</sup> This suggests that introduction of olefin side chains into functionalised proline may be a facile method to achieve a hydrocarbon cross-link in polyproline, through RCM and potentially stabilise the desired PolPro1 conformation in a short peptide. Previous success using ruthenium-catalysts on resin-bound peptides shows the viability of this method with conditions varying depending on the specific catalyst used. RCM of the resin-bound peptide is desirable as this limits the amount of cross-metathesis that can occur, however, depending on the functional groups present, this can result in high *mol%* of catalyst required to achieve full conversion. This presents an inelegant reaction as high concentrations ( $\leq 50$  *mol%*)<sup>[19]</sup> <sup>[21]</sup> essentially use the catalyst as a reagent, therefore attempting the reaction after cleavage may be a more desirable method ideally targeting minimal catalyst concentrations ( $\leq 5$  *mol%*). Catalysts requiring high temperatures to progress metathesis are not desirable as this can result in disruption of the helix and especially in this case where conformationally well-defined peptides are desired.<sup>[18]</sup> The versatility of this reaction, with an array of reagents available, is especially evidenced by recent success of RCM in aqueous conditions due to the high stability of ruthenium-carbene complexes developed by Grubbs, with high efficiency of aqueous reactions using versatile Hoveyda-Grubbs catalysts, where previously dry conditions were required.<sup>[21]</sup> Also, the 2<sup>nd</sup> generation Hoveyda-Grubbs, (**1**) catalyst often out-performs the 2<sup>nd</sup> generation Grubb's catalyst in challenging metathesis reactions with a faster initiation and longer catalytic life, and presents a more appropriate catalysts for this procedure. The recapture cycle of Grubbs 2<sup>nd</sup> generation is destructive and results in catalyst decomposition limiting productivity while 2<sup>nd</sup> generation Hoveyda-Grubbs has facile initiation with a recapture cycle post-metathesis and a relatively facile reintroduction into the catalytic metathesis cycle, resulting in increased productivity and catalyst lifetime.<sup>[22]</sup> The 3<sup>rd</sup> Generation Grubb's catalyst,  $[(H_2IMes)(3-Br-py)_2(Cl)_2Ru=CHPh]$  (**2**), also presents a promising RCM catalyst due to being a very fast initiator even at low temperatures and could be effective for the RCM of the polyproline bound olefins.<sup>[23]</sup>

Hoveyda-Grubbs 2<sup>nd</sup> Generation Catalyst, (1)Grubbs 3<sup>rd</sup> Generation Catalyst, (2)

As there is no hydrogen bonding in polyproline a significant factor determining the *cis* or *trans* conformation is steric bulk at various positions on the proline ring structure. This effect is mainly evidenced at 5 and 2 position substitutions with alkyl groups, while the 4-position (*Figure 4A*) shows little effect on helix conformation, due to their location being unfavourable to interact with proline dihedral geometries.<sup>[2]</sup> However, this effect is limited in affecting the entirety of the helix and only has significant local effects; favouring the *cis* conformation locally for a 5-position t-Bu substituted proline residue in water for example, while the *trans* conformation still remains in the rest of the helix. As steric bulk on a single residue seems insufficient, to promote interconversion from PolPro2 to PolPro1 type helix, spreading the induced *cis* conformation to a greater proportion of the helix, and increasing the constraint imposed on the helix, may present an improved result. The stability of the PolPro1 conformation may therefore be increased by forming a hydrocarbon bridge between the appropriate residues, over a single turn of the helix to induce the PolPro1 conformation throughout a larger portion of the short polyproline chain and hopefully extending this effect across the full length of the peptide, when the conformation would otherwise be disfavoured in a specific solvent.

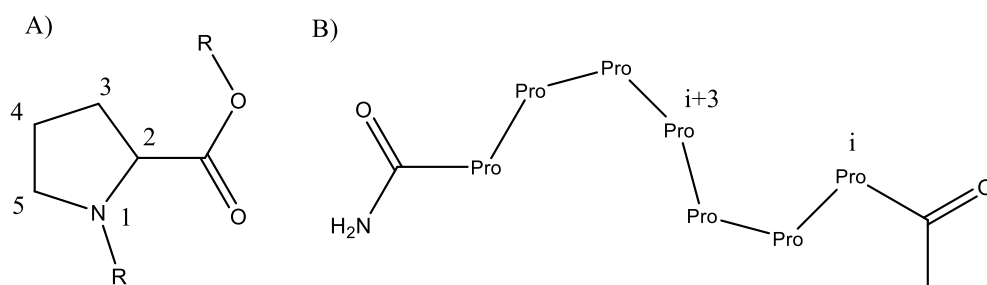


*Figure 4* - A) Example proline residue with carbon positions specified. B) Example Pro7 peptide with *i* and *i+3* residues shown.

The 5C and 3C positions on the proline ring present the best potential for an effective cross-link between the residues *i* and *i+3* (*Figure 4B*), both preserving the most faces of the peptide, with the cross-link being largely contained within the helix, and the positions being held closely

together in PolPro1 conformation. However, the addition of an olefin sidechain at the 4-position presents a remarkably facile synthesis with a significantly reduced number of steps comparative with the functionalisation of the 5 or 3 positions. Also, the 4-position shows limited steric effect on the conformation of polyproline, unlike the 5-position, so any observed effects on conformation can be largely attributed to constraint imposed by the linker and not simply due to steric bulk stabilising or destabilising the helix. This also reduces the chances of the added steric bulk counteracting the influence of the linker and potentially favouring the PolPro2 conformation. Although a cross-link between the 4-positions presents a more limited peptide mimetic, as a number of functionalisable faces of the peptide are removed, the ease of the synthesis and the potential to still effectively influence the conformation of the polyproline helix means functionalisation at this position presents a viable route to be investigated, alongside attempting to produce a cross-link between the 5 and 3C positions on the *i* and *i*+3 residues of a short polyproline chain.

The stability of the PolPro1 helix appears to vary with chain length, with greater chain lengths stabilising the PolPro1 helix, while peptides as short as 4 units can form a PolPro2 helix however with a reduced stability. *Oka et al.* suggests that the shortest polyproline chain that can form PolPro1 in propanol is P(Pro)<sub>6</sub> with a P(Pro)<sub>4</sub> peptide unable to form the PolPro1 helix, while a large P(Pro)<sub>13</sub> chain can form PolPro1 not only in propanol but also in methanol, after 21 days showing the expected shift to lower wavelengths on CD analysis (Figure 5).<sup>[3]</sup> This highlights the increased stability of the helix imposed by a greater chain length.

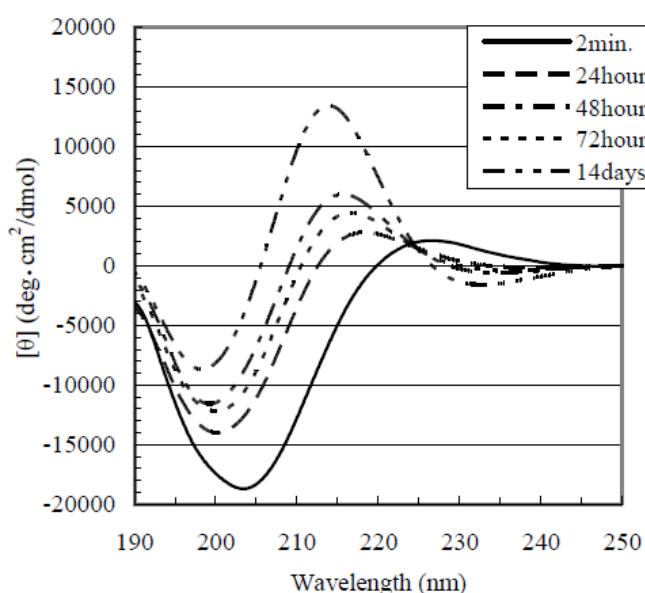


Figure 5 - Circular dichroism spectra of P(Pro)<sub>13</sub> in 1-propanol at 5 °C, showing the shift from PPII to PPI over time exhibited by the increase in intensity and shift to lower wavelengths<sup>[3]</sup>

Therefore, it seems feasible that an appropriate chain length for analysis of conversion between the two conformations would be P(Pro)<sub>6</sub> or greater, with shorter than P(Pro)<sub>13</sub> chains having a reduced helical stability but presenting a reduction in wastage of material and synthetic steps.

Circular dichroism (CD) spectrometry presents an effective method for the determination of the conformation of the polyproline peptides as there is a clear measurable difference between

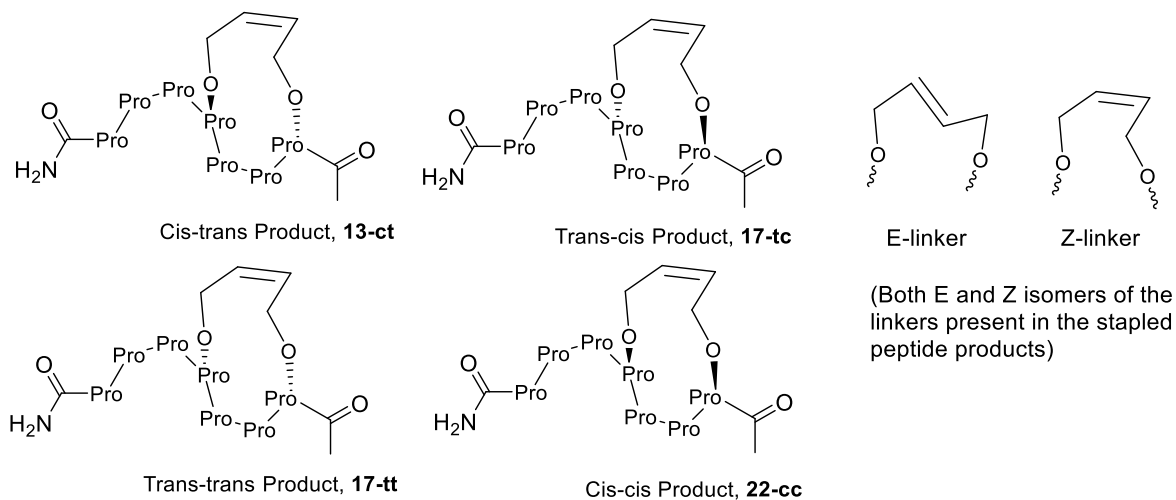
PolPro1 and PolPro2. PolPro1 presents a minima at  $\approx 200$  nm, a maxima at  $\approx 214$  nm and a small negative band at  $\approx 232$  nm while PolPro2 presents a reduced minima at  $\approx 204$  nm and a higher intensity maxima at  $\approx 226$  nm. This shift is well documented for polyproline chains 10 monomer units and larger. <sup>[1] [2] [3] [24]</sup>

Another potential method that has previously been used for the analysis of polyproline conformation is via the use of FT-IR spectroscopy, whereby, the exhibited wavenumber of the polyproline C=O amide band indicates the polyproline conformation present in the sample. PolPro1 should exhibit C=O amide stretching band at  $1635\text{ cm}^{-1}$  and PolPro2 should exhibit the band at  $1623\text{ cm}^{-1}$ , with an intermediate band suggested to form during the transition at  $1651\text{ cm}^{-1}$  when both conformations are present within the sample. <sup>[6]</sup> This suggests another clear observable shift can be utilised to observe the conformational change of PolPro1 to PolPro2.

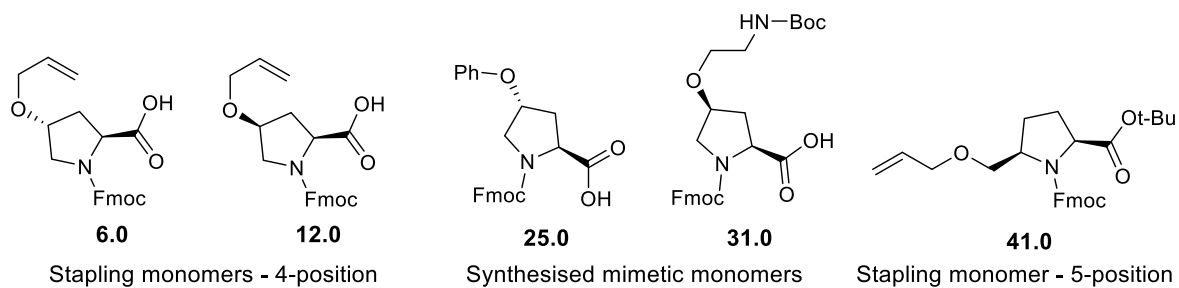
Ion-Mobility Mass Spectrometry (IM-MS) has been increasingly used for analysis of biomolecule structure <sup>[25]</sup> and is sensitive to *cis/trans* isomerism of proline peptide residues. <sup>[26]</sup> This has allowed investigation of PolPro1-PolPro2 transitions by *Clemmer et al.* Which has shown a number of stable intermediates forming during the transition of  $\text{P(Pro)}_{13}$  from PolPro1 to PolPro2, with partial *cis/trans* amide bond configurations and has also allowed for investigation of the energetics of formation of the possible stable structures. <sup>[4]</sup> This suggests that conversion from PolPro1-PolPro2 occurs at the N-terminus and then isomerisation is able to occur in the centre of the peptide backbone. As such IM-MS could be used for the detailed investigation of synthesised stapled polyproline peptides and give detailed information about the *cis/trans* isomerisation within the peptides.

## 2. Results and Discussion

Target Stapled Peptides:



Target Monomers:



The purpose of this investigation is to determine if a short all hydrocarbon linker can be used to staple a polyproline chain and therein favour an alternative conformation. It was theorised that the proposed staple would limit the ability of the peptide to form the polyproline-II (PolPro2) conformation and stabilise polyproline-I (PolPro1) due to constraint applied by the linker, limiting the formation of the extended type II conformation in an aqueous environment. Therefore, the synthesis of an array of functionalised polyproline peptides was proposed such that their ease of 'stapling' and propensity to form the desired type I conformation after stapling could be analysed. This information will then have the potential to present an exciting opportunity for this procedure to be applied in the development of alpha-helix mimetics containing a similar linker.

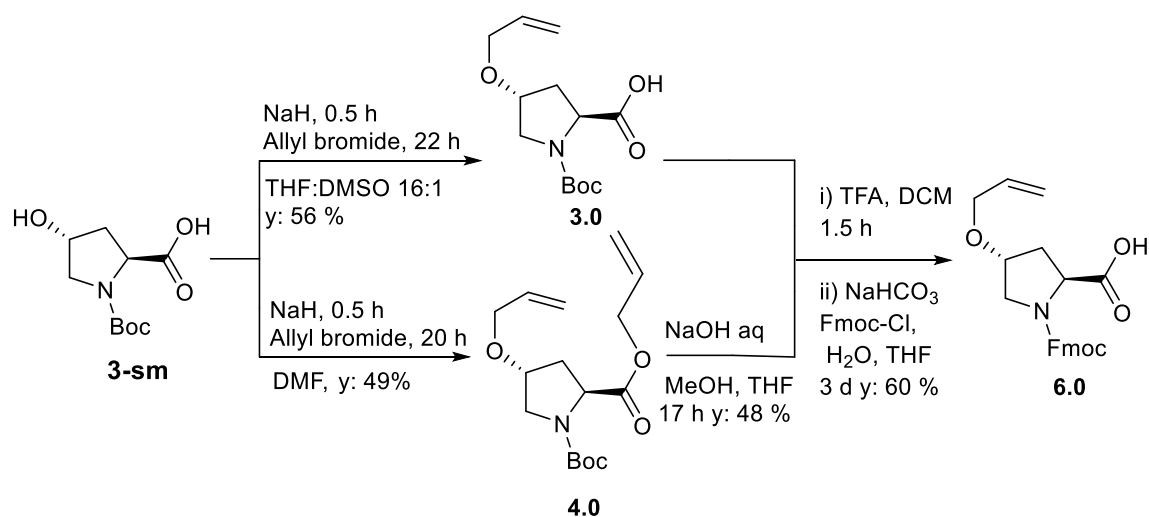
A polyproline peptide 'locked' into the PolPro1 conformation has the potential to act as a mimetic as the more condensed PolPro1 helix has structural similarity to the alpha-helix. It will also have a peptide chain wherein the location of sidechains could be easily predicted, with a well-defined conformation, and therefore used to mimic active regions of an alpha-helical peptide. Thereby, if a polyproline chain can be shown to have been effectively locked into

PolPro1 via a constraining 'staple' this would then allow for the development of promising new therapeutic molecules as well as other functional materials. Four target peptides were chosen with varying *cis-trans* isomerisation at the C4 position on the stapling residues. As such the synthesis of 4-C position functionalised prolines were required to be used in the Fmoc-based solid-phase peptide synthesis to produce functionalised peptides capable of undergoing ring-closing metathesis to produce an all-hydrocarbon linker. Upon which conformational analysis could then be carried out to study the propensity of the stapled peptides to form PolPro1 and PolPro2 helices.

## 2.1 Functionalised Monomer Synthesis Results and Analysis

Before peptide synthesis could be carried out, non-natural amino-acid monomers had to be synthesised to allow for RCM to be carried out to form the desired all-hydrocarbon 'staple'. As such both the *cis* and *trans* isomers of the 4-position functionalised prolines were synthesised with olefin-containing sidechains for use in peptide synthesis.

### 2.1.1 Synthesis of 4-position functionalised *trans*-proline monomer:

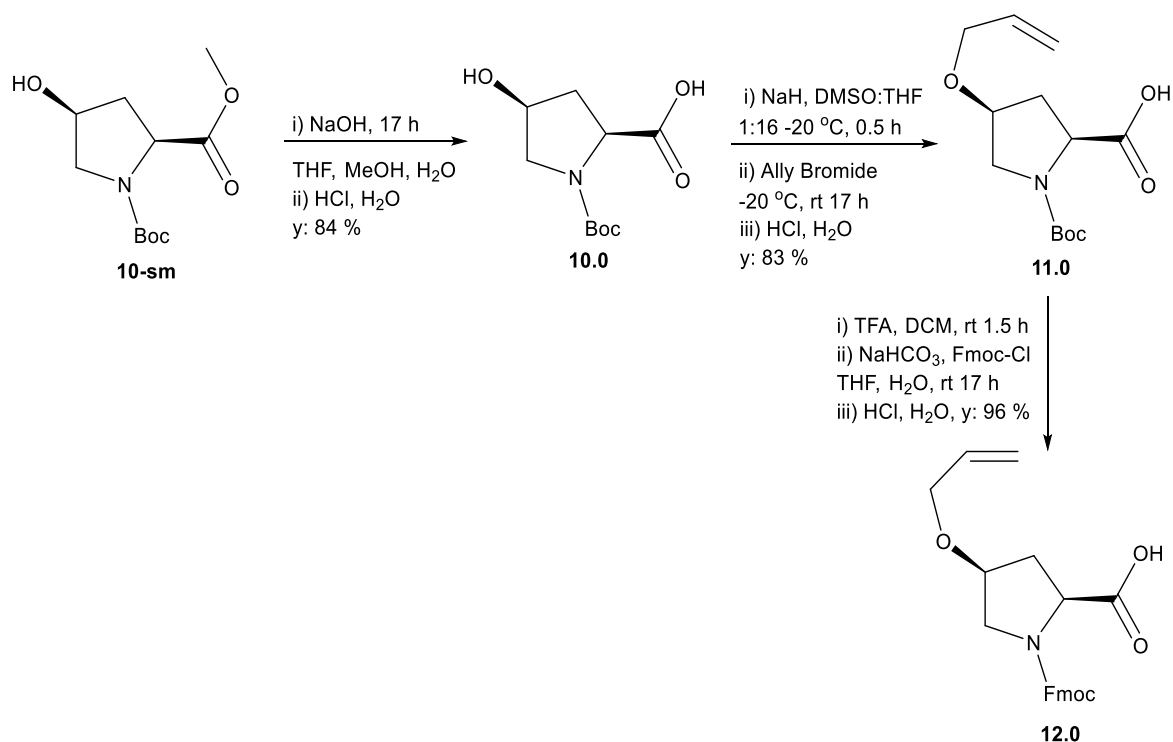


The first step in the synthesis of the 4-position functionalised proline involved the alkylation of the hydroxyl group. This was carried out on the *trans* isomer using the scheme proposed by *V.Mahali et al.* [27] Initially the ester was used in place of the carboxylic acid, **10-sm**, as a cheaper alternative and due to the comparatively more facile purification of an ester via FCC than the free acid. When the ester was used in the alkylation reaction sodium hydride was a strong enough base to deprotonate the carbon at the C2 position which, as it is no longer a non-chiral

centre, epimerisation occurs as the stereochemistry is not retained upon subsequent protonation, as such this yielded a non-stereospecific product. The acid was therefore used in place of the ester, which did not readily undergo this side-reaction. This gave a yield of 83 % of a clear colourless oil, **3.0**, and  $^1\text{H}$  NMR and  $^{13}\text{C}$  analysis showed that the alkylation was carried out successfully with two clear alkene bands between 5-6 ppm integrating correctly for 1 and 2 protons respectively. Dimethyl-sulfoxide was used as it specifically solvates the carboxy-anion under the strongly basic conditions reducing its nucleophilicity and therefore only the more nucleophilic oxy-anion is selectively alkylated.<sup>[27]</sup> This reduces the need for a second hydrolysis step which often results in low yields (**4.0**), as well as reducing the amount of alkylating agent required. Therefore, on repeating the reaction the carboxylic acid starting material was used. This yielded a crude viscous yellow oil which left a colourless oil, **3.1** (53 %), after base-acid extraction to remove impurities. This reaction was then scaled up using the same procedure giving a similar yield, **3.2** (55 %). Which was the main product used for the next stage of synthesis. The reaction was also repeated using DMF in place of THF and DMSO, this was not chemoselective and was carried out such that both the hydroxyl and carboxylic acid were alkylated. This then required a saponification step to selectively hydrolyse the ester giving a significantly reduced yield, **4.0-B** (22 %) of pure compound.  $^1\text{H}$  NMR analysis showed that the sample was usable for the next stage with only further drying required to remove residual DMF.

The next step carried out was Boc-deprotection and Fmoc-protection such that the compound can be used in Fmoc-based solid-state peptide synthesis. This reaction used the scheme proposed by *C.Peters et al*<sup>[28]</sup> with a few alterations such as using THF in place of DMF which is easier to remove and sodium bicarbonate as a base. Also, Fmoc-Cl was used as a safer and similarly effective alternative to Fmoc-Su (sensitizer). This was carried out on a sample of **3.2** and yielded a pink oily product which was freeze recrystallized to attempt to improve the purity of the sample to achieve a solid crystalline product, however only pink oily crystals were achieved. The pink colour was identified as the leeching of dye from the rubber seal of the flask via THF, and the product was therefore dissolved in DCM and mixed with activated carbon, which has been shown to remove contaminating dyes. After filtering and drying of the solution a white/off-white crystalline solid was yielded, **6.0** (60 %), with minimal loss of product (~5 %).  $^1\text{H}$  NMR analysis also showed that the Fmoc protection was successful and a high purity was achieved, with no residual  $\text{CH}_3$  peaks characteristic of the Boc protecting group and aromatic protons from the Fmoc protecting group visible in the 5.75-7.8 ppm region. The repeat of this reaction on a smaller scale yielded an off-white crystalline product, **6.2** (87 %).  $^1\text{H}$  NMR analysis of both products, **6.0** and **6.2**, showed they had an identical pattern of peaks.

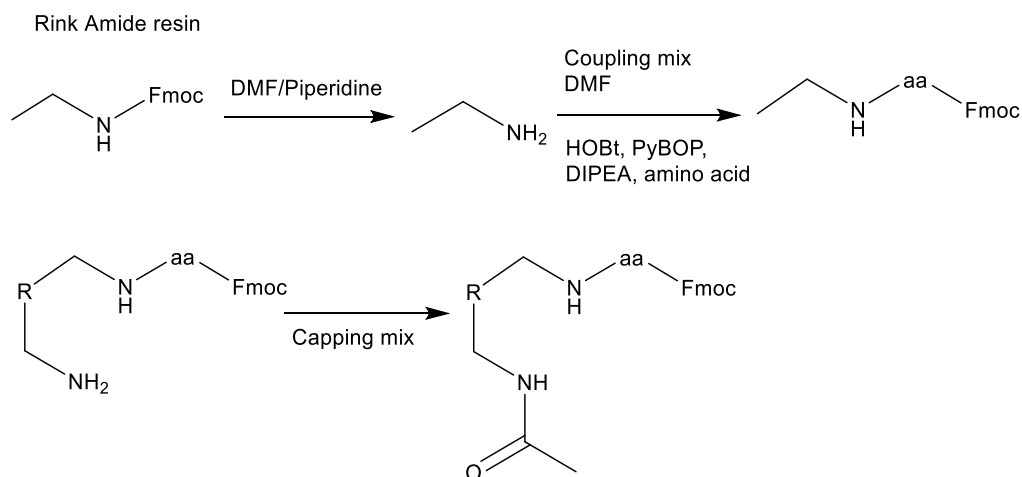
## 2.1.2 Synthesis of 4-position functionalised cis-proline monomer:



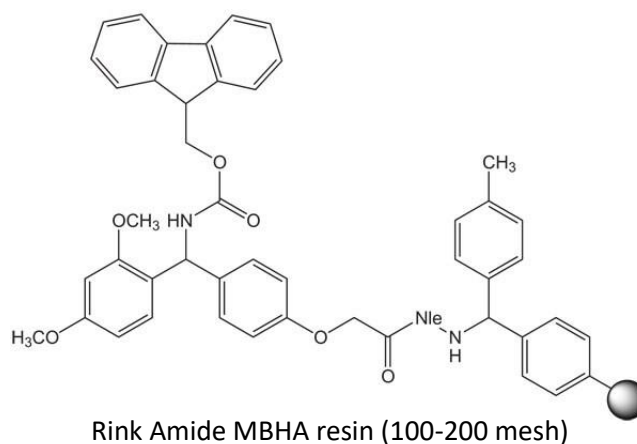
Initially O-alkylation of the hydroxyl-proline methyl-ester was attempted with hydrolysis of the methyl group to be attempted after isolating the alkylated compound, therefore allowing FCC to be used to be used more easily for purification. However, this was unsuccessful, with an epimerisation side-reaction causing significant impurities, with deprotonation and epimerisation occurring at the 2C-position resulting in flipping of the stereochemistry and partial formation of the (2*R*, 4*R*) product as opposed to the desired (2*S*, 4*R*). This then gave multiple different products which could not be separated by FCC. Therefore, it was decided that saponification of the methyl-ester starting material should be carried out before progressing to the alkylation step. This proved to be successful with base-acid extraction again proving to be an effective method for purification of the alkylated carboxylic acid compound with an **84 %** yield for the hydrolysis, **10.0**, and **83 %** after purification of the alkylated product, **11.0**. The product was then carried forward for de-protection of the Boc group with TFA and protection using Fmoc-Cl as was previously used for the trans-monomer, which again gave a high yield (**83 %**), with <sup>1</sup>H NMR analysis showing no residual CH<sub>3</sub> peaks characteristic of the Boc protecting group and aromatic protons from the Fmoc protecting group visible in the 5.75-7.8 ppm region. However, the removal of residual DMSO from the alkylation step proved to be difficult as NMR analysis indicated the solvent's presence in both products. The DMSO signal was only reduced by placing the sample under high vacuum at 60 °C. Which then gave the Fmoc-protected

compound **12.0** as a white crystalline product. This product was then used for SPPS with no further purification after recrystallization.

## 2.2 Peptide Synthesis Results and Analysis:



After synthesis of required non-natural amino-acid monomers SPPS was begun, using Fmoc-based peptide synthesis on a rink-amide resin. The coupling reactions were carried out using DIPEA as the base for amide coupling, HOBt and PyBOP as an in-situ activator. DMF was used as the solvent and 20% Piperidine in DMF for Fmoc-



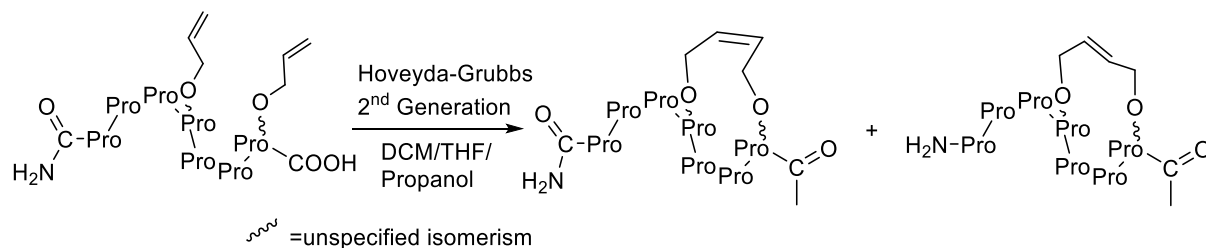
deprotection reactions. The Kaiser test was used to monitor success of initial capping of excess primary amines using acetic anhydride as the amino acid. Further couplings of proline monomers were confirmed by use of the chloranil test with colourless resin beads indicating a successful coupling. Finally, TFA (95 %, in DCM) was used for cleavage of the peptide after initial attempts with a reduced percentage of TFA for milder cleavage conditions giving reduced peptide yields.

*Table 1: Successful SPPS conditions used*

Procedure	Compound	Amount	Time
<b>Resin swelling</b>	DCM	3 ml	20 min
<b>Coupling Mixture</b>	HOBt	2 eq	1.5-2 h
	PyBOP	4 eq	
	DIPEA	4 eq	
	Amino Acid	2 eq	
	DMF	2 ml	
<b>Deprotection Mixture</b>	DMF/Piperidine 20 %	2 ml	40 min
<b>Capping Mixture</b>	Acetic Anhydride	10 eq	1 h
	DIPEA	8 eq	
	DMF	2 ml	
<b>Cleavage Mixture</b>	TFA 95 % in DCM	2 ml	1 h
		2 x 1 ml	30 sec
<b>Wash</b>	DMF	3 x 2 ml	30 sec

Although initial coupling reactions were successful using two equivalents of PyBOP, couplings gradually became less successful, increasing the amount of activating agent improved the success of coupling reactions back to initial levels. It was also noted that coupling reactions were often complete after 30 mins, however, hour long reaction times were chosen to reduce the likelihood of partially incomplete coupling. After partially unsuccessful couplings, removing the reacted mixture and adding more coupling mixture, often with slightly reduced masses of reagents, lead to the completion of the reaction whereas extending the reaction time was largely ineffectual. Therefore, it was theorised that carrying out two shorter coupling reactions (10 mins) would result in a successful coupling in a reduced amount of time. This proved to be successful when trialled using Fmoc-Pro-OH, however, this was not applicable when using functionalised monomers due to the precious nature of the materials, ideally only requiring a single coupling reaction to prevent wastage of the synthesised compounds. Electrospray ionisation mass spec confirmed the correct chain length had been synthesised for all four peptides with the expected 851.47 [M-H]<sup>+</sup> peak. Also, analytical reverse-phase HPLC indicated only a single product peak, suggesting a high purity of the desired peptide had been achieved.

## 2.2.1 RCM Reactions



General RCM reaction with unspecified *cis/trans* sidechains/staple

Ring-closing metathesis (RCM) reactions were initially attempted with the 3<sup>rd</sup> generation Grubb's catalyst due to its high reactivity and quick rate of reaction, and while the peptide was bound to the resin to limit any cross-metathesis. The 3<sup>rd</sup> generation Grubb's reactions proved to be unsuccessful after a series of attempts in various solvents. The Grubb's catalyst gave no significant degree of metathesis, especially in unfavourable solvents such as propanol, this was shown after LCMS analysis with no new product peaks produced. Therefore, 2<sup>nd</sup> generation Hoveyda-Grubbs catalyst was used as an alternative due to observed success in literature and high versatility, with RCM reportedly possible in protic coordinating solvents such as those that were to be used in this synthesis to achieve the desired PolPro1 conformation.<sup>[21]</sup> This proved to be significantly more effective than the 3<sup>rd</sup> generation catalyst, so further attempts with the 3<sup>rd</sup> generation catalyst were discarded to prevent wastage of peptide and the expensive catalyst. Attempts to carry out RCM on the resin-bound peptide were unsuccessful, likely due to a high dilution of catalyst as the amount of solvent required to cover the resin sufficiently resulted in a low catalyst concentration beyond ideal levels when using 5-10 % catalyst. It is possible that using higher percentages of catalyst would lead to successful resin-bound metathesis, however, due to the high cost of ruthenium-catalysts increasing the amount used any further would make the reaction unfeasible except on very small-scale reactions.

Four solvents were initially trialled to compare their effect on the degree of stapling and the amount of PolPro1 vs PolPro2 stapled product, ethyl acetate was shown to not dissolve the peptide so was discounted. Propanol was chosen as one of the solvents due the propensity of polyproline to form PolPro1 in propanol even though this is a disfavoured solvent for metathesis reactions. It was theorised that the formation of PolPro1 and the subsequent reduced distance between sidechains would increase the likelihood of metathesis as the staple in the PolPro1 conformation bridges a shorter distance than in PolPro2. However, propanol reactions proved to be less successful than those carried out in DCM or THF with most RCM reactions carried out in propanol giving little to no product. The degassed propanol being used was likely causing decomposition of the catalyst preventing any metathesis of the product.

The RCM reactions were carried out overnight which led to problems when using DCM as the small volumes used led to evaporation of the solvent, therefore reducing the length of reaction time. To mitigate this effect, smaller reaction vessels were used, and the atmosphere was initially attempted to be saturated with DCM by allowing an initial amount of solvent to evaporate, prior to adding reagents in solution. Also, excess DCM was either added initially or added after a reduction in solution volume was observed, however, concentration of the solution was kept as high as possible, as a high dilution limits the progress of the metathesis reaction.

### 2.2.2 HPLC Analysis

The RCM products were analysed via reverse phase analytical HPLC before the individual products were isolated via reverse-phase preparatory HPLC. The isolated products taken for further analysis are shown in *figures 6a-c*. The analytical HPLC indicated the presence of four products in each successful reaction. The majority of the HPLC spectra showed one major peak, excluding the starting material, with a second slightly smaller peak and two significantly smaller peaks that in some of the spectra were partially overlapped by the two larger peaks such as in *Figure 6* with only 3 clear product peaks. However, LC-MS confirms the presence of four products with the same mass. The degree of metathesis varied for each peptide with the *trans-trans* peptide showing the largest consumption of the starting material while *cis-cis* showed minimal consumption. ESI mass spec was then carried out on the crude product mixtures and showed that all the four product peaks from all four peptides had the same mass ( $M^+ 823.44$ ), this showed that all the products from each RCM were successfully stapled peptides. This peak pattern suggested that the four products were E/Z isomers with both the PolPro1 and PolPro2 conformation. Subsequent hydrogenation would ideally be used to remove the E/Z isomerisation and thus provide a clearer picture with only the PolPro1 and PolPro2 products present. Therefore, in the interest of time most of the further analysis was focused on the most successful products with the largest consumption of starting material, peptide **17-tt**. Also, Ion-Mobility Mass spectrometry (IM-MS) was to be carried out on the final peptides to provide further characterisation of the conformation of the products present, however, due to time constraints and limited access to equipment this was not possible within the timeframe of the project.

The differences between products from RCM reactions in THF vs DCM were minimal with only slight variations in peak intensities and degree of metathesis. For example, for peptide **13-ct**, the peak pattern was very similar (*Figure 7a*) and when the samples were combined there was complete overlap of product peaks (*Figure 7c*) suggesting the same products were being produced in either case with similar ratios. However, RCM reactions carried out in propanol (*Figure 7b*) consistently showed minimal metathesis in comparison to RCM carried out in DCM and THF. Also, the product ratios appeared to be the same suggesting there is no benefit to the formation of either isomer from using propanol over other solvents which combined with the reduced yield suggests propanol is not an effective solvent for this synthesis.

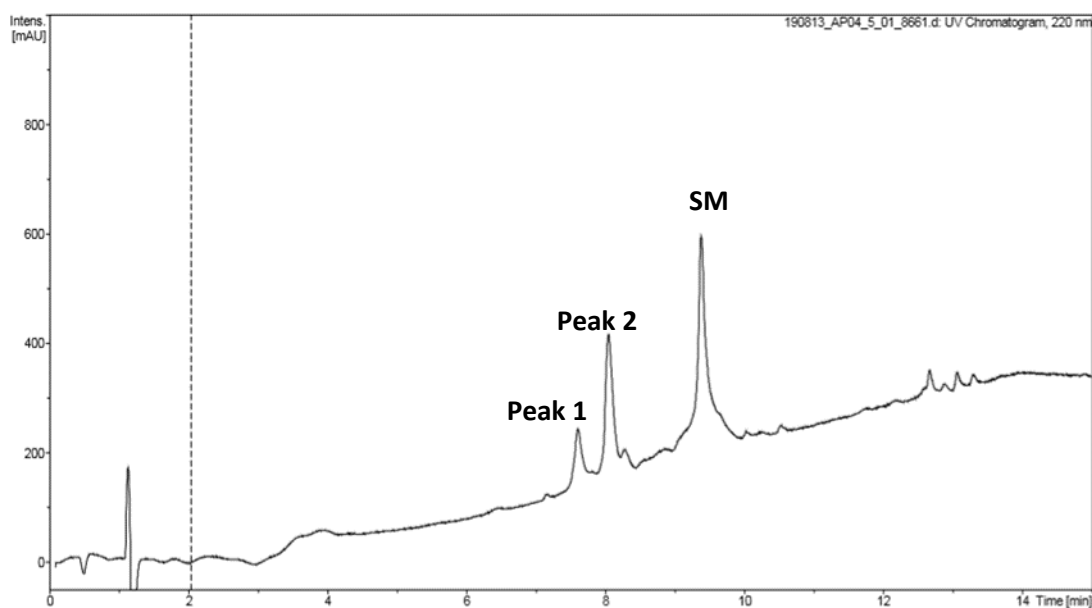


Figure 6a – **13-ct** peptide stapled RCM products isolated via prep-HPLC for further analysis

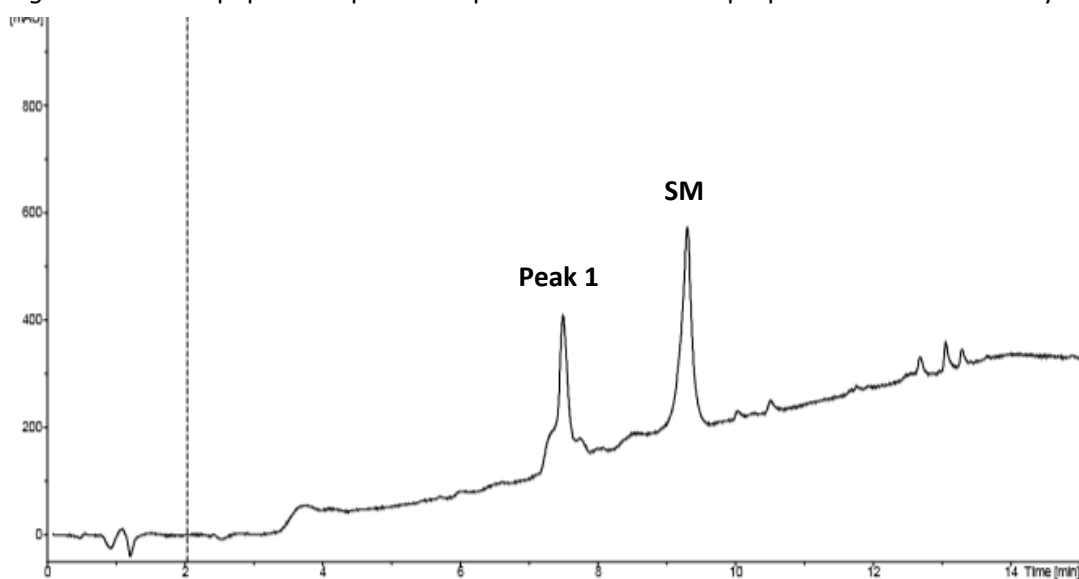


Figure 6b – **17-tc** peptide stapled RCM products isolated via prep-HPLC for further analysis

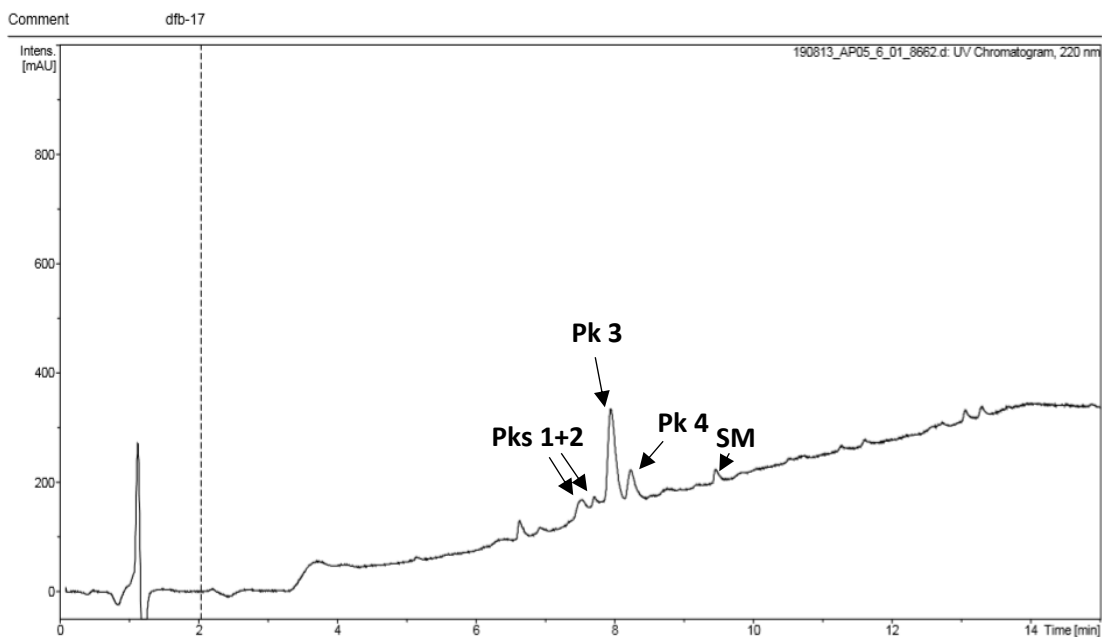


Figure 6c – 17-tt peptide stapled RCM products isolated via prep-HPLC for further analysis

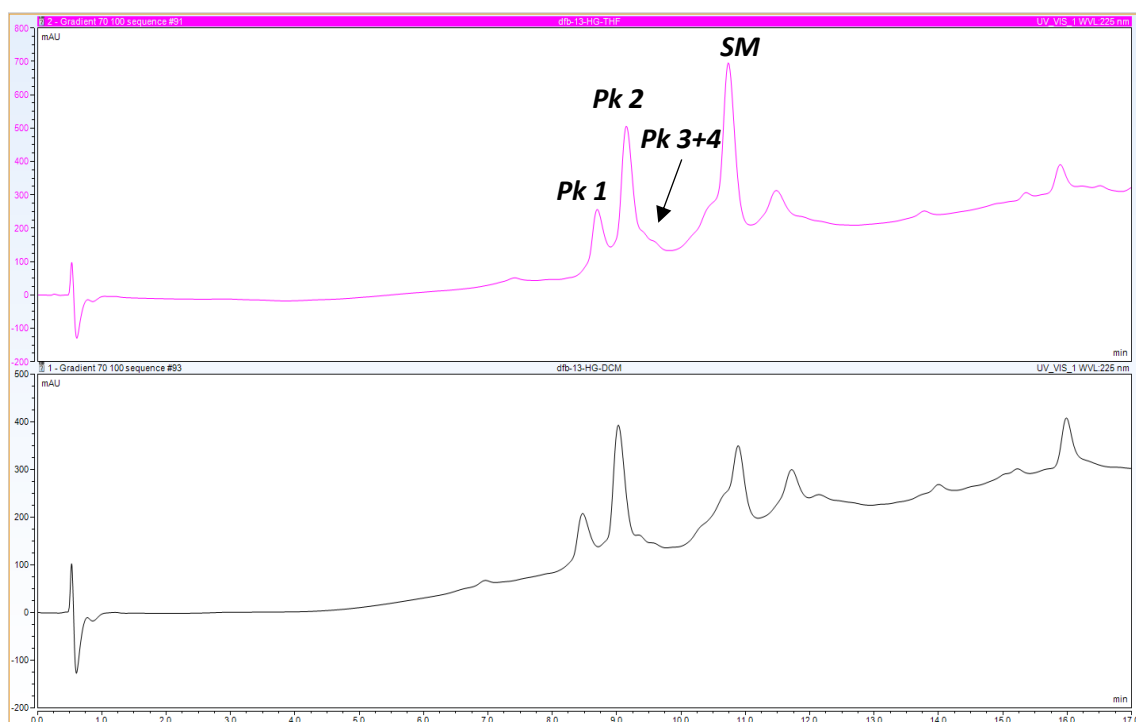


Figure 7a – Reverse-phase analytical HPLC results of peptide 13-ct in THF (top) and DCM (bottom) exhibiting very similar product peaks.

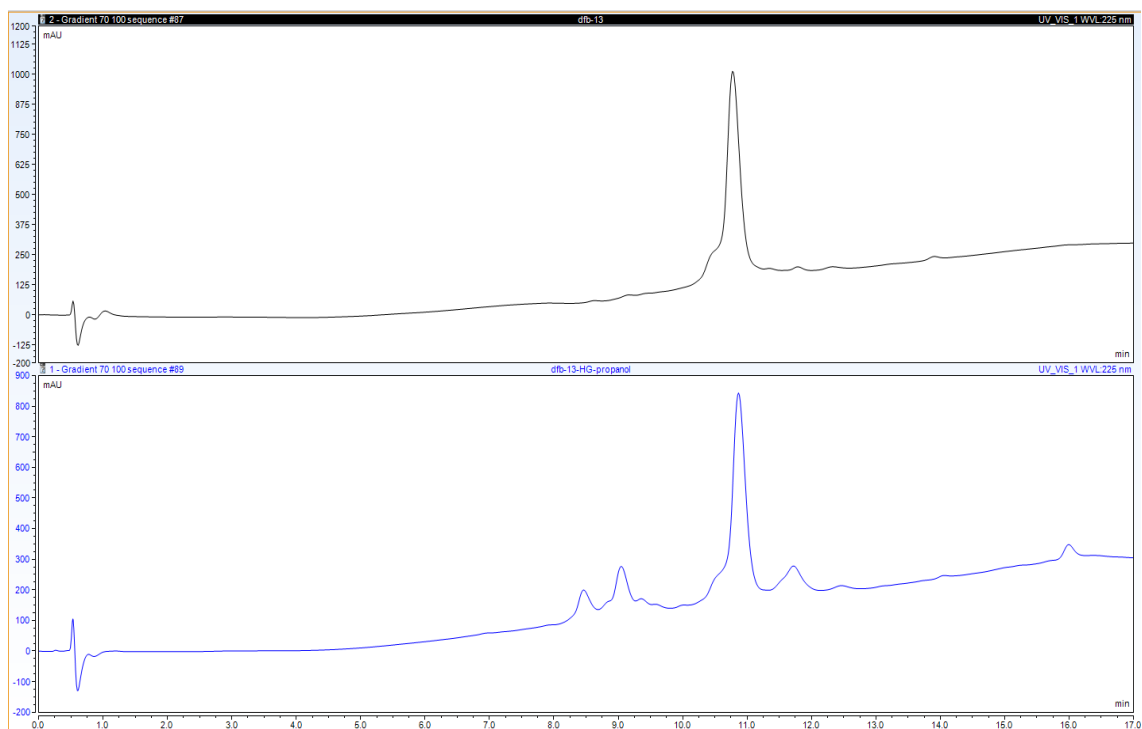


Figure 7b – Reverse-phase analytical HPLC results of peptide **13-ct** starting material (top) and RCM in propanol product (bottom).

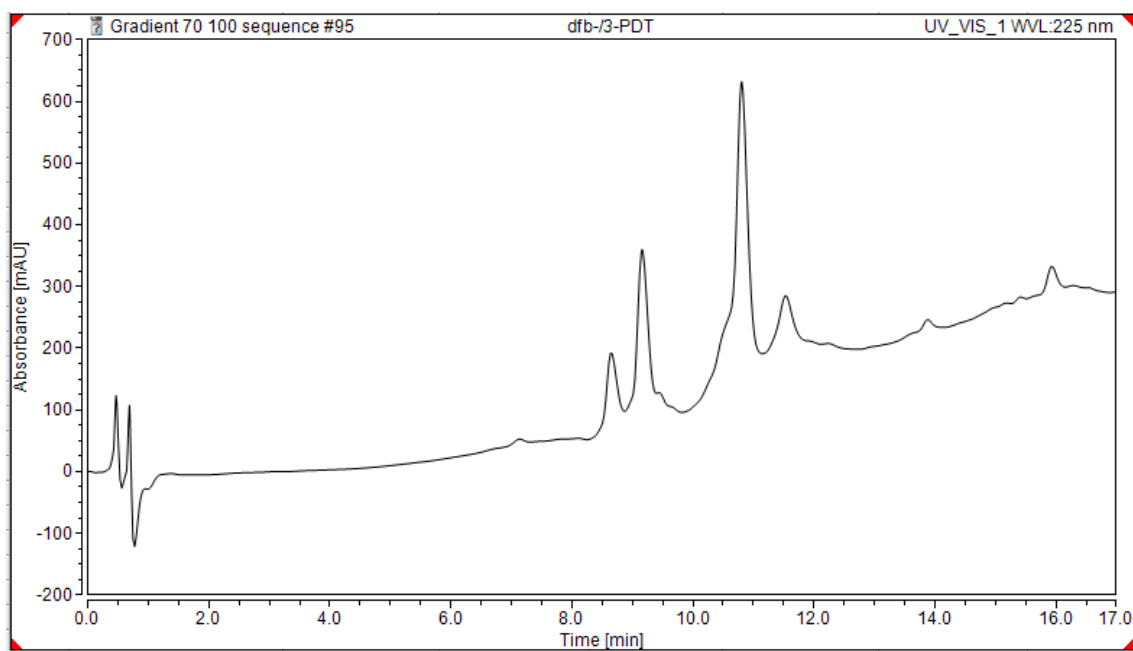


Figure 7c – Reverse-phase analytical HPLC results for peptide **13-ct** of combined samples of DCM, THF and Propanol RCM reaction products.

### 2.2.3 CD Spectroscopy Results

Initially CD spectroscopy was carried out on the starting materials after incubation in propanol or water for at least 6 days at 20 °C. PolPro2 should exhibit a spectrum with a weak positive band at 225-229 nm and a strong negative band at 202-206 nm.<sup>[3]</sup> PolPro1 should exhibit a medium intensity negative band at 198-200 nm, a strong positive band at 214-215 nm and a weak negative at 231-232 nm. This makes CD spectroscopy an effective method for conformational analysis of polyproline. However, after analysis none of the starting material samples showed significant shift of the maxima from 226 nm to 214 nm as expected for the peptides incubated in propanol (*Appendix C*) which would be indicative of PolPro1. The peptide **17-tt** was chosen an example of this as the CD spectra of the starting material shows no shift of the maxima to 214 nm (*Figure 8*). However, there was a noticeable shift in intensities which suggests that a conformational change is occurring, yet the difference from the expected spectrum suggests PolPro1 may not be fully stable for this length of peptide and that some intermediary structure may be forming,<sup>[4]</sup> which results in the lack of shift to lower wavelengths as was expected.

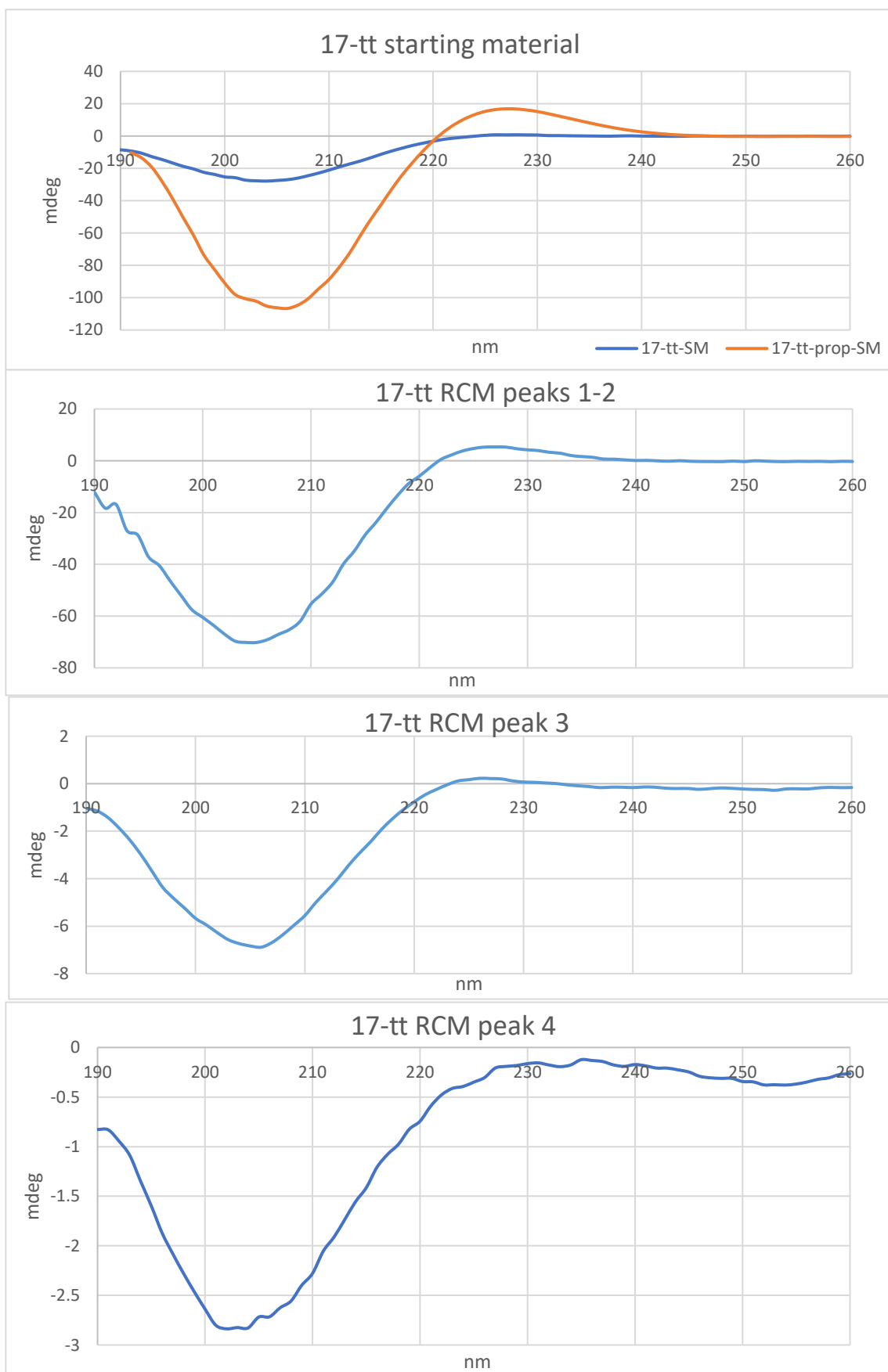
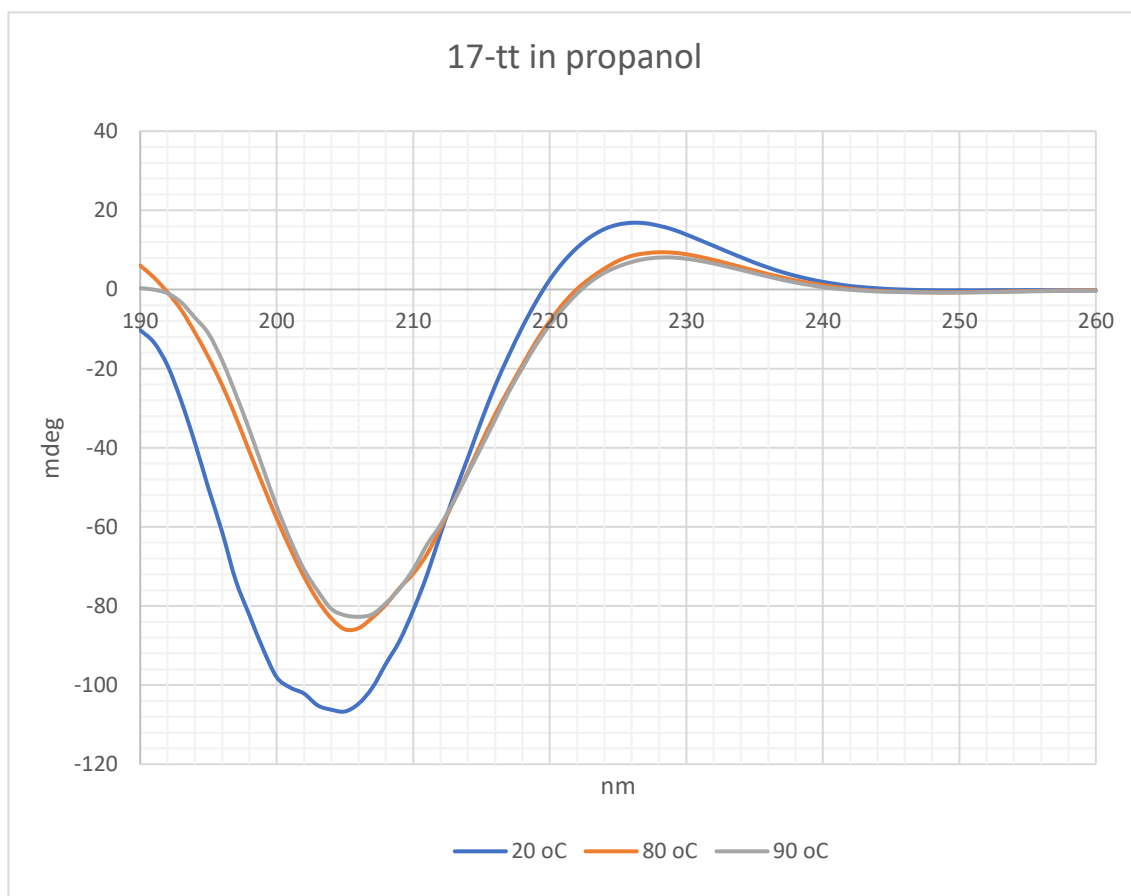


Figure 8 – CD spectra of functionalised **17-tt** (*trans-trans*) P(Pro)<sub>7</sub> in aqueous solution (blue) and in propanol (orange), and RCM products **1-4** in water (<10 % MeOH), at 20 °C and ≈100 μM.

Due these results a variable temperature CD analysis (*Figure 10*) was carried out on the 17-tt unstapled peptide to determine if increasing the temperature of the polyproline samples would cause a distinct change in the spectra at 226 nm, as well as carrying out full spectra analysis at various temperatures (*Figure 9*). As temperature increases the PolPro2 conformation is favoured over the PolPro1 conformation and as such there should be a further shift to a more PolPro2 like character.<sup>[3]</sup> This analysis showed that as temperature increased the intensity of the peak at 226 nm reduced and shifted to 228 nm which shows that there is a clear conformational change occurring.

Analysis of the isolated RCM products was also carried out, however, these again did not show any shift of the maxima to 214 nm as expected. The main differences exhibited for the **17-tt** RCM products (**pk1-4**) was formation of a trough after 240 nm in both the **peak 3 + 4** products which similarly appears in PolPro1 CD spectra which is not present in the minor products CD spectrum. Which may suggest that major product is PolPro1 in this case. Also, the intensity of both the minima and maxima varied significantly between each sample, however the wavelength of the minima/maxima did not differ between each sample as would be expected. The CD spectra for the peptide **17-tt** are shown as an example above (*Figure 8*).



*Figure 9* – CD spectra of unstapled **17-tt** *trans-trans* P(Pro)<sub>7</sub> in propanol at 20 °C, 80 °C and 90 °C and 100  $\mu$ M.

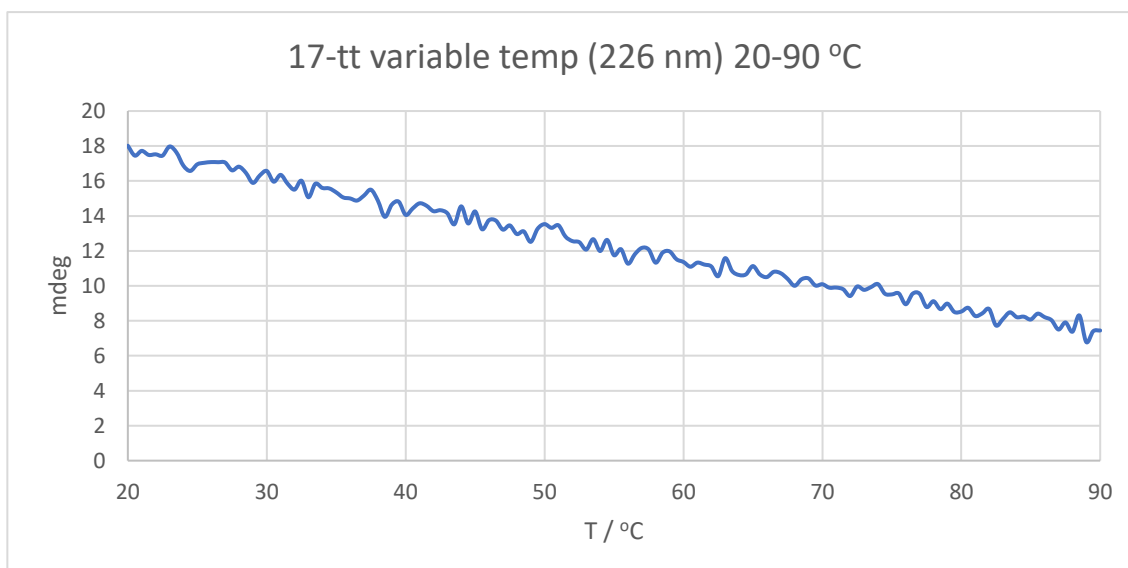


Figure 10 – CD spectrum of unstapled **17-tt** *trans-trans* P(Pro)<sub>7</sub> in propanol from 20-90 °C at 226 nm and 100 μM (*Appendix C*, further temperature information)

#### 2.2.4 FT-IR Spectroscopy Analysis of Peptides

Due to the good indication of a transition occurring from CD spectroscopy FT-IR analysis was carried out as another method to indicate the conformation of the peptides. In this case PolPro1 should exhibit a strong peak at  $1635\text{ cm}^{-1}$  while PolPro2 should exhibit a strong peak at  $1623\text{ cm}^{-1}$ .<sup>[6]</sup> This was proven to be the case after analysis of the starting materials as those that were incubated in propanol showed a shift to  $1635$  as expected, suggesting PolPro1 was forming in this solvent, while those in water showed the expected band at  $1623\text{ cm}^{-1}$ , the IR spectrum of **17-tc** is given as an example below exhibiting alternate shifts when incubated in propanol vs aqueous solvent (*Figure 11 + 12, Appendix D*). All the starting materials except for the *trans-trans* peptide showed this shift from  $\approx 1623\text{ cm}^{-1}$  to  $1635\text{ cm}^{-1}$  after incubating in propanol.

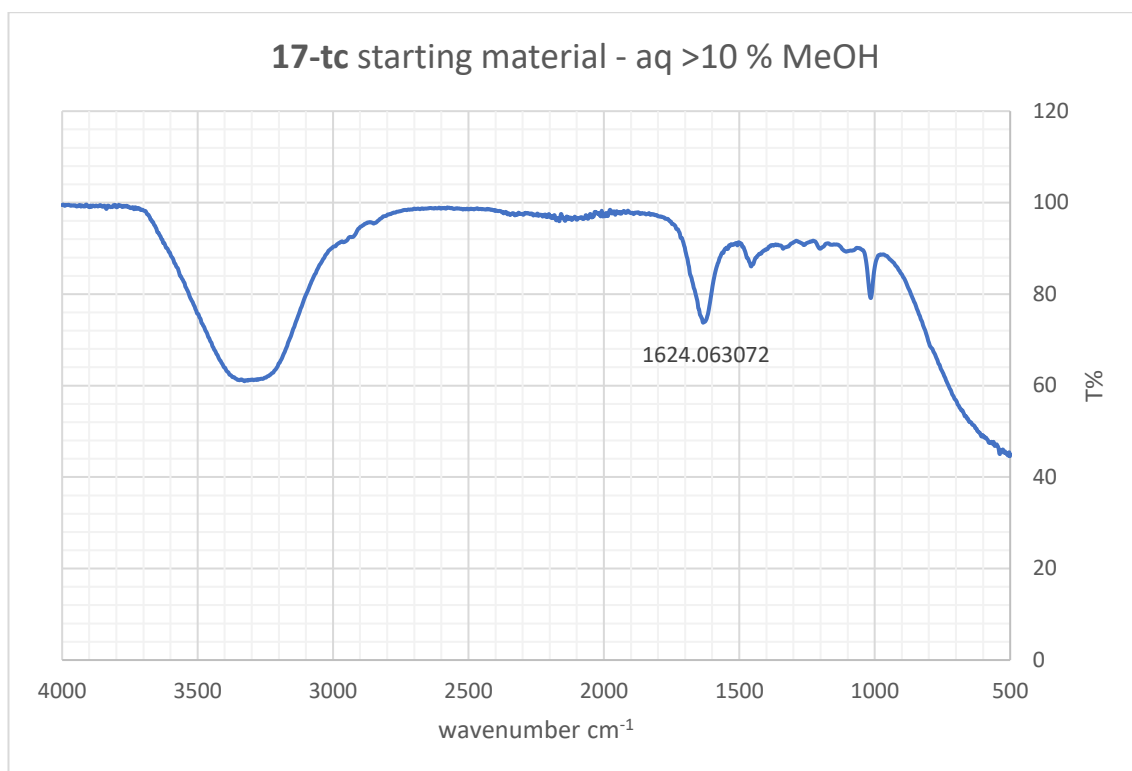


Figure 11 – FT-IR spectrum of unstapled peptide **17-tc** (*trans-cis*) incubated in aqueous solvent, exhibiting a C=O band at  $1624 \text{ cm}^{-1}$ , suggesting a PPII conformation.

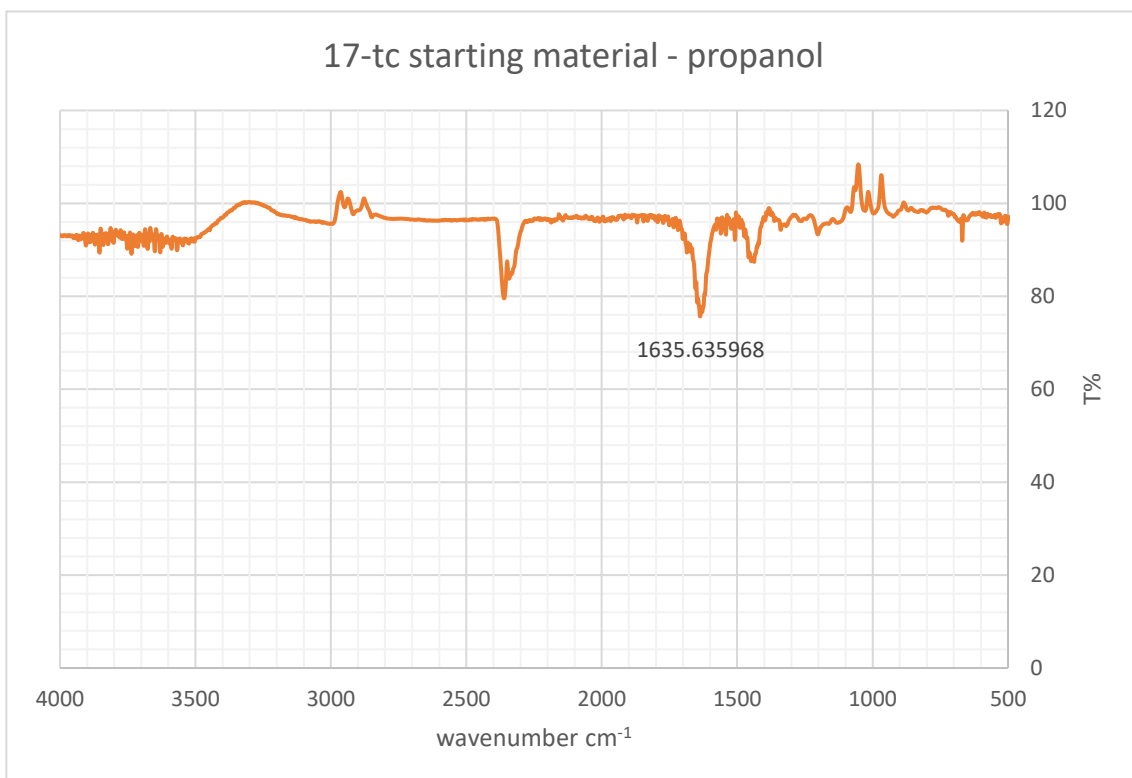
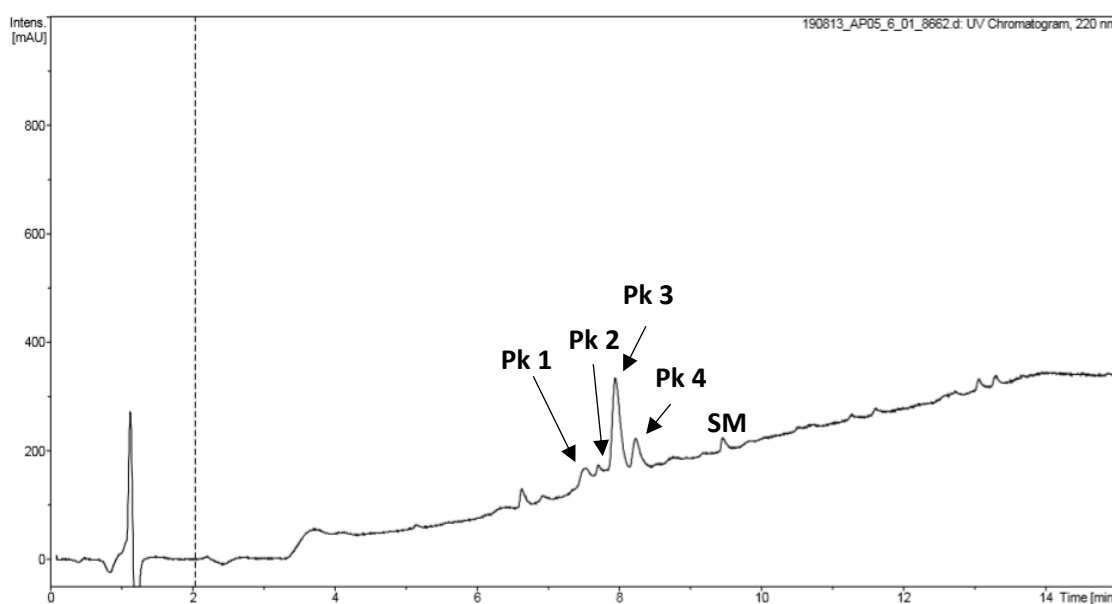


Figure 12– FT-IR spectrum of unstapled peptide **17-tc** (*trans-cis*) incubated in propanol, exhibiting a C=O band  $1635 \text{ cm}^{-1}$ , suggesting a PPI conformation.

Therefore, analysis of the purified RCM products from prep-HPLC was carried out. These all gave a strong broad peak at  $1635.7\text{-}1637.5\text{ cm}^{-1}$ , suggesting that the peptide was no longer exhibiting PolPro2 structure even though the samples were in an aqueous environment. This information indicates that after stapling the conformation of the peptide is no longer strongly influenced by the solvent. However, this is also contrary to the idea that both PolPro1 and PolPro2 are forming as the products do not express different C=O bands as would be expected if the 4 products (*Figure 13*) represented E/Z isomers of 'locked' PolPro1 and PolPro2. *Figure 14* shows the IR analysis of the **17-tt** RCM (in THF) products (*Figure 13*, products **1 + 2** isolated together) and shows how all the products appear to give the same C=O band at the same position given by the PolPro1 conformation however, there must clearly be difference in conformation as the products are separable via chromatography. This suggests that the conformation of the products may differ from that of the well-defined PolPro1 and PolPro2 conformations and may lay somewhere in between. However, the location of the band at 1635 suggests a more PolPro1 character than PolPro2.



*Figure 13* – ESI-MS UV chromatogram of peptide **17-tt** (*trans-trans*) after RCM in THF. Four RCM products are all clearly visible and peaks **1+2**, **3** and **4** were isolated and further analysed.

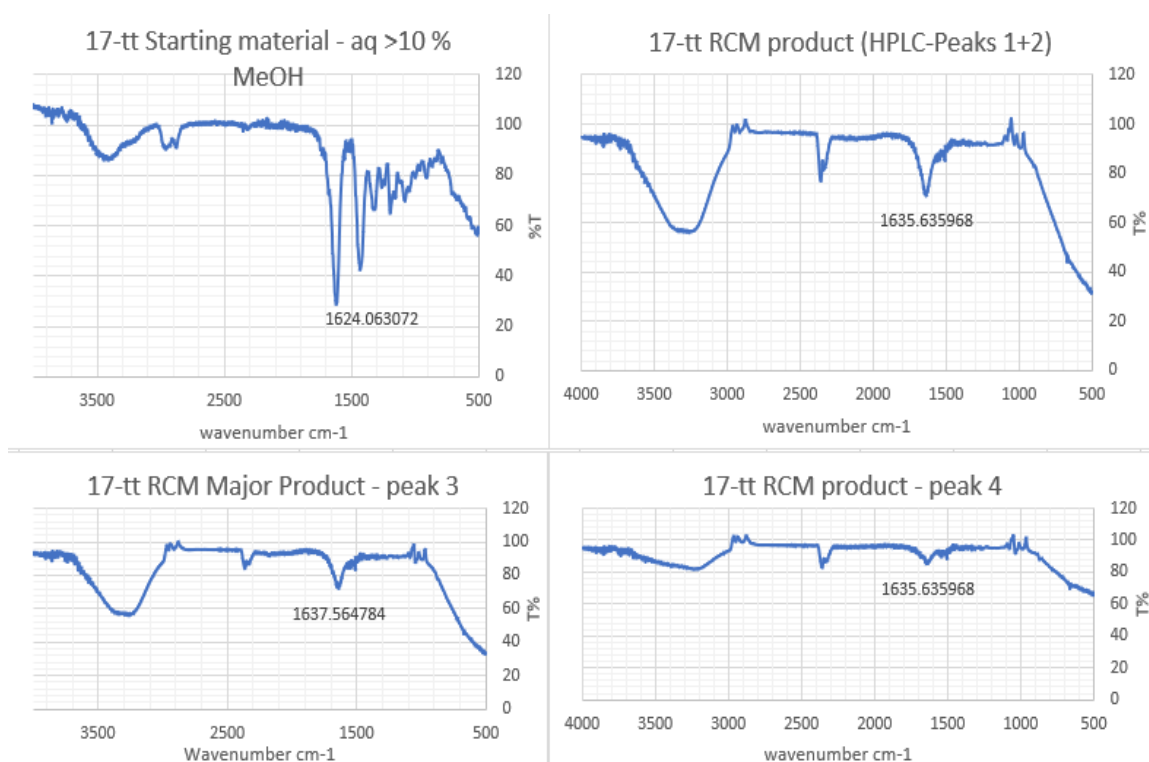


Figure 14 – FT-IR spectra of **17-tt** starting material and the RCM products, highlighting the shift in the C=O band from  $1624\text{ cm}^{-1}$  in the unstapled peptide to  $1635\text{ cm}^{-1}$  in the stapled peptides (peaks from *figure 11*). This matches the proposed shift seen in the transition from PPII to PPI outlined by *R.K.Dukorm et al.* [6]

## 2.4 Mimetic-peptide Monomer Synthesis Results and Analysis

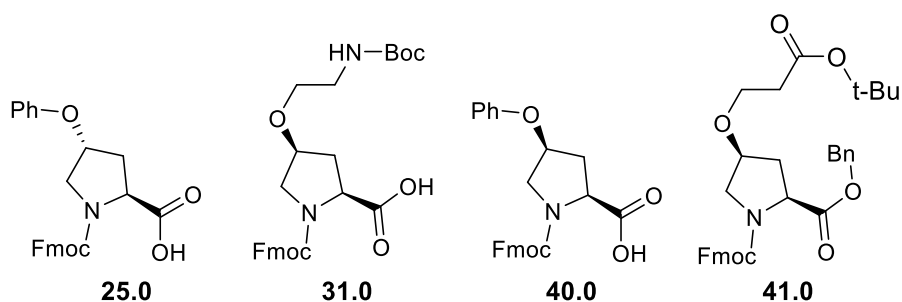
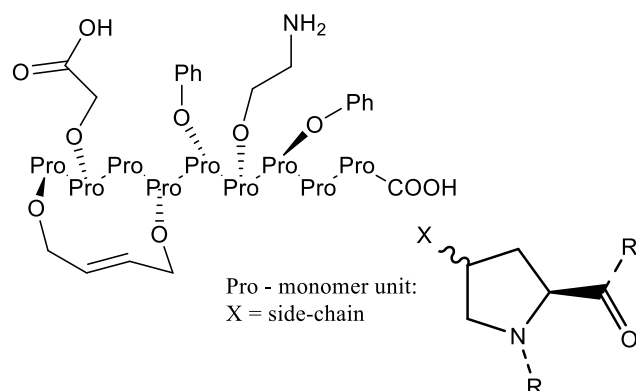


Figure 15 - Further non-natural amino-acids required for the synthesis of proposed mimetic peptide, **32.0** (*Figure 16*). Compound **25.0** fully synthesised, **31.0** – steps towards synthesis carried out, **40.0** previously synthesised within the Palma group.

After completion of synthesis of stapled test peptides work was begun on synthesising monomers required to synthesise a modelled peptide mimetic (*Figure 15*) of a peptide that interacts with a section of the protein Talin. This protein and its interaction with a model peptide, **33.0**, has been extensively studied by our collaborator in the School of Biosciences here at Kent. The Goult group has indeed identified key contact points between the alpha helix and the Talin segment. [29] [30] This system should enable thorough investigation of the interactions of

the Talin protein and our mimetic. The overlap (*figure 17*) of the two peptides indicates that the active region of the mimetic closely resembles that of the peptide, **32.0**, and therefore should interact effectively with the target protein. Key contact points which we will aim to mimic are associated with the tyrosine, phenylalanine and lysine side chains. Therefore, the synthesis of several non-natural amino acids was required for this mimetic detailed above (*Figure 15*). Work was completed on synthesising a trans-phenol functionalised proline, compound **23.0** (*section. 2.4.1*), and begun on synthesising a lysine mimetic proline, compound **31.0** (*section. 2.4.2*).



*Figure 16* – Proposed ‘stapled’ peptide mimetic structure, **32.0**, with all visible non-natural sidechains bound at the C4 position.

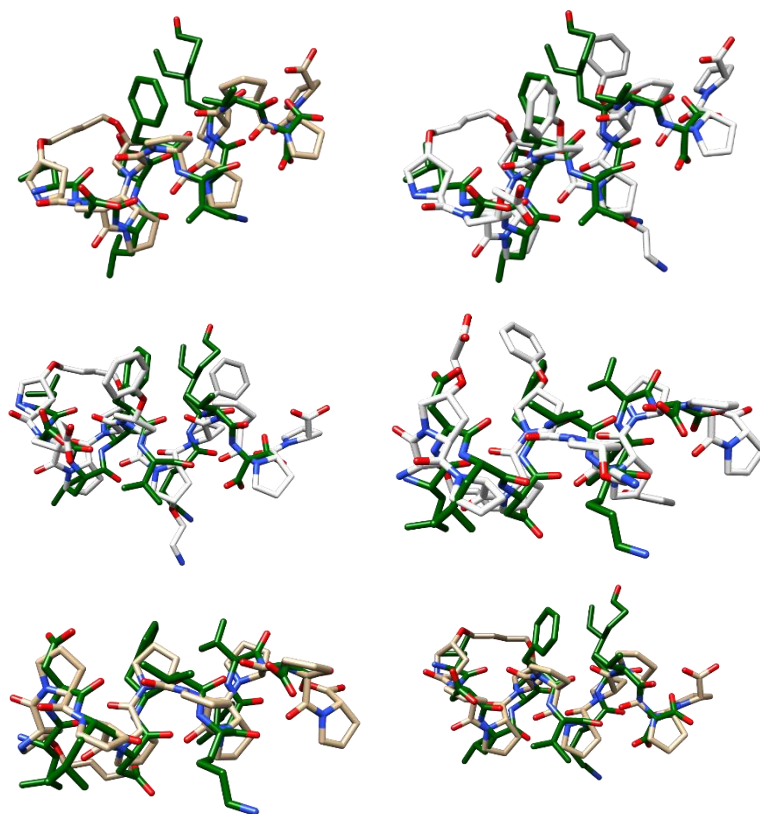
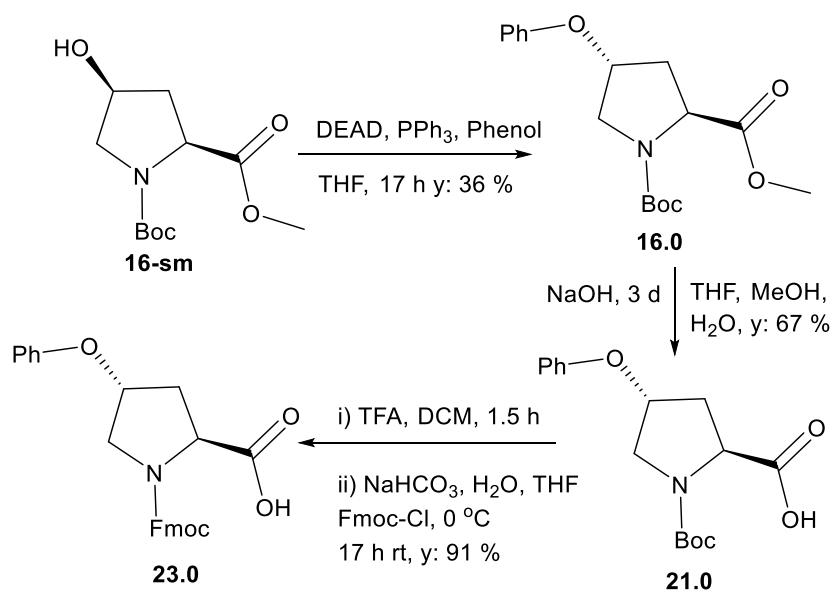


*Figure 17* – Overlap of proposed ‘stapled’ polyproline mimetic, **32.0** (*white*), with target peptide, **33.0**, (*green*) that interacts with a portion of the Talin protein.

## 2.4.1 Synthesis of trans-phenol proline monomer:

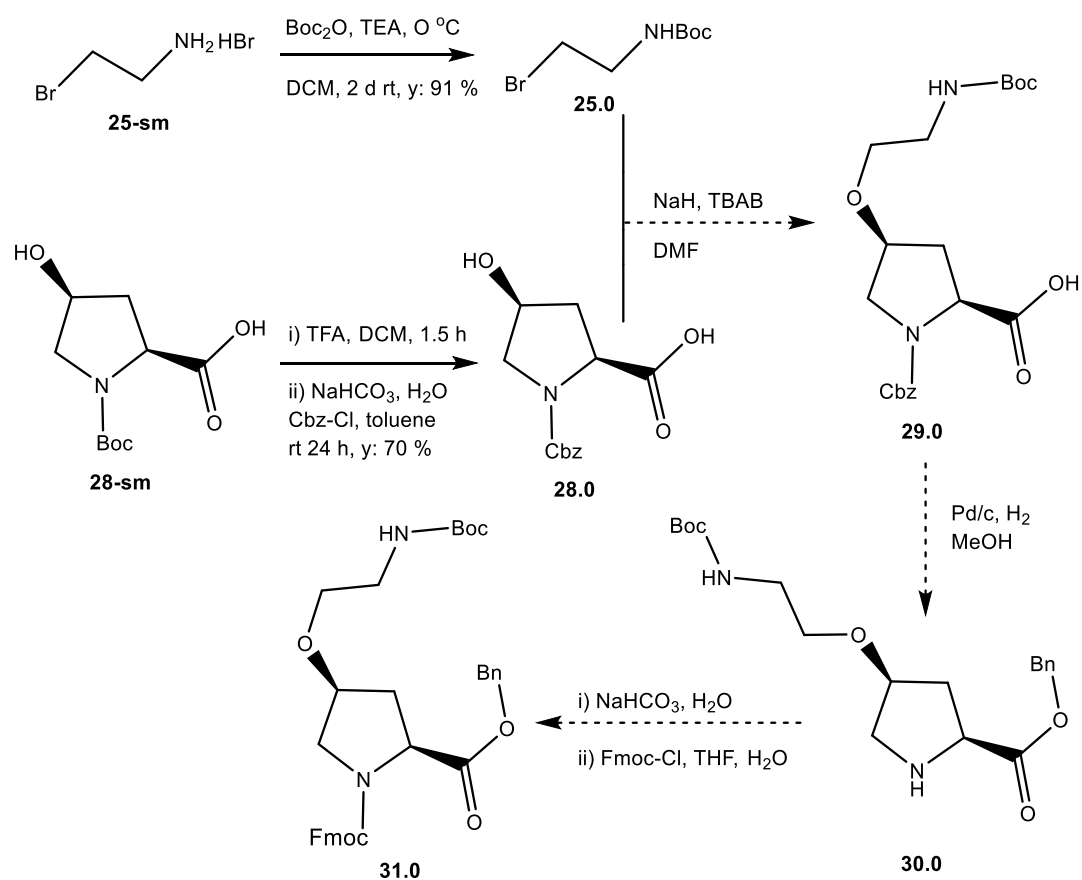


Initially the Mitsunobu reaction, utilising diethyl azodicarboxylate, was used to functionalise proline with the desired phenol group and to produce the trans product, 1-(tert-butyl) 2-methyl (2S,4R)-4-phenoxyproline-1,2-dicarboxylate, **16.0**. This proved to be successful as evidence by the presence of 3 new peaks around 7 ppm, representative of the 5 aromatic protons from phenol, however, FCC had to be carried out twice to remove significant contaminants. These are likely due to the presence of PPh<sub>3</sub>O and hydrazine dicarboxylate, but also possibly side products produced from the addition of the azodicarboxylate in place of the desired nucleophile, which is common for the Mitsunobu reaction. Finally, activated carbon was added to the product in solution to attempt to remove contaminants visible between 0-1 ppm on <sup>1</sup>H NMR analysis, as this method had previously been used to successfully remove contaminants from this region. This produced a significantly cleaner spectrum, however, the yield achieved was relatively low (36%). The yield (0.5 g) was sufficient such that the product could be carried forward to the next step with no further purification.

The free acid, **21.0**, was then produced using a simple hydrolysis with NaOH as in previously stated methods, achieving a 67% yield. The success of which was clearly evidenced by the loss of the methyl protons peak at 3.75 ppm on the <sup>1</sup>H NMR spectrum. TFA was then used to remove the Boc protecting group so that it could be replaced with the Fmoc required SPPS. The deprotection and protection using Fmoc-Cl was carried out successfully achieving a high yield (91%) and a pure compound, **23.0**, 1-((9H-fluoren-9-yl)methyl) 2-methyl (2S,4R)-4-phenoxyproline-1,2-dicarboxylate. No residual Boc protected compound was present shown by the lack of the characteristic CH<sub>3</sub> peak under <sup>1</sup>H NMR analysis. Also, a number of new aromatic

proton peaks, from the Fmoc, present around 7.5 ppm were clearly visible.

#### 2.4.2 Synthesis of tert-butyl ethylcarbamate proline monomer:



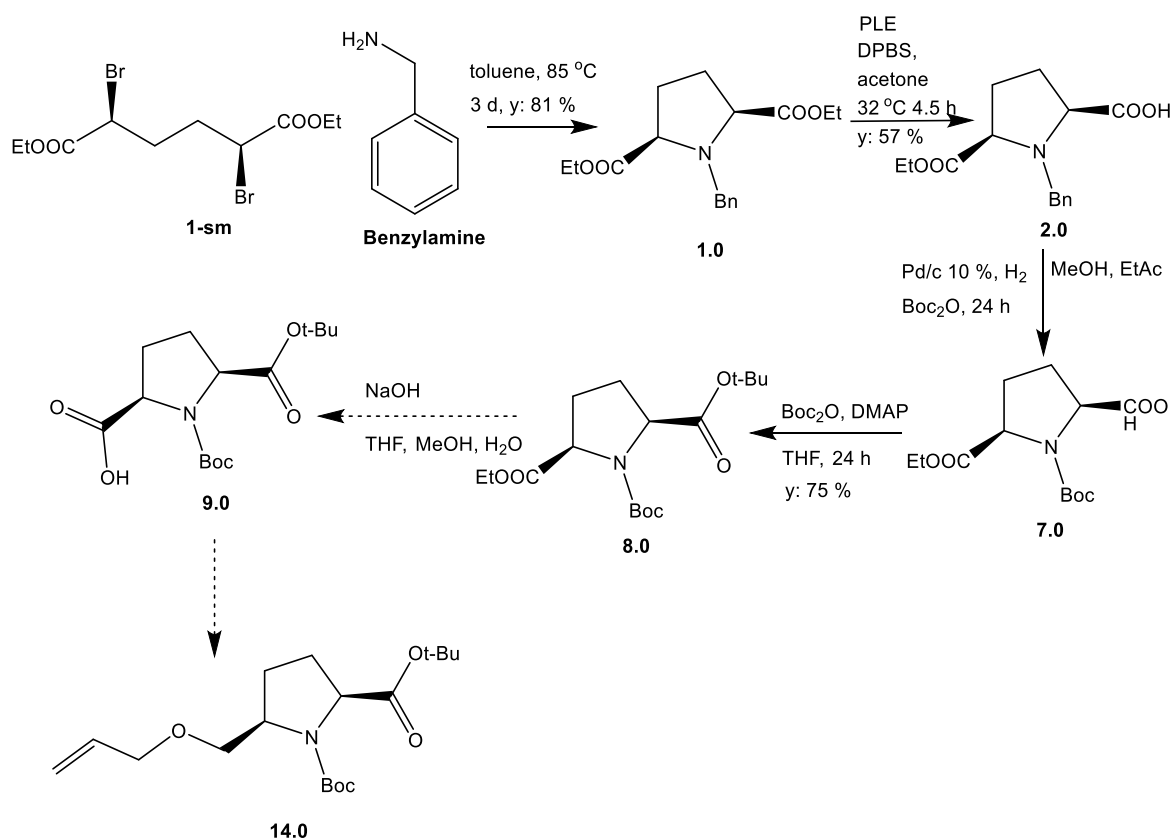
Initially the Boc-protected amine alkylating agent, **25**, tert-butyl (2-bromoethyl) carbamate (**25.0**), was synthesised using  $\text{Boc}_2\text{O}$  and bromoethylamine hydrobromide, with TEA used as the base in the reaction. This proved to be successful (**67 %** yield) with the product isolated after extraction.  $^1\text{H}$  NMR analysis showed residual  $\text{Boc}_2\text{O}$  with a second tert-butyl proton peak present at 1.45 ppm (1:9 product, molar ratio) with the integrals for the 3 other peaks giving the expected number of protons. The  $^{13}\text{C}$  NMR analysis shows extra peaks for all the Boc-group carbons, again showing that there is residual unreacted  $\text{Boc}_2\text{O}$ . When this reaction was repeated a higher yield was achieved (**91 %**).

Alongside this de-protection of cis-Boc-proline and protection with Cbz was carried out. This was done to introduce an orthogonal protecting group to the Boc-group on the primary amine to prevent coupling occurring at the sidechain during peptide synthesis. Removal of the Boc-group would be required after the cleavage of the peptide from the resin. This used a similar method to the previously used Fmoc-protection. First deprotecting with TFA, before drying and addition

of Cbz-Cl with no previous purification step. After work-up and extraction of the product, (2*S*,4*S*)-1-((benzyloxy)carbonyl)-4-hydroxypyrrolidine-2-carboxylic acid (**28.0**), was isolated as a viscous oil (70 %). <sup>1</sup>H NMR analysis showed the removal of the tert-butyl CH<sub>3</sub> proton peak at 1.37 ppm, confirming the Boc-protecting group was successfully removed. The presence of peaks in the aromatic region representing the 5 benzyl protons from the Cbz group indicated the protection was successful.

## 2.5 5-position functionalised monomer synthesis

An alternative location for the hydrocarbon staple was initially proposed between the 5 and 3 positions as the staple would be contained more within the helix and preserves more faces of the helix for functionalisation. This would therefore lead to a more adaptable mimetic, with more locations available for sidechains. Ideally, a peptide with a linker at this location would have also been synthesised and the efficacy of their binding affinities to target proteins could be compared. However, due to the length of the synthesis to acquire both monomers, time-constraints meant that the shorter synthesis of 4-position functionalised prolines was prioritised to allow time for peptide synthesis and analysis. Work was partially carried out towards the synthesis of the 5-position functionalised monomer, compound **8.0**, pictured below.



Compound **1.0** was synthesised by the heating of a solution of diethyl (2R,5R)-2,5-dibromohexanedioate and benzylamine in toluene over 3 days. This reaction proved not to be chemoselective even though enantiopure starting material was used and both *trans* and *cis* products were isolated via FCC (Ethyl acetate: hexane). However, a high yield (81 %) was still achieved even though some product was lost in racemization and this was also successfully scaled up to a 15 g scale. Pig-liver esterase was then used for the asymmetric hydrolysis of the diester, **2.0**, such that the position 2 acid group could be protected to allow for functionalisation of the position-5 functional group while preserving the carboxylic acid required for amide coupling in peptide synthesis. This reaction proved to be successful although with a reduced yield compared to the previous step (57 %), several problems were also encountered on scaling up of the reaction. The larger amount of enzyme used lead to difficulty in the co-solvent's (acetone) ability to dissolve the enzyme in the PBS solution which may have reduced the yield. Also, this led to mixing of the aqueous and organic layers during extraction. To prevent this the solution had to be first filtered through a layer of celite to remove the enzyme before extraction was possible, which may also have contributed to loss of material. The success of the reaction was confirmed by NMR analysis as both the proton and carbon spectra showed splitting of the proline ring peaks after hydrolysis as the molecules loses symmetry. Also, the peaks representative of the ethyl groups was reduced such that the CH<sub>3</sub> peak integrates for 3 H as opposed to 6 H for the starting material (*Appendix A, 1.1-2.2*).

The benzyl group had to first be removed and replaced with a Boc-protecting group before addition of the acid-protecting group. This was done via hydrogenation with Boc<sub>2</sub>O removing the benzyl protecting group and adding the Boc group in situ. After removal of solvent the product was used for the next step with no further purification as the next step also required Boc<sub>2</sub>O therefore residual Boc-anhydride is not a problem. This resulted in an excessive yield (121 %), however removal of the benzyl group was confirmed by <sup>1</sup>H NMR analysis as no aromatic region protons were present.

The DMAP catalysed reaction of the proline carboxylic acid with Boc-anhydride was then used to protect the acid with tert-butyl group which will survive under the hydrolysing conditions to be used to remove the 5-position ester alkyl group. This was carried out overnight under a nitrogen atmosphere and the product was isolated via FCC (ethyl acetate: petroleum ether) giving an orange oil, **8.0**, with a reasonably high yield (75 %). The success of the reaction was confirmed via <sup>1</sup>H NMR analysis which showed the added 9 t-Bu protons. Mass spectrometry also confirmed the correct product had been synthesised. The previous two steps were not attempted at a larger scale due to prioritisation of the alternative monomer synthesis.

### 3. Conclusion

It has been shown that RCM using the Hoveyda-Grubbs 2<sup>nd</sup> generation catalyst is a viable method to form an all-hydrocarbon staple between olefin sidechains on **i,i+3** proline residues. ‘Stapling’ was possible on all the various *cis/trans* isomers, however, the isomers present had a significant impact on the degree of metathesis occurring. The *trans-trans* peptide had almost complete consumption of starting material while the *cis-cis* peptide had a very low degree of metathesis, suggesting that an ideal positioning of olefins is required to favour formation of the staple. Mass-spec analysis showed that four stapled products were produced in every reaction which indicated that two different conformations were being exhibited with E/Z isomerism of both occurring. This suggested that both PolPro1 and PolPro2 stapled peptides were synthesised during metathesis. After both CD and FT-IR analysis it was clearly shown that the staple produced a conformational change from the original PolPro2 starting material in an aqueous environment and that more similarities were shown to the PolPro1 conformation produced in propanol, especially after FT-IR analysis, while still in an aqueous environment. However, differences between the four RCM products were not clearly shown, as the products generally exhibited the PolPro1 band at 1635 cm<sup>-1</sup> under FT-IR analysis [3] and maxima/minima did not vary significantly from each other under CD analysis, however, slight differences between product data was shown suggesting slightly differing conformations. Therefore, it was not possible to identify which products had the desired PolPro1 structure, yet the data collected herein does suggest that constraining staple on a polyproline peptide does produce a clear conformational difference between the stapled and unstapled peptides. This indicates that polyproline can successfully be ‘locked’ into an alternative conformation than what is typically exhibited in an aqueous environment and that this may potentially have a more PolPro1 type structure.

Samples of the RCM products from the *trans-trans* peptide (**17-tc**) and the *cis-trans* peptide (**13-ct**) have also been submitted for DOSY NMR and IM-MS analysis for full characterisation of the four product structures, however, this data is not yet available at the time of submission of this report due to delays from sample queues and raw data analysis.

### 4. Future Plan

As a ‘stapled’ peptide was successfully synthesised, however full characterisation of the conformation was not successful due to different analysis methods not corroborating with the definite polyproline conformations formed, the results are still indicative of a successfully ‘locked’ polyproline and further investigation potentially with a longer peptide, and therefore a

more stabilised PolPro1 structure, may give clearer results. Specifically, under circular dichroism analysis, removing any contention as to the exact 'stapled' products being formed. Further analytical methods are also currently being carried out, DOSY NMR and IM-MS, to allow confirmation of the proposed conclusions from the current data. Also, hydrogenation of the stapled products would allow removal of the E/Z isomerism such that only two products would be visible via HPLC analysis, allowing clearer determination of which product is PolPro1 or PolPro2. The work carried out would allow streamlining of this synthesis such that a larger peptide could be more quickly synthesised and characterised, allowing confirmation of the theory that the PolPro1 structure is not sufficiently stabilised in a 7-unit polyproline peptide for analysis using CD spectroscopy.

Full investigation of the use of a stapled polyproline mimetic, incorporating the analysed linker, in interactions with a protein against an alpha-helical peptide could then be carried out, by completion of the synthesis of the proposed mimetic (*Figure 16*). The interaction of the protein Talin and the target alpha-helical peptide has been fully characterised,<sup>[29] [30]</sup> which would allow a detailed analysis of the binding method and affinity of the mimetic with the protein Talin. More detailed information about the binding of a stapled polyproline mimetic with a protein would allow translation of this information into the development of mimetics for other protein-protein interactions with potential medical applications.

## 5. Experimental

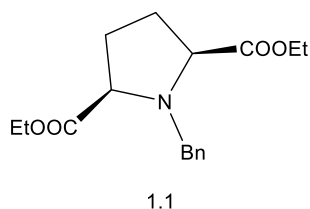
**General Aspects:** Purchased compounds were used as received with no further purification steps unless otherwise specified. Reactions were monitored by thin layer chromatography (TLC) using Merck silica gel 60 aluminium plates. TLC compounds were visualized by UV and vanillin stain. Flash column chromatography (FCC) was performed using ultrapure Silica Gel 60A, particle size 60-200  $\mu\text{m}$ .  $^1\text{H}$  and  $^{13}\text{C}$  were recorded on a Bruker Avance II 400 MHz spectrometer. Chemical shifts are reported in ppm using TMS as a reference. Electrospray ionisation (ESI) mass spectrometry was used for molecular mass measurements. Analytical HPLC was carried out on a Phenomenex Hyper Sil 5 C8 column (50 mm x 2.00 mm, 5 microns). Preparative HPLC was carried out on a Phenomenex Hyper Sil 5 C8 column (50 mm x 2.00 mm, 5 microns). Jasco J-715 spectropolarimeter was used for CD measurements. For FT-IR measurements a Shimadzu IRaffinity-1S Spectrophotometer was used.

**General Protocols for CD-Spectroscopic analysis:** CD spectra were recorded using a spectral bandwidth of 190-260 nm, at 20 °C. CD data are given as mean residual molar ellipticities ( $\text{deg cm}^2 \text{dmol}^{-1}$ ) unless otherwise stated. The spectra are formed of 4 accumulations. A Quartz cell

was used with a 1 mm path length using approximately 100  $\mu$ M peptide solutions. All samples were incubated for at least 6 days.

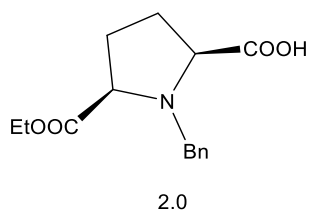
## 5.1 Synthesis of 5-position functionalised proline-monomer

### *Synthesis (scale-up) of diethyl (2R,5S)-1-benzylpyrrolidine-2,5-dicarboxylate (1.1):*



**Diethyl (2R,5R)-2,5-dibromohexanedioate** ( 15 g, 41.7 mmol, 1 eq) was dissolved in toluene (300 ml). **Benzylamine** (14.0 ml, 125.0 mmol, 3 eq) was added with constant stirring and the reaction mixture was heated at 85 °C for 3 days. TLC (4:6, Diethyl ether: Hexane),  $R_f$  0.35, was used to monitor the progress of the reaction. The white/pink crystalline precipitate was filtered off and the orange oil extracted with ethyl acetate (500 ml x 3). The combined organic layers were then washed with aqueous sodium bicarbonate and dried with anhydrous magnesium sulphate before being concentrated under reduced pressure (12.5 g crude yield). FCC was then used to isolate the product. Both *trans* and *cis*-products were recovered separately, with impurities present in the *trans*-product, yielding a yellow oil, **compound 1.1 (10.3 g, 33.8 mmol, 81 % yield)**.  $^1\text{H}$  NMR (400 MHz,  $\text{CDCl}_3$ )  $\delta$  7.33 (dd,  $J = 8.1, 1.4$  Hz, 2H), 7.30 – 7.25 (m, 2H), 7.24 – 7.19 (m, 1H), 4.08 – 3.96 (m, 4H), 3.45 – 3.38 (m, 2H), 2.11 – 2.01 (m, 4H), 1.18 (t,  $J = 7.1$  Hz, 6H).  $^{13}\text{C}$  NMR (101 MHz,  $\text{CDCl}_3$ )  $\delta$  173.54 (s), 137.75 (s), 129.63 (s), 128.14 (s), 127.31 (s), 65.73 (s), 60.68 (s), 57.91 (s), 28.83 (s), 14.27 (s). FT-IR =  $\nu_{\text{max}}/\text{cm}^{-1}$  1186,1249 (C-O), 1724 (C=Os). Mass spectrometry: ESI-MS( $m/z$ ):  $[\text{M-H}]^+$  calcd. for  $\text{C}_{17}\text{H}_{24}\text{NO}_4$ , 306.4; found, 306.2.

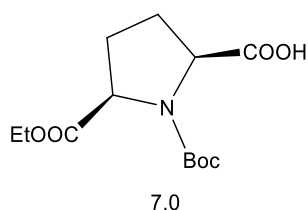
### *Synthesis of (2R,5S)-1-benzyl-5-(ethoxycarbonyl)pyrrolidine-2-carboxylic acid (2.0):*



**Compound 1.0** (1.3091 g, 4.3 mmol, 1 eq) was dissolved in acetone (15 ml) and PBS (125 ml, pH 8). **PLE** (150 mg, 2700 units) was added and the emulsion stirred at 32 °C for 4.5 hours. TLC (6:4, pet ether: ethyl acetate),  $R_f$  0.35 was used to monitor the progress of the reaction. The solution was then acidified to pH 2 with hydrochloric acid (1 M) and extracted with ethyl acetate (200 ml x 3). The combined organic layers were then washed with water and dried with magnesium sulphate before being concentrated under reduced pressure yielding a viscous yellow oil **2.0**

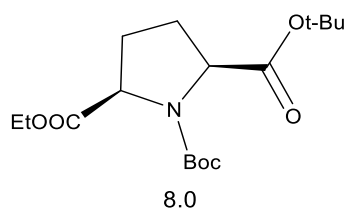
(0.68 g, 2.5 mmol, 57 %).  $^1\text{H}$  and  $^{13}\text{C}$  NMR analysis were carried out on the product.  $^1\text{H}$  NMR (400 MHz,  $\text{CDCl}_3$ )  $\delta$  7.36 – 7.25 (m, 5H), 4.12 – 4.04 (m, 2H), 3.96 – 3.87 (m, 2H), 3.76 – 3.67 (m, 2H), 2.31 – 2.19 (m, 2H), 2.16 – 2.08 (m, 1H), 1.93 – 1.81 (m, 1H), 1.20 (t,  $J = 7.1$  Hz, 3H).  $^{13}\text{C}$  NMR (101 MHz,  $\text{CDCl}_3$ )  $\delta$  174.79 (s), 174.15 (s), 135.60 (s), 129.54 (s), 128.96 (s), 128.47 (s), 67.03 (s), 66.55 (s), 61.93 (s), 59.07 (s), 30.55 (s), 30.32 (s), 14.14 (s).

*Synthesis of (2S,5R)-1-(tert-butoxycarbonyl)-5-(ethoxycarbonyl)pyrrolidine-2-carboxylic acid (7.0):*



Palladium on activated carbon 10 % (251 mg) was placed in a three-neck flask under a nitrogen atmosphere and dissolved in ethyl acetate. **(2S,5R)-1-benzyl-5-(ethoxycarbonyl)pyrrolidine-2-carboxylic acid, compound 2.0** (630 mg, 2.3 mmol, 1 eq), and Boc-anhydride (590 mg, 2.7 mmol, 1.1 eq) were dissolved in methanol (12 ml) and added slowly to the solution with constant stirring. The reaction was then placed under a hydrogen atmosphere for 24 h. The solution was then filtered through celite and concentrated under reduced pressure yielding a yellow oil (0.85 g, 120 %) containing residual Boc-anhydride [1.52 ppm (s, 13H)].  $^1\text{H}$  NMR (400 MHz,  $\text{CDCl}_3$ )  $\delta$  4.63 – 4.27 (m, 4H), 2.45 – 2.24 (m, 2H), 2.15 – 1.99 (m, 2H), 1.45 (s, 9H), 1.37 – 1.31 (m, 3H).

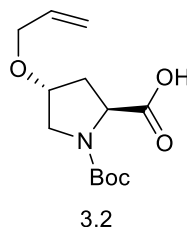
*Synthesis of 1,2-di-tert-butyl 5-ethyl (2S,5R)-pyrrolidine-1,2,5-tricarboxylate (8.0):*



**Compound 7.0** (0.85 g, 3.0 mmol) and Boc-anhydride (1.4033 g, 6.4 mmol, 2.17 eq) were dissolved in dry THF (30 ml). DMAP (0.1362 g, 1.1 mmol, 0.38 eq) was added under a nitrogen atmosphere at rt with constant stirring forming an orange solution. The solution was stirred for 24 h and then acidified with hydrochloric acid (1 M) and extracted with dichloromethane (50 ml x 3). The combined organic layers were then dried with magnesium sulphate and concentrated under reduced pressure to yield an orange oil. FCC (85:15, pet ether: ethyl acetate) was then carried out yielding a yellow/orange oil **8.0** (740 mg, 2.2 mmol, 75 %).  $^1\text{H}$  NMR (400 MHz,  $\text{CDCl}_3$ )  $\delta$  4.33 – 4.03 (m, 4H), 2.06 (m, 4H), 1.39 (d,  $J = 4.3$  Hz, 9H), 1.35 (d,  $J = 7.1$  Hz, 9H), 1.19 (dd,  $J = 15.4, 8.0$  Hz, 3H). Mass spectrometry: ESI-MS( $m/z$ ):[M-Na]<sup>+</sup>calcd.for  $\text{C}_{17}\text{H}_{29}\text{NNaO}_6$ , 366.4; found, 366.1.

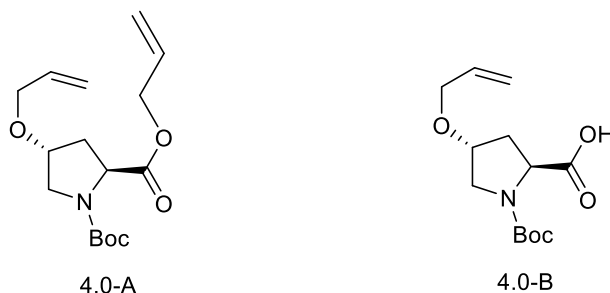
## 5.2 Synthesis of *trans*-4-position functionalised proline monomer

Synthesis (scale-up) of (2*S*,4*R*)-4-(allyloxy)-1-(*tert*-butoxycarbonyl)pyrrolidine-2-carboxylic acid (**3.2**)<sup>[27]</sup>:



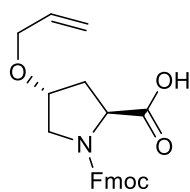
Sodium hydride, 60 % in mineral oil (1.816 g, 54.1 mmol, 2.5 eq) was placed in an oven-dried two-neck flask cooled under a nitrogen atmosphere. A solution of **(2*S*,4*R*)-1-(*tert*-butoxycarbonyl)-4-hydroxypyrrolidine-2-carboxylic acid** (5.013 g, 21.7 mmol, 1 eq) in anhydrous THF (21 ml) and DMSO (2.1 ml) was slowly added at -25 °C with constant stirring, significant gas release occurring throughout addition. The temperature was then raised to 0 °C for 0.5 h. The temperature was then reduced to -25 °C and a solution of allyl bromide (4.67 ml, 54.1 mmol, 2.5 eq) in anhydrous THF (12.6 ml) was added. The solution was then stirred at 25 °C for 22 h. TLC (8:2, ethyl acetate: methanol),  $R_f$  0.3, used to monitor the reaction. The reaction was then acidified with HCl (1 M) and aqueous ammonia to pH 3 and quickly extracted with ethyl acetate (60 ml x 3). The combined organic layers were then washed with brine and aqueous sodium bicarbonate before drying with anhydrous magnesium sulphate. The solution was then concentrated under reduced pressure (4.92 g crude yield). Base-acid extraction was then carried out. The compound was dissolved in sodium hydroxide (1 M) and washed with dichloromethane. The aqueous layer was then acidified at 0 °C to pH 2 with hydrochloric acid (1 M) and extracted with dichloromethane (60 ml x 3). The combined organic layers were then concentrated under reduced pressure yielding a colourless oil **3.2 (3.42 g, 0.5 mmol, 56 %)**.  $^1\text{H}$  and  $^{13}\text{C}$  NMR analysis were carried out on the product.  $^1\text{H}$  NMR (400 MHz,  $\text{CDCl}_3$ )  $\delta$  9.93 (s, 1H), 5.93 – 5.79 (m, 1H), 5.26 (dq,  $J = 17.2, 1.5$  Hz, 1H), 5.18 (dd,  $J = 10.4, 1.2$  Hz, 1H), 4.37 (dt,  $J = 15.7, 7.5$  Hz, 1H), 4.16 – 4.08 (m, 1H), 4.03 – 3.89 (m, 2H), 3.65 – 3.46 (m, 2H), 2.43 – 2.35 (m, 1H), 2.34 – 2.21 (m, 1H), 2.14 – 2.06 (m, 1H), 1.42 (d,  $J = 22.0$  Hz, 9H).  $^{13}\text{C}$  NMR (101 MHz,  $\text{CDCl}_3$ )  $\delta$  178.76 (s), 176.16 (s), 155.87 (s), 153.97 (s), 134.27 (s), 117.55 (d,  $J = 6.9$  Hz), 81.42 (s), 80.84 (s), 76.33 (s), 76.01 (s), 70.24 (d,  $J = 3.7$  Hz), 57.91 (d,  $J = 9.3$  Hz), 52.04 (s), 51.43 (s), 36.69 (s), 34.84 (s), 28.36 (d,  $J = 13.7$  Hz). FT-IR =  $\nu_{\text{max}}/\text{cm}^{-1}$  1670 (C=Os), 1157, 1128 (C-O)

*Synthesis of (2S,4R)-4-(allyloxy)-1-(tert-butoxycarbonyl)pyrrolidine-2-carboxylic acid (4.0-B):*



Sodium hydride, 60 % in mineral oil (431 mg, 10.8 mmol, 2.5 eq) was placed in an oven-dried two-neck flask cooled under a nitrogen atmosphere. A solution of **(2S,4R)-1-(tert-butoxycarbonyl)-4-hydroxypyrrolidine-2-carboxylic acid, 3-sm** (1.0 g, 4.3 mmol, 1 eq) in dry DMF (21 ml) was slowly added at -25 °C with constant stirring, significant gas release occurring throughout addition. The temperature was then raised to 0 °C for 0.5 h. The temperature was then reduced to -25 °C and a solution of allyl bromide (0.93 ml, 10.8 mmol, 2.5 eq) in anhydrous DMF (3 ml) was added. The solution was then stirred at 25 °C for 20 h. TLC (8:2, ethyl acetate: methanol),  $R_f$  0.3 was used to monitor the reaction. The reaction was then acidified with HCl (0.1 M) to pH 2 and quickly extracted with ethyl acetate (60 ml x 3). The combined organic layers were then washed with brine and aqueous sodium bicarbonate before drying with anhydrous magnesium sulphate. The solution was then concentrated under reduced pressure yielding a clear colourless oil **2-allyl 1-(tert-butyl) (2S,4R)-4-(allyloxy)pyrrolidine-1,2-dicarboxylate, 4.0-A** (660 mg, 2.1 mmol, 49 %). The product was then saponified overnight in THF (2 ml), methanol (4 ml) and sodium hydroxide (4 ml, 1 M). The organic solvents were then removed under reduced pressure and the solution then acidified to pH 2 with hydrochloric acid (1 M) and extracted with ethyl acetate (50 ml x 3). Combined organic layers then dried and concentrated under reduced pressure yielding a yellow oily product **4.0-B (0.2749 g, 1.0 mmol, 22 %)**.  $^1\text{H}$  and  $^{13}\text{C}$  NMR analysis were carried out on the product, small amount of DMF still present in the product.  $^1\text{H}$  NMR (400 MHz,  $\text{CDCl}_3$ )  $\delta$  9.65 (s, 1H), 5.81 (ddt,  $J = 17.2, 10.5, 5.5$  Hz, 1H), 5.21 (dq,  $J = 17.2, 1.5$  Hz, 1H), 5.12 (d,  $J = 10.4$  Hz, 1H), 4.30 (dt,  $J = 15.6, 7.5$  Hz, 1H), 4.10 – 4.03 (m, 1H), 3.60 – 3.40 (m, 2H), 2.38 – 2.01 (m, 2H), 1.37 (d,  $J = 18.2$  Hz, 9H).  $^{13}\text{C}$  NMR (101 MHz,  $\text{CDCl}_3$ )  $\delta$  175.47 (s), 175.06 (s), 163.07 (s), 154.63 (s), 153.82 (s), 134.13 (s), 116.82 (d,  $J = 5.5$  Hz), 80.00 (s), 76.31 (s), 75.75 (s), 69.76 (d,  $J = 3.9$  Hz), 57.79 (s), 57.56 (s), 51.66 (s), 51.11 (s), 36.52 (s), 36.27 (s), 35.05 (s), 31.37 (s), 28.00 (d,  $J = 18.3$  Hz). FT-IR =  $\nu_{\text{max}}/\text{cm}^{-1}$  1741 (C=O) 1647 (C=Os).

*Synthesis of (2S,4R)-1-(((9H-fluoren-9-yl)methoxy)carbonyl)-4-(allyloxy)pyrrolidine-2-carboxylic acid (6.0):* [28]

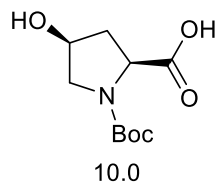


6.0

Trifluoroacetic acid (7.5 ml, 98.0 mmol, 20 eq) was added to **(2S,4R)-4-(allyloxy)-1-(tert-butoxycarbonyl)pyrrolidine-2-carboxylic acid, compound, 3.2** (1.2825 g, 4.5 mmol, 1 eq) in dichloromethane (7.5 ml). The solution was stirred at rt for 90 mins then concentrated under reduced pressure. Sodium bicarbonate (1.161 g, 13.8 mmol, 3 eq) in deionised water (12 ml) and THF (12 ml) were added slowly at 0 °C. Fmoc-Cl (1.2793 g, 4.9 mmol, 1.1 eq) was then added at 0 °C and the solution was stirred for 30 mins. The solution was then stirred for 3 days at rt, forming a cloudy off-white solution. This was then concentrated under reduced pressure with a pink foam forming as the colour leached from the rubber seal on the reaction flask. The product was then partitioned between hydrochloric acid (1 M) and dichloromethane (60 ml x 3). The combined organic layers were then dried with magnesium sulphate and concentrated under reduced pressure yielding a pink oily product. This was then freeze recrystallized with pet ether and diethyl ether yielding pink oily crystals (1.7687 g, 65 %). The product was then dissolved in dichloromethane and activated carbon was added to the solution and stirred for 30 mins. The solution was then filtered through celite and concentrated under reduced pressure to yield orange/off-white crystals **6.0** (1.06 g, 2.7 mmol, 60 %). NMR analysis carried out.  $[\alpha]_D^{20}$  (-38.0) ( $c = 1.002$ , MeOH, 25.5 °C), lit:  $[\alpha]_{D20}^{20}$  (-27.9)  $^1\text{H}$  NMR (400 MHz,  $\text{CDCl}_3$ )  $\delta$  7.74 (dd,  $J = 24.2, 7.5$  Hz, 3H), 7.64 – 7.51 (m, 3H), 7.43 – 7.27 (m, 5H), 5.95 – 5.81 (m, 1H), 5.33 – 5.16 (m, 2H), 4.52 (t,  $J = 7.5$  Hz, 1H), 4.48 – 4.31 (m, 2H), 4.27 (t,  $J = 7.0$  Hz, 1H), 4.19 – 4.09 (m, 1H), 4.02 – 3.90 (m, 2H), 3.78 – 3.58 (m, 2H), 2.48 – 2.10 (m, 2H).  $^{13}\text{C}$  NMR (101 MHz,  $\text{CDCl}_3$ )  $\delta$  177.51 (s), 175.71 (s), 156.10 (s), 154.72 (s), 144.42 (s), 144.11 (s), 143.83 (d,  $J = 6.3$  Hz), 141.63 (s), 141.42 (s), 134.25 (s), 127.89 (s,  $J = 18.3$  Hz), 127.76 (d,  $J = 2.2$  Hz), 127.71 (s), 127.21 (d,  $J = 2.9$  Hz), 125.35 – 124.75 (m), 120.11 (t,  $J = 7.6$  Hz), 117.67 (s), 76.45 (s), 75.83 (s), 70.34 (s), 68.15 (s), 68.00 (d,  $J = 26.8$  Hz), 65.27 (s), 58.24 (s), 57.55 (s), 52.11 (s), 51.88 (s), 50.40 (s), 47.24 (d,  $J = 7.5$  Hz), 36.98 (s), 35.09 (s). FT-IR =  $\nu_{\text{max}}/\text{cm}^{-1}$  3442 (OHbr) 1682 (C=Os) Mass spectrometry: ESI-MS( $m/z$ ):[M-Na] $^{+}$ calcd.for  $\text{C}_{23}\text{H}_{23}\text{NNaO}_5$ , 416.4;found, 416.0.

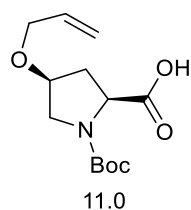
### 5.3 Synthesis of *cis*-4-position functionalised proline monomer

*Synthesis of (2S,4S)-1-(tert-butoxycarbonyl)-4-hydroxypyrrolidine-2-carboxylic acid (10.0):*



**1-(tert-butyl) 2-methyl (2S,4S)-4-hydroxypyrrolidine-1,2-dicarboxylate** (1.5014 g, 6.1 mmol, 1 eq) was dissolved in THF (12 ml) and methanol (12 ml). NaOH (0.32 g, 8.0 mmol, 1.3 eq) was added. Excess NaOH was then added after stirring overnight as the reaction was incomplete. The organic solvents were then removed under reduced pressure forming a yellowish solution. The solution was then acidified to pH 0 with hydrochloric acid forming a colourless solution. This was then extracted with ethyl acetate (50 ml x 3) and the combined organic layers were washed with brine (x 2) and dried with anhydrous MgSO<sub>4</sub>. This was then concentrated under reduced pressure yielding a white crystalline solid **10.0 (1.1959 g, 84 %, 5.2 mmol)**. <sup>1</sup>H NMR (400 MHz, CDCl<sub>3</sub>) δ 4.47 – 4.30 (m, 2H), 3.73 – 3.43 (m, 2H), 2.46 – 2.20 (m, 2H), 1.46 (d, *J* = 17.6 Hz, 9H). FT-IR =  $\nu_{\max}/\text{cm}^{-1}$  1668 (C=O) 3194 (O-Hbr). Mass spectrometry: ESI-MS(*m/z*):[M-Na]<sup>+</sup>+calcd.for C<sub>10</sub>H<sub>17</sub>NNaO<sub>5</sub>, 254.2;found, 254.1.

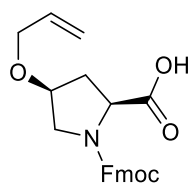
*Synthesis of 11.0, (2S,4S)-4-(allyloxy)-1-(tert-butoxycarbonyl)pyrrolidine-2-carboxylic acid:*



NaH (60 % in mineral oil, 0.3086 g, 12.9 mmol, 2.5 eq) was placed in a flamed dried flask under a N<sub>2</sub> atmosphere. **(2S,4S)-1-(tert-butoxycarbonyl)-4-hydroxypyrrolidine-2-carboxylic acid** (1.1895 g, 5.1 mmol, 1 eq) in dry DMSO (1 ml) and THF (16 ml) was then added at -18°C. The solution was stirred for 30 mins at 0°C. Allyl Bromide (1.5556 g, 1.1 ml, 12.9 mmol, 2.5 eq) in DMSO (0.2 ml) and THF (2.8 ml) was then added at -10°C. The solution was stirred at room temperature overnight, the reaction monitored by TLC (8:2, Pet ether: ethyl acetate), forming a white solid. The product was then acidified to pH 0 with hydrochloric acid, forming a yellow solution, and quickly extracted with ethyl acetate (50 ml x 3) and washed with brine (x 2). The organic layer was then dried with anhydrous and MgSO<sub>4</sub> and concentrated under reduced

pressure to give a yellow oil (0.7702 g). The product was then dissolved in aqueous NaOH (0.1 M) and washed with DCM. The aqueous layer was then acidified with hydrochloric acid and extracted with DCM (50 ml x 3). The DCM extraction layers were then combined and dried, before removing the solvent under reduced pressure to yield a colourless oil **11.0** (**1.1581 g, 4.3 mmol, 83 %**).  $^1\text{H}$  NMR (400 MHz,  $\text{CDCl}_3$ )  $\delta$  9.50 (s, 1H), 5.83 (qd,  $J = 10.4, 5.2$  Hz, 1H), 5.24 (dd,  $J = 17.2, 1.5$  Hz, 1H), 5.15 (ddd,  $J = 10.4, 2.7, 1.3$  Hz, 1H), 4.46 – 4.25 (m, 1H), 4.12 – 4.06 (m, 1H), 4.05 – 3.86 (m, 2H), 3.62 – 3.42 (m, 2H), 2.60 – 2.09 (m, 2H), 1.44 (d,  $J = 19.1$  Hz, 9H).  $^{13}\text{C}$  NMR (101 MHz,  $\text{CDCl}_3$ )  $\delta$  176.59 (s), 174.68 (s), 156.17 (s), 154.10 (s), 134.08 (d,  $J = 26.5$  Hz), 117.58 (s), 81.53 (s), 80.81 (s), 76.27 (s), 75.80 (s), 69.81 (d,  $J = 33.9$  Hz), 69.60 – 69.26 (m), 57.95 (s), 52.93 (s), 51.52 (s), 40.28 (s), 35.85 (s), 33.40 (s), 28.39 (d,  $J = 11.8$  Hz). Mass spectrometry: ESI-MS( $m/z$ ):[M-Na] $^+$ +calcd.for $\text{C}_{13}\text{H}_{21}\text{NNaO}_5$ , 294.3;found, 294.6.

*Synthesis of 12.0, (2S,4S)-1-(((9H-fluoren-9-yl)methoxy)carbonyl)-4-(allyloxy)pyrrolidine-2-carboxylic acid:*



12.0

Trifluoroacetic acid (9.15 ml, 76.1 mmol, 20 eq) was added to **(2S,4S)-4-(allyloxy)-1-(tert-butoxycarbonyl)pyrrolidine-2-carboxylic acid**, compound **11.0** ( 1.0323 g, 3.8 mmol, 1 eq) in dichloromethane (4 ml). The solution was stirred at rt for 90 mins then concentrated under reduced pressure. Sodium bicarbonate (96 mg, 11.4 mmol, 3 eq) in deionised water (15 ml) and THF ( 15 ml) was added slowly at 0 °C. Fmoc-Cl (1.0829 g, 4.2 mmol, 1.1 eq) was then added at 0 °C and the solution was stirred for 30 mins. The solution was then stirred for overnight at rt, forming a cloudy off-white solution. This was then concentrated under reduced pressure. The product was then partitioned between hydrochloric acid (1 M) and dichloromethane (50 ml x 3). The combined organic layers were then dried with anhydrous magnesium sulphate and concentrated under reduced pressure yielding a viscous orange oily product. This was then freeze recrystallized from diethyl ether and hexane, The product was placed under vacuum at 60 °C for 4 hours yielding a white crystalline solid **12.0** with some orange oil present (**1.4607 g, 3.7 mmol, 96 %**).  $[\alpha]_D^{25}$  (-16.0) ( $c = 1.002$ , MeOH, 25.5 °C).  $^1\text{H}$  NMR (400 MHz,  $\text{CDCl}_3$ )  $\delta$  7.80 – 7.69 (m, 2H), 7.64 – 7.53 (m, 2H), 7.44 – 7.27 (m, 4H), 5.92 – 5.76 (m, 1H), 5.27 (d,  $J = 16.9$  Hz, 1H), 5.17 (d,  $J = 10.2$  Hz, 1H), 4.59 – 3.88 (m, 7H), 3.60 (s, 2H), 2.61 – 2.14 (m, 2H).  $^{13}\text{C}$  NMR (101 MHz,  $\text{CDCl}_3$ )  $\delta$  174.01 (s), 156.34 (s), 143.85 (d,  $J = 19.9$  Hz), 141.79 – 141.01 (m), 134.13 (s), 127.91 (s), 127.26 (s), 125.14 (s), 120.12 (s), 117.63 (s), 69.79 (s), 68.15 (s), 58.38 (s), 52.69 (s), 47.30 (s),

33.79 (s). FT-IR =  $\nu_{\max}/\text{cm}^{-1}$  1701 (C=Os) Mass spectrometry: ESI-MS(m/z):[M-H]<sup>+</sup>+calcd.forC<sub>23</sub>H<sub>24</sub>NO<sub>5</sub>, 394.4;found, 394.0.

## 5.4 Synthesis of polyproline peptides

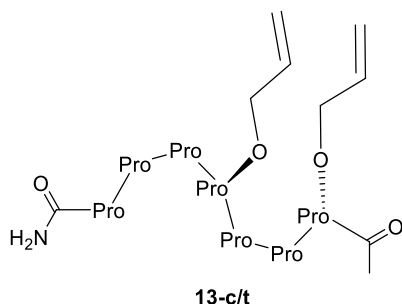
### 5.4.1 General Solid Phase Peptide Synthesis Protocol:

<i>Table 1: General SPPS conditions</i>			
Procedure	Compound	Amount	Time
<b>Resin swelling</b>	DCM	3 ml	20 min
<b>Coupling Mixture</b>	HOBt	2 eq	1.5-2 h
	PyBOP	4 eq	
	DIPEA	4 eq	
	Amino Acid	2 eq	
	DMF	2 ml	
<b>Deprotection Mixture</b>	DMF/Piperidine 20 %	2 ml	40 min
<b>Capping Mixture</b>	Acetic Anhydride	10 eq	1 h
	DIPEA	8 eq	
	DMF	2 ml	
<b>Cleavage Mixture</b>	TFA 95 % in DCM	2 ml	1 h
		2 x 1 ml	30 sec
<b>Wash</b>	DMF	3 x 2 ml	30 sec

The rink amide resin (0.5-1.0 g) was swollen in DCM for 20 mins. It was then washed with DMF (2 ml x 3). DMF/Piperidine (20 %) was then added, to cover resin, with spinning for 40 mins before it was again washed with DMF (2 ml x 3). The coupling mixture [HOBt (2 eq), PyBOP (4 eq), DIPEA (4 eq) and Fmoc-Pro-OH (2 eq) for unfunctionalised residues in DMF] was then sonicated for 5 mins and then added for 1.5-2h with constant stirring. Resin was again washed with DMF (2 ml x 3). The capping mixture was then added [Acetic anhydride (10 eq) and DIPEA (8 eq) in DMF] for 1 hour with stirring. Then washed with DMF (2 ml x 3). The Kaiser test was carried out on a small sample of resin beads to confirm successful capping. The de-protection step through to coupling step were then repeated to add a second residue. The chloranil test was used to confirm the success of the coupling reaction, if unsuccessful, the coupling step was repeated. These steps were then repeated to build the full peptide. After completion of desired the peptide chain DMF/Piperidine (20 %) was added. This was then washed with DMF (2 ml x 3). Then the capping step was repeated. The resin was then washed with DMF (2 ml x 3). The chloranil test was carried out to confirm completed capping. The capped peptide was then cleaved from the resin with TFA (95 % in DCM) for 1h. The resin was then washed with the cleavage cocktail (1 ml x 2) and TFA removed under reduced pressure. The product was then dissolved in cold diethyl ether and centrifuged. The solution was then decanted and the solid re-

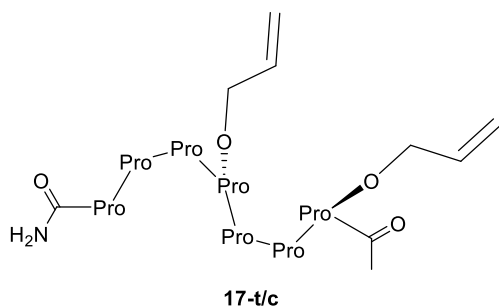
dissolved in diethyl ether and again centrifuged to isolate the solid peptide after drying. Reverse-phase HPLC was then used to confirm isolation of the peptide.

#### Synthesis of 13-Pro7-C/T:



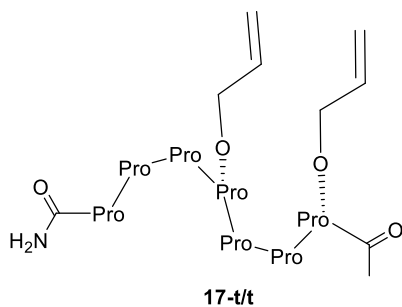
Synthesised using general solid-phase peptide synthesis protocol. The 4<sup>th</sup> and 7<sup>th</sup> couplings utilised previously synthesised Fmoc-Pro-OCH<sub>2</sub>CHCH<sub>2</sub> monomers, *cis* (**12.0**) and *trans* (**6.0**) respectively. *m/z* 851.47 (C<sub>43</sub>H<sub>62</sub>N<sub>8</sub>O<sub>10</sub>)

#### Synthesis of 17-Pro7-T/C:



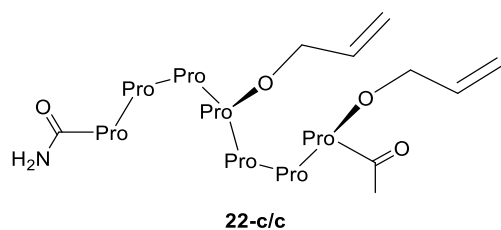
Synthesised using general solid-phase peptide synthesis protocol. The 4<sup>th</sup> and 7<sup>th</sup> couplings utilised previously synthesised Fmoc-Pro-OCH<sub>2</sub>CHCH<sub>2</sub> monomers, *trans* and *cis* respectively. *m/z* 851.47 (C<sub>43</sub>H<sub>62</sub>N<sub>8</sub>O<sub>10</sub>)

#### Synthesis of 17-Pro7-T/T:



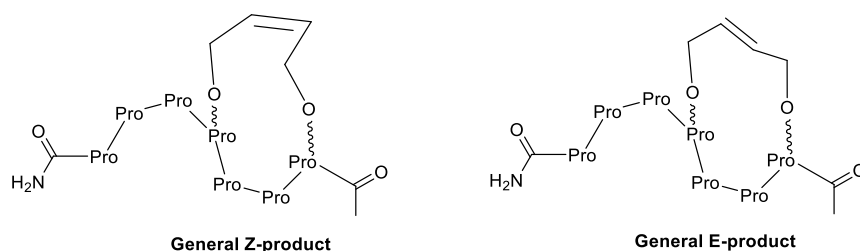
Synthesised using general solid-phase peptide synthesis protocol. The 4<sup>th</sup> and 7<sup>th</sup> couplings utilised previously synthesised *trans*-Fmoc-Pro-OCH<sub>2</sub>CHCH<sub>2</sub>. *m/z* 851.47 (C<sub>43</sub>H<sub>62</sub>N<sub>8</sub>O<sub>10</sub>)

### Synthesis of 22-Pro7-C/C:



Synthesised using general solid-phase peptide synthesis protocol. The 4<sup>th</sup> and 7<sup>th</sup> couplings utilised previously synthesised *cis*-Fmoc-Pro-OCH<sub>2</sub>CHCH<sub>2</sub>.  $m/z$  851.47 (C<sub>43</sub>H<sub>62</sub>N<sub>8</sub>O<sub>10</sub>)

### 5.4.2 Ring-closing Metathesis Reactions:



All reactions were carried out under a N<sub>2</sub> atmosphere and in dry solvents. The peptides (7-20 mg) were dissolved in the relevant dry solvent (*table 2 + 3*) under a nitrogen atmosphere with a magnetic stirrer before addition of catalyst (~5-10 %) dissolved in minimal amount of same solvent. Reactions were then left stirring overnight before removal of solvent under reduced pressure, analysis and isolation were carried out via reverse-phase HPLC. All Hoveyda-Grubb's 2<sup>nd</sup> Generation reactions in THF and DCM produced four products with the same  $m/z$  showing successful stapling had occurred to varying degrees. Minimal metathesis was observed in reactions carried out in propanol as well as for those using 3<sup>rd</sup> generation Grubb's catalyst. ESI used for mass analysis. Stapled products:  $m/z$  823.44 (C<sub>41</sub>H<sub>58</sub>N<sub>8</sub>O<sub>10</sub>)

*Table 2: Hoveyda Grubbs 2<sup>nd</sup> Gen. catalyst RCM reaction conditions*

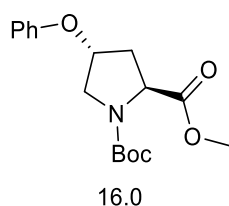
Olefin Confo.	Trans/Cis			Cis/Trans			Trans/Trans			Cis/Cis		
	Prop	DCM	THF	Prop	DCM	THF	Prop	DCM	THF	Prop	DCM	THF
Peptide / mg	15.0	19.7	16.7	9.6	7.0	10.3	14.0	15.1	14.5	15.2	16.0	14.9
Catalyst / %	6.0	7.5	5.0	10.0	6.0	12.5	10.0	7.5	8.0	6.0	10.0	6.0
Volume / ml	0.1	0.2	0.2	0.3	0.3	0.4	0.2	0.2	0.2	0.2	0.2	0.2
Major Product <i>m/z</i>	-	823. 44	823. 44	-	823. 44	823. 44	-	823. 44	823. 44	-	823. 44	823. 44

*Table 3: 3<sup>rd</sup> Generation Grubbs catalyst. RCM reaction conditions*

Olefin Confo.	Trans/Cis		
	Prop	DCM	THF
Peptide / mg	15.1	15.1	15.0
Catalyst / %	8.5	5.0	7.5
Volume / ml	0.2	0.3	0.3

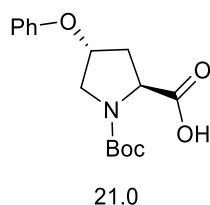
## 5.5 Mimetic-peptide specific monomers synthesis

### Synthesis of 16.0, 1-(tert-butyl) 2-methyl (2S,4R)-4-phenoxyproline-1,2-dicarboxylate:



DEAD ( 6.2 mmol, 0.975 ml, 1.5 eq) added to PPH<sub>3</sub> ( 6.2 mmol, 1.6215 g, 1.5 eq) , **1-(tert-butyl) 2-methyl (2S,4S)-4-hydroxyproline-1,2-dicarboxylate** ( 1.0 g, 4.1215 mmol, 1 eq) and phenol ( 0.5818 g, 6.2 mmol, 1.5 eq) in dry THF (16 ml) at 0°C. Stirred overnight at rt. The reaction was monitored via TLC (7:3, pet ether: ethyl acetate). Solvents were then removed under vacuum to afford an orange slurry/oil. This was then placed in diethyl ether and the white solid precipitate was filtered off. The ether solution was then dried under reduced pressure to yield a crude orange oil (4.4401 g). FCC was then used to purify the product (0.759 g) however this was repeated (0.6117 g) due to residual impurities. <sup>1</sup>H NMR analysis showed the presence of contaminants between 0-1 ppm from the solvent used. The product was dissolved in DCM and activated carbon was added and the solution stirred for 2 h. The solution was then filtered and concentrated under reduced pressure to yield a colourless oil, **16.0 (0.5061 g, 1.5 mmol, 36 %)**. <sup>1</sup>H NMR (400 MHz, CDCl<sub>3</sub>) δ 7.33 – 7.26 (m, 2H), 6.98 (q, *J* = 7.2 Hz, 1H), 6.88 – 6.83 (m, 2H), 4.95 – 4.88 (m, 1H), 4.46 (dt, *J* = 29.8, 7.9 Hz, 1H), 3.84 – 3.65 (m, 5H), 2.60 – 2.48 (m, 1H), 2.22 (ddd, *J* = 13.4, 6.7, 3.8 Hz, 1H), 1.43 (d, *J* = 11.3 Hz, 9H). <sup>13</sup>C NMR (101 MHz, CDCl<sub>3</sub>) δ 173.61 (s), 156.96 (s), 129.80 (s), 121.59 (s), 115.69 (d, *J* = 4.9 Hz), 80.57 (s), 77.36 (s), 75.40 (s), 74.68 (s), 58.15 (s), 57.74 (s), 52.51 (s), 52.28 (s), 52.05 (s), 36.71 (s), 35.76 (s), 28.43 (d, *J* = 11.3 Hz). FT-IR = ν<sub>max</sub>/cm<sup>-1</sup> 1749 (C=Os) 1697 (C=Os)

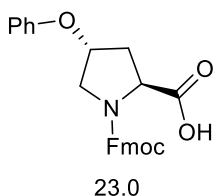
### Synthesis of 21.0, (2S, 4R)-1-(tert-butoxycarbonyl)-4-phenoxyproline-2-carboxylic acid:



**Compound 16.0** (0.5003 g, 1.6 mmol, 1 eq) dissolved in THF (4 ml) and MeOH (4 ml). aq 1 M NaOH (1.8 ml, 1.1 eq) added, forming a yellow solution. This was then stirred for 3 days before removing organic solvents under reduced pressure. Oily product was then acidified to pH 0 with 3 M HCl and quickly extracted with EtOAc (40 ml x 3). The combined organic layers were then

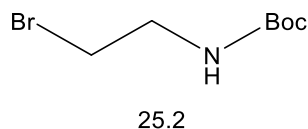
washed with brine (x 2) and dried with anhydrous MgSO<sub>4</sub>. This was then concentrated under vacuo to yield a viscous yellow oil (0.34 g, 71 %). This impure product was dissolved in NaOH 1 M and washed with DCM (20 ml x 2). Then acidified to pH 0-2 with 3 M HCl and extracted with DCM (40 ml x 3). The combined organic layers were then washed with brine (x 2), dried with anhydrous MgSO<sub>4</sub> and concentrated under vacuo to yield a white crystalline product, **21.0** (**0.33 g, 1.1 mmol, 67 %**).  $[\alpha]_D = -37.5^\circ$  (c = 0.5, CDCl<sub>3</sub>, 26 °C) <sup>1</sup>H NMR (400 MHz, CDCl<sub>3</sub>) δ 7.29 (dd, *J* = 15.2, 7.5 Hz, 2H), 6.99 (dd, *J* = 15.2, 7.6 Hz, 1H), 6.87 (d, *J* = 7.8 Hz, 2H), 4.94 – 4.88 (m, 1H), 4.51 (dt, *J* = 43.4, 7.8 Hz, 1H), 3.86 – 3.63 (m, 2H), 2.66 – 2.24 (m, 2H), 1.46 (d, *J* = 13.7 Hz, 9H). <sup>13</sup>C NMR (101 MHz, CDCl<sub>3</sub>) δ 178.30 (s), 174.30 (s), 156.95 (s), 129.86 (s), 121.78 (d, *J* = 13.3 Hz), 115.82 (d, *J* = 15.4 Hz), 82.37 (s), 81.06 (s), 74.83 (d, *J* = 21.0 Hz), 58.12 (d, *J* = 21.4 Hz), 52.36 (s), 52.07 (s), 36.69 (s), 34.50 (s), 28.42 (d, *J* = 7.3 Hz).

*Synthesis of 23.0, 1-((9H-fluoren-9-yl)methyl) 2-methyl (2S,4R)-4-phenoxyproline-1,2-dicarboxylate:*



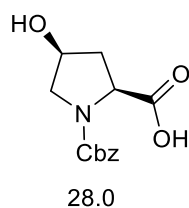
**Compound 21** (0.33 g, 1.1 mmol, 1 eq) dissolved in DCM (1.5 ml) and TFA (20 eq, 21.5 mmol, 2.4485 g, 1.64 ml), the solution was then stirred at rt for 90 mins. Excess TFA was then removed under vacuo. NaHCO<sub>3</sub> (0.2706 g, 3.2 mmol, 3 eq) in THF (8 ml) and H<sub>2</sub>O (8 ml) was then added at 0 °C. Fmoc-Cl (1.1 eq, 1.2 mmol, 0.3056 g) added at 0 °C forming a cloudy white solution. This was then stirred overnight forming a clear solution. THF was then removed under reduced pressure before acidifying to pH 0-2 with 3 M HCl, which caused a white precipitate to form. This was then extracted with DCM (50 ml x 3). The combined organic layers were then washed with brine (x 2) and dried with anhydrous MgSO<sub>4</sub>, before being concentrated under vacuo to yield a white crystalline solid, **23.0** (**0.42 g, 1.0 mmol, 91 %**). <sup>1</sup>H NMR (400 MHz, CDCl<sub>3</sub>) δ 7.83 – 6.83 (m, 13H), 4.70 – 3.73 (m, 8H), 2.71 – 2.27 (m, 2H). <sup>13</sup>C NMR (101 MHz, CDCl<sub>3</sub>) δ 156.60 (s), 143.54 (s), 141.29 (s), 129.80 (d, *J* = 11.8 Hz), 127.73 (d, *J* = 17.8 Hz), 127.13 (s), 125.05 (s), 121.76 (s), 120.06 (t, *J* = 6.6 Hz), 115.54 (d, *J* = 5.1 Hz), 74.78 (s), 68.33 (s), 58.30 (s), 52.14 (s), 46.98 (s), 34.88 (s). FT-IR =  $\nu_{\max}/\text{cm}^{-1}$  1701 (C=O)s 1232, 1170, 1126 (C-O). Mass spectrometry: ESI-MS(*m/z*):[M-Na]<sup>+</sup>+calcd.for C<sub>26</sub>H<sub>23</sub>NNaO<sub>5</sub>, 452.5;found, 452.0.

*Synthesis of 25.2, tert-butyl (2-bromoethyl)carbamate:*



A flame dried 100 ml flask was charged with Boc<sub>2</sub>O (1.2157 g, 5.6 mmol, 1 eq) in dry DCM (24 ml). **2-bromoethylamine hydrobromide** (1.11 eq, 6.2 mmol, 1.2669 g) was added in one portion at 0 °C. TEA (1.5 eq, 8.4 mmol, 0.8455 g, 1.10 ml) was added dropwise over 10 mins at 0 °C. The solution was then stirred for 2 days at rt. The solution was then diluted with DCM (150 ml) and washed with sat. aq. NH<sub>4</sub>Cl (x 2, 10 ml), sat. aq. NaHCO<sub>3</sub> (x 2, 20 ml) and brine (x3, 20 ml). The combined DCM layers were then dried over anhydrous MgSO<sub>4</sub> and filtered before concentrating under vacuo to yield a colourless oil, **25.2 (1.152 g, 5.1 mmol, 91 %)**. <sup>1</sup>H NMR (400 MHz, CDCl<sub>3</sub>) δ 5.15 (s, 1H), 3.49 – 3.35 (m, 4H), 1.37 (s, 9H). <sup>13</sup>C NMR (101 MHz, CDCl<sub>3</sub>) δ 155.66 (s), 146.68 (s), 85.17 (s), 79.67 (s), 42.32 (s), 32.62 (s), 28.32 (s), 27.36 (s). Mass spectrometry: ESI-MS(m/z): [M-Na]<sup>+</sup>+calcd.forC<sub>7</sub>H<sub>14</sub>BrNNaO<sub>2</sub>, 247.1;found, 247.9.

*Synthesis of 28.0-B, (2S,4S)-1-((benzyloxy)carbonyl)-4-hydroxypyrrolidine-2-carboxylic acid:*



**(2S,4S)-1-(tert-butoxycarbonyl)-4-hydroxypyrrolidine-2-carboxylic acid** (0.2709 g, 1.2 mmol, 1 eq) was dissolved in DCM (2 ml). TFA (20 eq, 23.4 mmol, 2.82 ml) was added, this was then stirred for 90 mins at rt. The solution was then concentrated under vacuo to yield (2S,4S)-4-hydroxypyrrolidine-2-carboxylic acid as an oil. NaHCO<sub>3</sub> (2.5 eq, 2.9 mmol, 246 mg) in H<sub>2</sub>O (5 ml) was then added to the oily product. A solution of benzylchloroformate (1.15 eq, 1.3 mmol, 0.2298 g) in toluene (0.5 ml) was added dropwise to the stirred solution. This was then stirred at rt for 24 hrs. The aqueous layer was then separated and washed with diethyl ether (x 4). This was then acidified to pH 0 with 4 N HCl before extracting with DCM (50 ml x 3). The combined DCM layers were then dried over anhydrous MgSO<sub>4</sub>, this was then filtered and concentrated under vacuo to yield a viscous oil, **28.0 (0.2106 g, 0.8 mmol, 70 %)**. <sup>1</sup>H NMR (400 MHz, CDCl<sub>3</sub>) δ 7.41 – 7.28 (m, 5H), 5.14 (p, *J* = 12.3 Hz 3H), 4.52 – 4.36 (m, 2H), 3.74 – 3.51 (m, 2H), 2.39 – 2.19 (m, 2H). <sup>13</sup>C NMR (101 MHz, CDCl<sub>3</sub>) δ 176.16 (s), 175.73 (s), 156.15 (s), 155.10 (s), 136.20 (d, *J* = 18.0 Hz), 128.66 (d, *J* = 8.9 Hz), 128.30 (d, *J* = 22.8 Hz), 127.96 (s), 127.19 (s), 70.87 (s), 69.98 (s),

67.98 (s), 67.70 (s), 65.48 (s), 58.39 (s), 57.92 (s), 55.53 (s), 53.56 (s), 38.76 (s), 37.49 (s), 29.84 (s). FT-IR =  $\nu_{\max}/\text{cm}^{-1}$  1670 (C=Os)

## 6. Acknowledgements

I would like to thank Dr. Aniello Palma for his supervision and support. I would also like to thank Athina Fotopoulou and Dr Kevin Howland for MS data.

## References

- [1] **Michael Kümin, Louis-Sebastian Sonntag, Helma Wennemers**, "Azidoproline Containing Helices: Stabilization of the Polyproline II Structure by a Functionalizable Group," *Journal of American Chemical Society*, vol. 129, no. 3, pp. 466-467, 2007.
- [2] **Eric Beausoleil, William Lubell**, "An examination of the steric effects of 5-tert-butylproline on the conformation of polyproline and the cooperative nature of type II to type I helical interconversion," *Biopolymers*, vol. 53, no. 3, pp. 249-256, 2000.
- [3] **Sachiro Kakinoki, Yoshiaki Hirano, and Masahito Oka**, "On the Stability of Polyproline-I and II Structures of Proline Oligopeptides," *Polymer Bulletin*, vol. 53, pp. 109-115, 2005.
- [4] **Liuqing Shi, Alison E. Holliday, Matthew S. Glover, Michael A. Ewing, David H. Russell, David E. Clemmer**, "Ion Mobility-Mass Spectrometry Reveals the Energetics of Intermediates that Guide Polyproline Folding," *Journal for the American Society for Mass Spectrometry*, vol. 27, no. 1, pp. 22-30, 2016.
- [5] **Liuqing Shi, Alison E. Holliday, Neelam Khanal, David H. Russell, and David E. Clemmer**, "Configurational-Coupled Protonation of Polyproline-7," *Journal of the American Chemical Society*, vol. 137, no. 37, pp. 8680-8683, 2015.
- [6] **Rina K Dukorm, Timothy A keiderling**, "Reassessment of the random coil conformation: Vibrational CD study of proline oligopeptides and related polypeptides," *Biopolymers*, vol. 31, no. 14, pp. 1747-1761, 1991.
- [7] **Christopher H. Douse, Sabrina J. Maas, Jemima C. Thomas, James A. Garnett, Yunyun Sun, Ernesto Cota, and Edward W. Tate**, "Crystal Structures of Stapled and Hydrogen Bond Surrogate Peptides Targeting a Fully Buried Protein-Helix Interaction," *ACS Chemical Biology*, vol. 9, pp. 2204-2209, 2014.
- [8] **Peter S. Kutchukian, Jae Shick Yang, Gregory L. Verdine, and Eugene I. Shakhnovich**, "All-Atom Model for Stabilization of  $\alpha$ -Helical Structure in Peptides by Hydrocarbon Staples," *JACS*, vol. 131, no. 13, pp. 4622-4627, 2009.
- [9] **Loren D. Walensky and Gregory H. Bird**, "Hydrocarbon-Stapled Peptides: Principles, Practice, and Progress," *Journal of Medicinal Chemistry*, vol. 57, no. 15, pp. 6275-6288, 2014.
- [10] **Yugong Cheng, Tanguy LeGall, Christopher J. Oldfield, James P. Mueller**, "Rational drug design via intrinsically disordered proteins," *TRENDS in biotechnology*, vol. 24, no. 10, pp. 435-442, 2006.
- [11] **Agnieszka Gembarska, Flavie Luciani, Clare Fedele, Elisabeth A Russell, Michael Dewaele, Stéphanie Villar, Aleksandra Zwolinska, Sue Haupt, Job de Lange, Dana Yip, James Goydos, Jody J Haigh, Ygal Haupt, Lionel Larue, Aart Jochemsen and Hubing Shi**,

- "MDM4 is a key therapeutic target in cutaneous melanoma," *Nature Medicine*, vol. 18, pp. 1239-1247, 2012.
- [12] **Yong S. Chang, Bradford Graves, Vincent Guerlavais, Christian Tovar, Kathryn Packman, Kwong-Him To, Karen A. Olson, Kamala Kesavan, Pranoti Gangurde, Aditi Mukherjee, Theresa Baker, Krzysztof Darlak, Carl Elkin, Zoran Filipovic, Farooq Z. Qureshi, Honglia,** "Stapled  $\alpha$ -helical peptide drug development: A potent dual inhibitor of MDM2 and MDMX for p53-dependent cancer therapy," *Proceedings of the National Academy of Sciences*, vol. 110, no. 36, pp. 3445-3454, 2013.
- [13] **Koki Sakagami, Toshihiro Masuda, Kenichi Kawano, and Shiroh Futaki,** "Importance of Net Hydrophobicity in the Cellular Uptake of All-Hydrocarbon Stapled Peptides," *Molecular Pharmaceutics*, vol. 15, no. 3, pp. 1332-13340, 2018.
- [14] **Gregory H Bird, Emanuele Mazzola, Kwadwo Opoku-Nsiah, Margaret A Lammert, Marina Godes, Donna S Neuberger & Loren D Walensky,** "Biophysical determinants for cellular uptake of hydrocarbon-stapled peptide helices," *Nature Chemical Biology*, vol. 12, pp. 845-852, 2016.
- [15] **Laura Henchey, Andrea Jochim, Paramjit Arora,** "Contemporary Strategies for the Stabilization of Peptides in the  $\alpha$ -Helical Conformation," *Current Opinion in Chemical Biology*, vol. 12, no. 6, pp. 692-697, 2008.
- [16] **Qian Chu, Raymond E. Moellering, Gerard J. Hilinski, Young-Woo Kim, Tom N. Grossmann, Johannes T.-H. Yeh and Gregory L. Verdine,** "Towards understanding cell penetration by stapled peptides," *MedChemComm*, vol. 6, no. 1, pp. 111-119, 2015.
- [17] **Tzu-Lin Sun, Yen Sun, Chang-Chun Lee, and Huey W. Huang,** "Membrane Permeability of Hydrocarbon-Cross-Linked Peptides," *Biophysical Journal*, vol. 104, no. 9, pp. 1923-1932, 2013.
- [18] **Christian E. Schafmeister, Julia Po, and Gregory L. Verdine,** "An All-Hydrocarbon Cross-Linking System for Enhancing the Helicity and Metabolic Stability of Peptides," *Journal of the American Chemical Society*, vol. 122, no. 24, pp. 5891-5892, 2000.
- [19] **Young-Woo Kim, Tom N Grossmann, Gregory L Verdine,** "Synthesis of all-hydrocarbon stapled  $\alpha$ -helical peptides by ring-closing olefin metathesis," *Nature Protocols*, vol. 6, no. 6, pp. 761-771, 2011.
- [20] **Helen E. Blackwell and Robert H Grubbs,** "Highly Efficient Synthesis of Covalently Cross-Linked Peptide Helices by Ring-Closing Metathesis," *Angew. Chem. Int. Ed.*, vol. 37, no. 23, pp. 3281-3284, 1998.
- [21] **Daniel Burtcher, Karol Grela,** "Aqueous Olefin Metathesis," *Angewandte Chemie International Edition*, vol. 48, no. 3, pp. 442-454, 2008.
- [22] **Jennifer M Bates, Justin A M Lummiss, Gwendolyn A. Bailey, and Deryn E. Fogg,** "Operation of the Boomerang Mechanism in Olefin Metathesis Reactions Promoted by the Second-Generation Hoveyda Catalyst," *American Chemical Society*, vol. 4, no. 7, pp. 2387-2394, 2014.
- [23] **Jennifer A Love, John P Morgan, Tina M Trnka, Robert H Grubbs,** "A Practical and Highly Active Ruthenium-Based Catalyst that Effects the Cross Metathesis of Acrylonitrile," *Angewandte Chemie International Edition*, vol. 41, no. 21, pp. 4035-4037, 2002.
- [24] **Wen-Hsiu Tseng, Meng-Che Li, Jia-Cherng Horng, Sheng-kai Wang,** "Strategy and effect of polyproline peptide stapling by copper(I) catalyzed alkyne-azide cycloaddition reaction," *CHEMBIOCHEM*, vol. 20, pp. 153-158, 2019.
- [25] **Brian C. Bohrer, Samuel I. Merenbloom, Stormy L. Koeniger, Amy E. Hilderbrand, and David E. Clemmer,** "Biomolecule Analysis by Ion Mobility Spectrometry," *Annual Review of Analytical Chemistry*, vol. 1, p. 2008, 293-327.
- [26] **Liuqing Shi, Alison E. Holliday, Huilin Shi, Feifei Zhu, Michael A. Ewing, David H. Russell,**

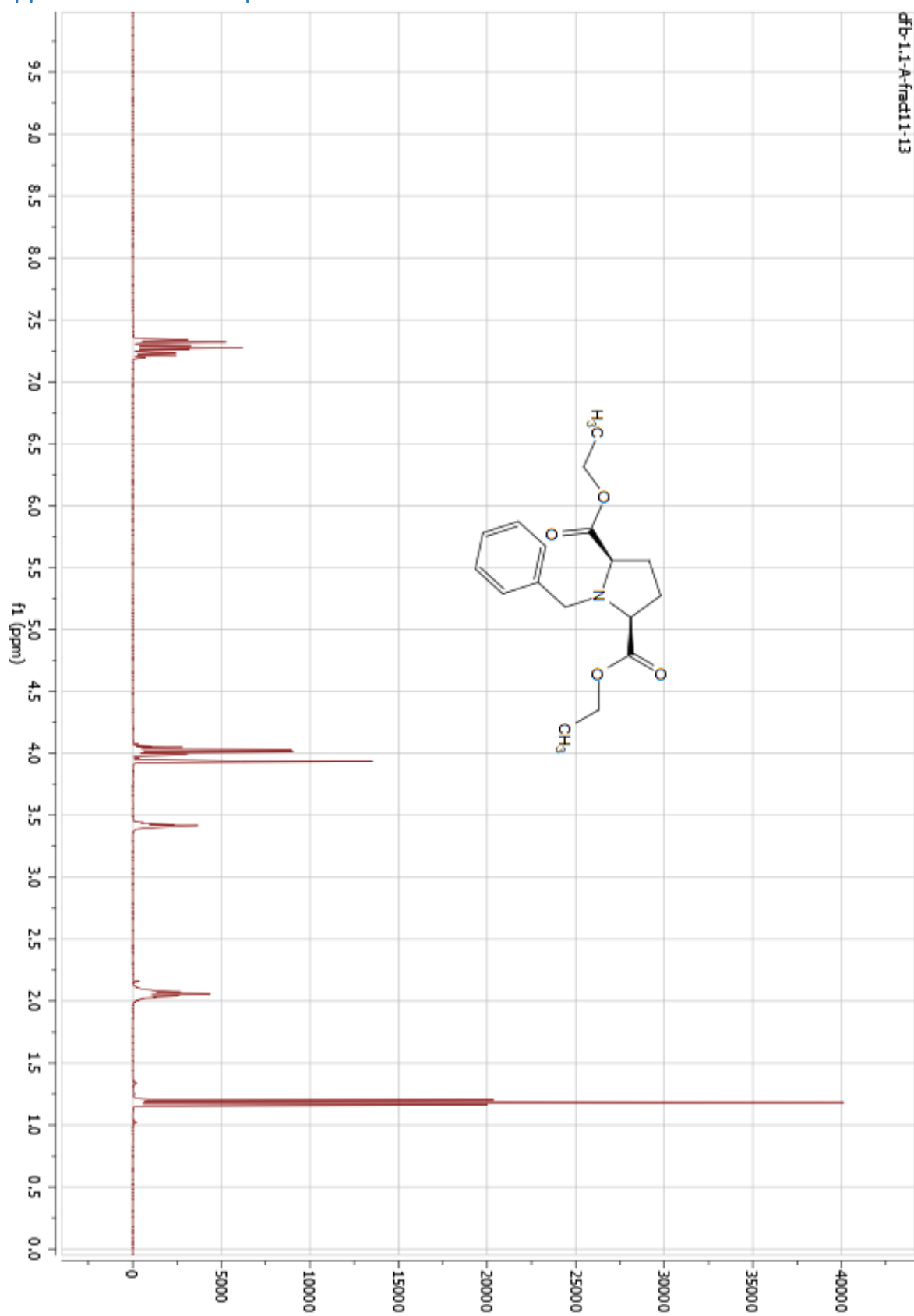
- David E. Clemmer**, "Characterizing Intermediates Along the Transition from Polyproline I to Polyproline II Using Ion Mobility Spectrometry-Mass Spectrometry," *Journal of the American Chemical Society*, vol. 136, no. 36, pp. 12702-12711, 2014.
- [27] **Voichita Mihali, Francesca Foschi, Michele Penso, and Gianluca Pozzi**, "Chemoselective Synthesis of N-Protected Alkoxyprolines under Specific Solvation Conditions," *Journal of Organic Chemistry*, vol. 24, pp. 5351-5355, 2014.
- [28] **Carsten Peters, Markus Bacher, Christoph L. Buenemann, Franz Kricek, Jean-Michel Rondeau, and Klaus Weigand**, "Conformationally Constrained Mimic of the Membrane-Proximal Domain of FceRIa," *ChemBioChem*, vol. 8, pp. 1785-1789, 2007.
- [29] **Paul R. Elliott, Benjamin T. Goult, Petra M. Kopp, Neil Bate, J. Gunter Grossmann, Gordon C.K. Roberts, David R. Critchley and Igor L. Barsukov**, "The Structure of the Talin Head Reveals a Novel Extended Conformation of the FERM Domain," *Structure*, vol. 18, no. 10, pp. 1289-1299, 2010.
- [30] **Benjamin T. Goult, Jie Yan, and Martin A. Schwartz**, "Talin as a mechanosensitive signaling hub," *Journal of Cell Biology*, vol. 217, no. 11, p. 3776, 2018.
- [31] **Richard Mimna, Gabriele Tuchscherer, Manfred Mutter**, "Toward the Design of Highly Efficient, Readily Accessible Peptide N-caps for the Induction of Helical Conformations," *IJPRT*, vol. 13, no. 1-2, pp. 237-244, 2007.
- [32] **K. M. Engle, L. Pfeifer, G. W. Pidgeon, G. T. Giuffredi, A. L. Thompson, R. S. Paton, J. M. Brown and V. Gouverneur**, "Coordination diversity in hydrogen-bonded homoleptic fluoride-alcohol complexes modulates reactivity," *Chemical Science*, vol. 6, no. 9, pp. 5293-5302, 2015.
- [33] **Nicolas Pétry, Hafid Benakki, Eric Clot, Pascal Retailleau, Farhate Guenoun, Fatima Asserar, Chakib Sekkat, Thomas-Xavier Métro, Jean Martinez, Frédéric Lamaty**, "A mechanochemical approach to access the proline-proline diketopiperazine framework," *Bellstein Journal of Organic Chemistry*, vol. 13, pp. 2169-2178, 2017.
- [34] **Altmann Eva et al**, "Indole compounds or analogs thereof as complement factor D inhibitors useful for the treatment of age-related macular degeneration and their preparation," *From PCT Int. Appl.*, Vols. 2012093101,, 12 July 2012.
- [35] **K.Takeda, A.Akiyama, H.Nakamura, S.I.Takizawa, Y.Mizuno, H. Takayanagi, Y.Harigaya**, "Dicarbonates: Convenient 4-DMAP catalysed esterification reagents," *ChemInform*, vol. 26, no. 9, pp. 1063-1066, 1994.
- [36] **Raines, Jia-Cherng Horng and Ronald T**, "Stereo-electronic effects on polyproline conformation," *Protein Science*, vol. 5, pp. 74-75, 2005.
- [37] **Aimee L. Boyle**, "3 - Applications of de novo designed peptides," *Peptide Applications in Biomedicine, Biotechnology and Bioengineering*, pp. 51-86, 2018.

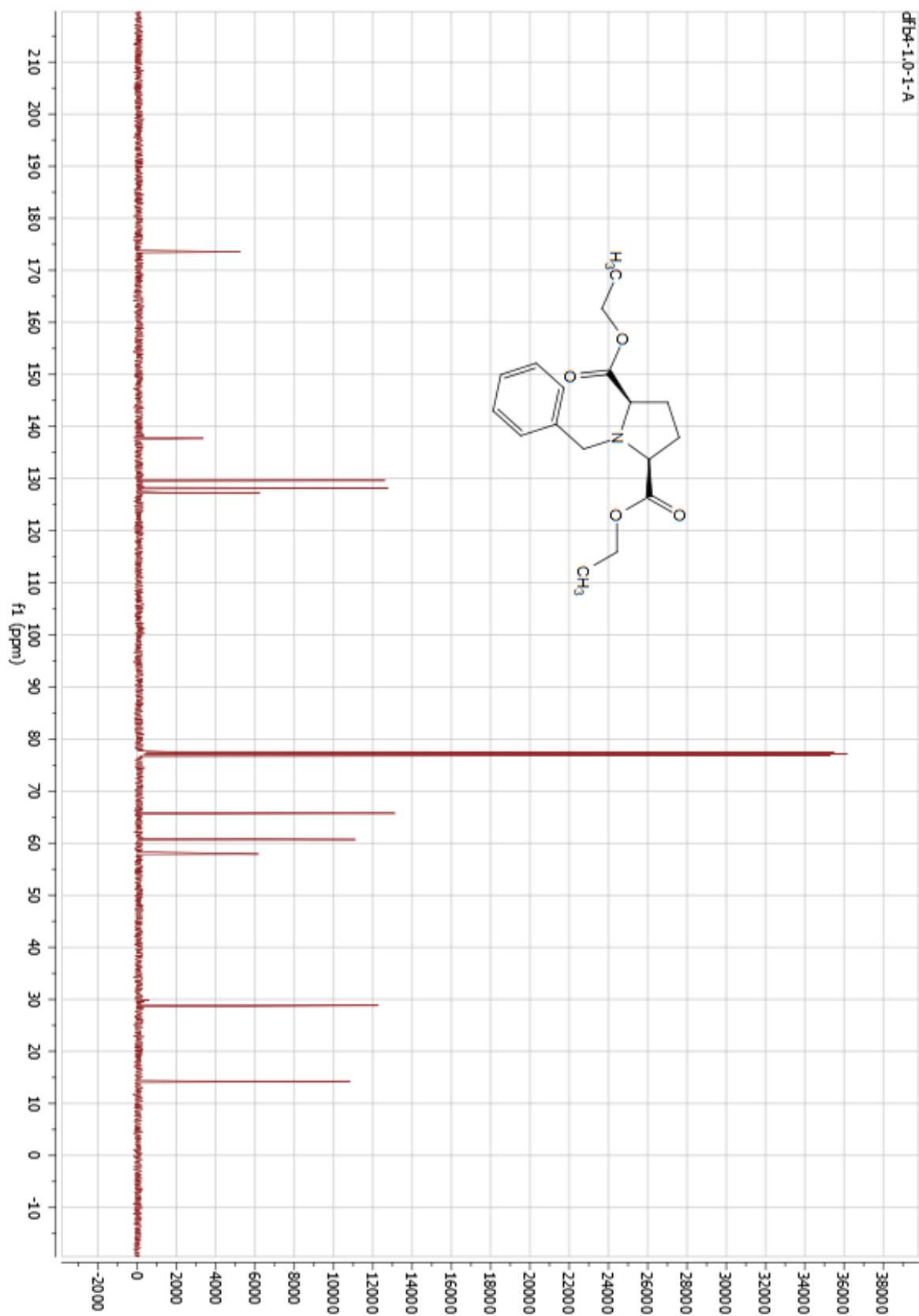
## Appendices

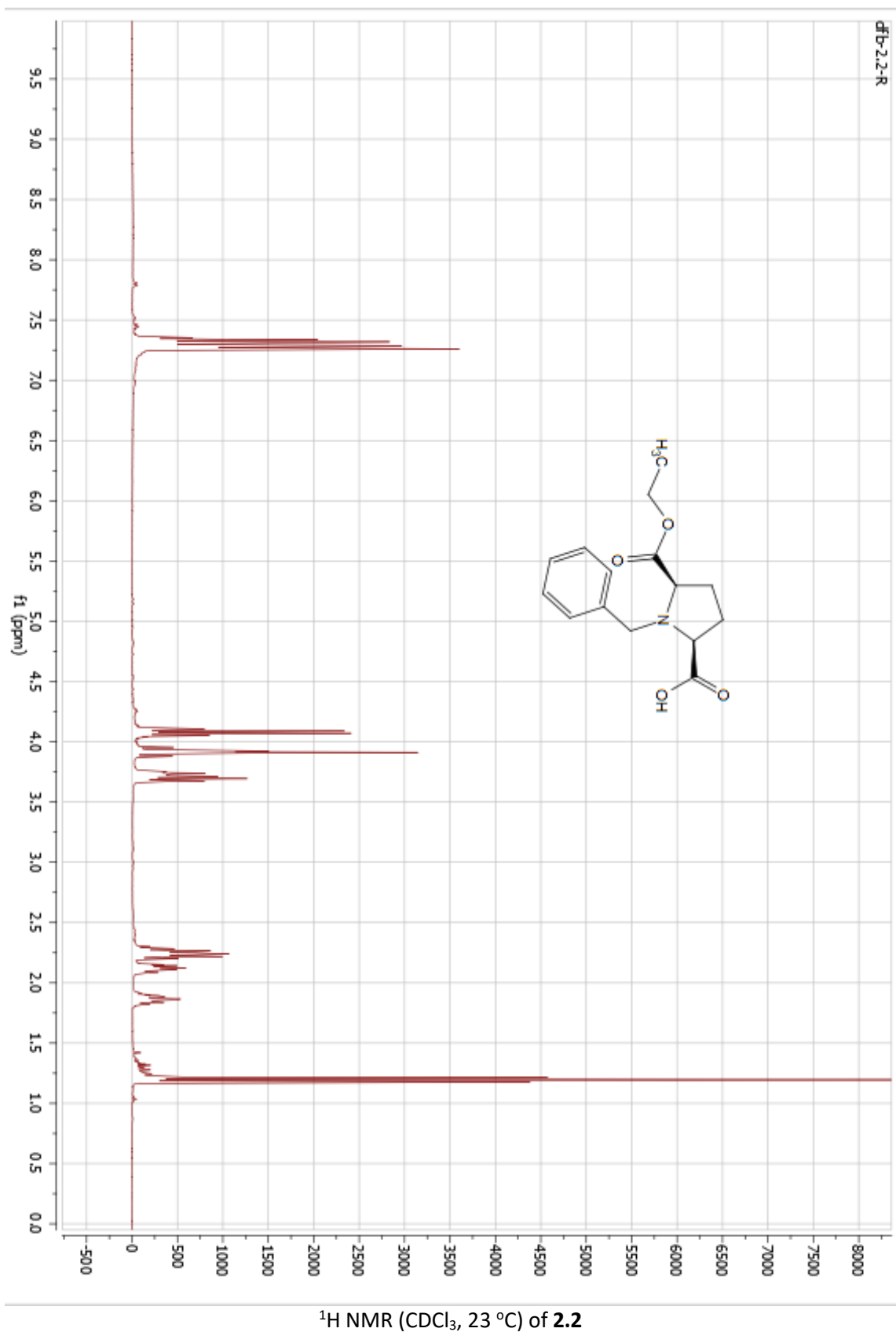
### Appendix – Contents:

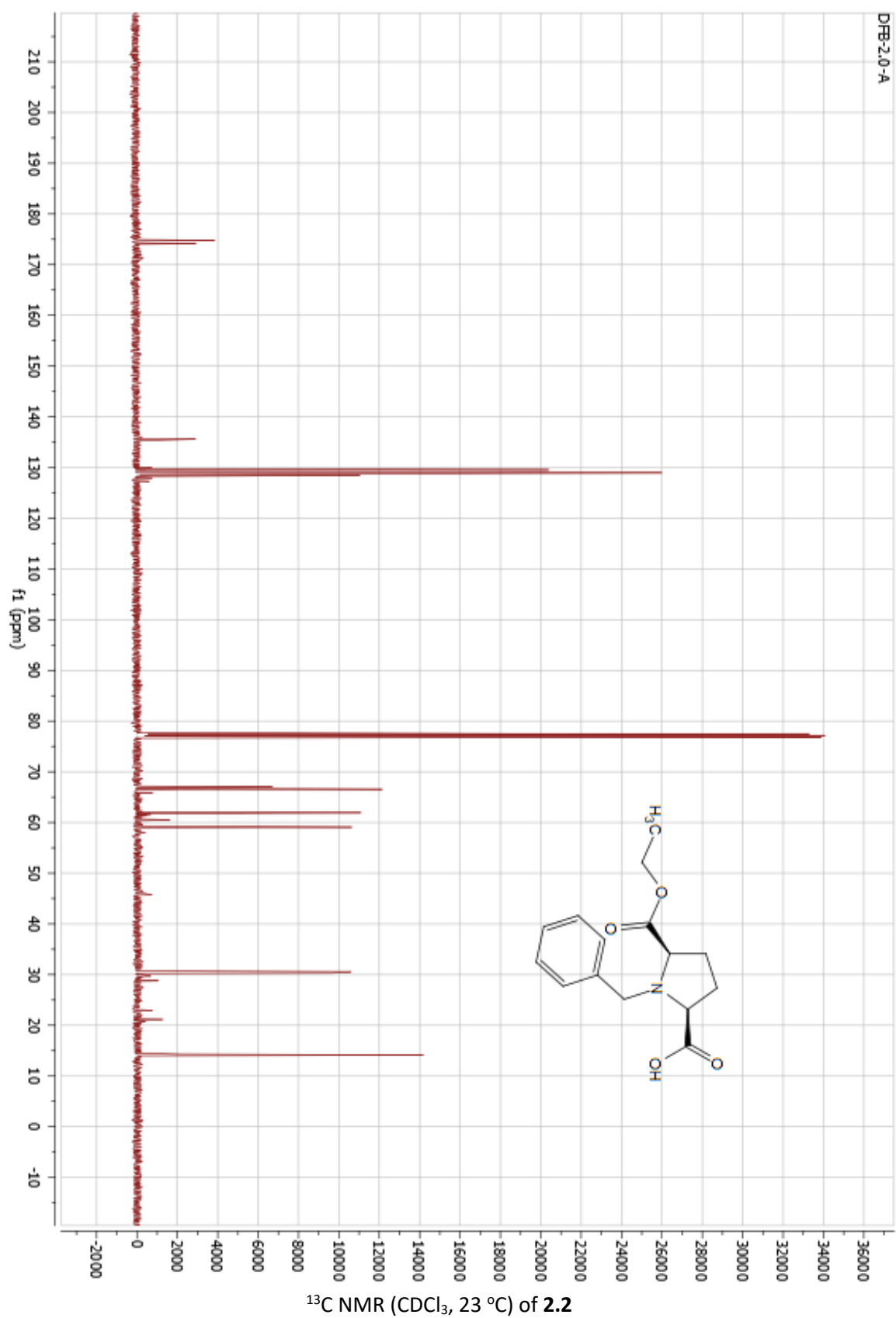
Appendix – <b>A</b> – NMR spectra .....	<b>52</b>
Appendix – <b>B</b> – Mass spec and isolated RCM products data ...	<b>79</b>
Appendix – <b>C</b> – CD spectra .....	<b>86</b>
Appendix – <b>D</b> – FT-IR spectra .....	<b>94</b>

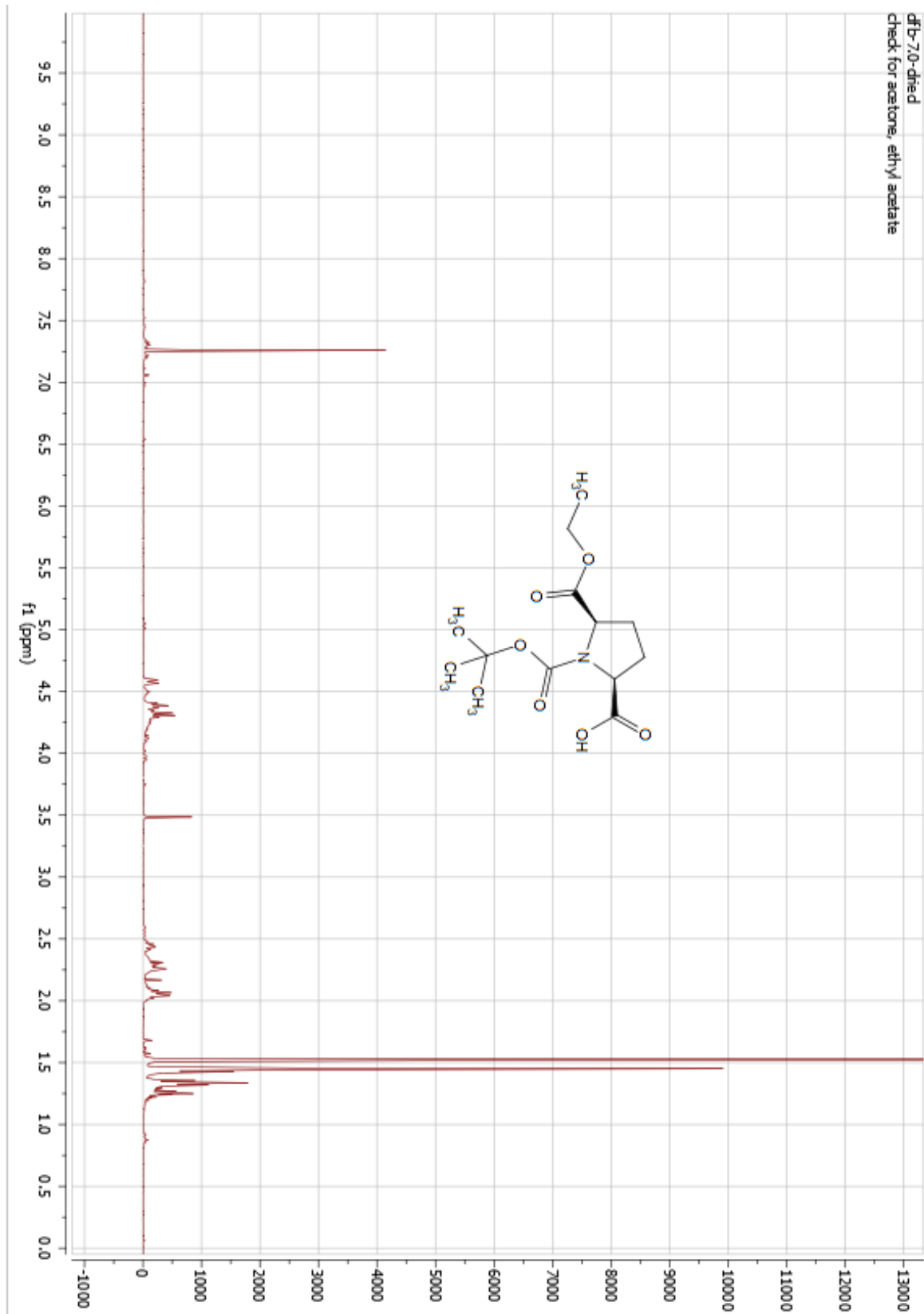
## Appendix – A – NMR Spectra

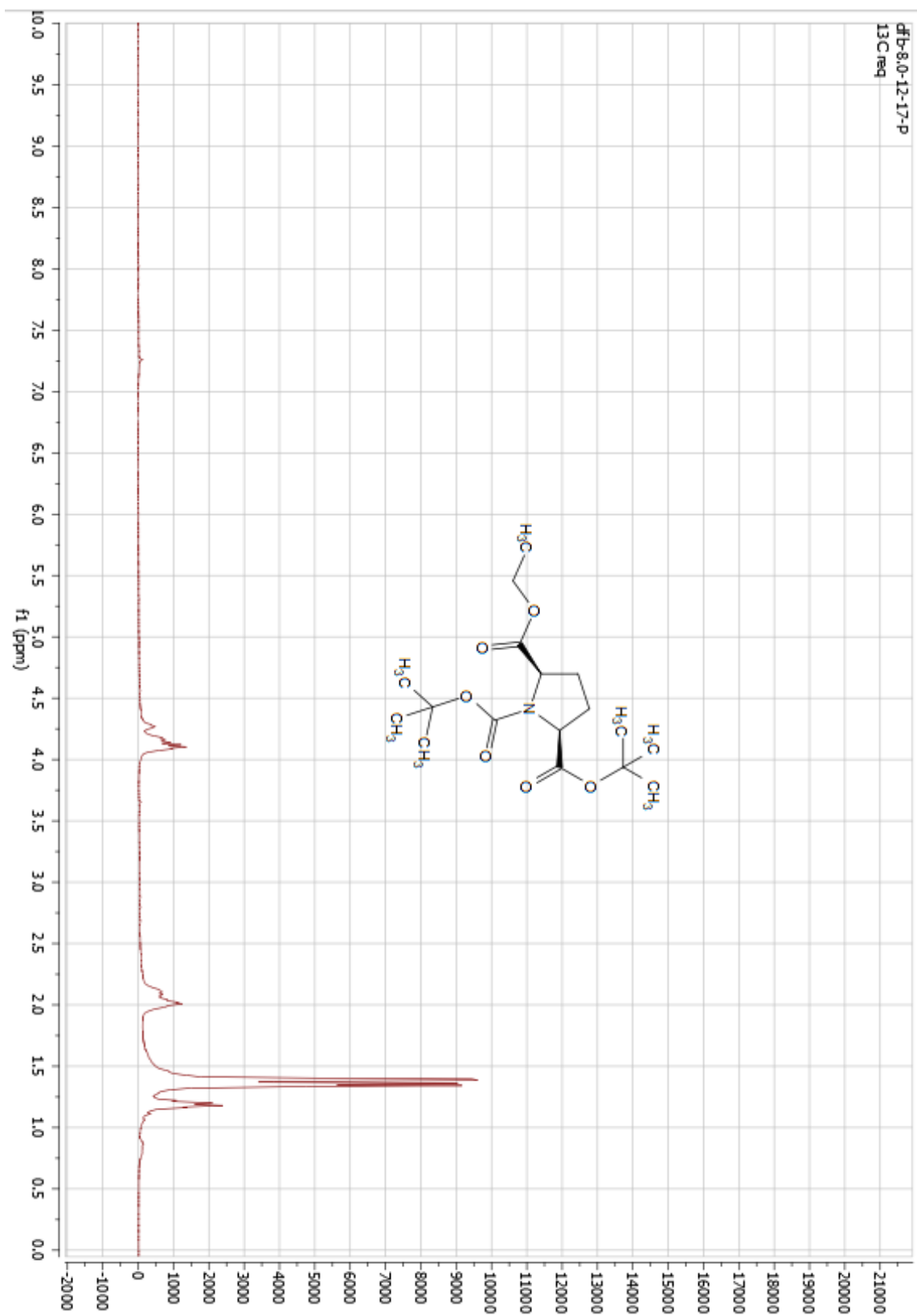
 $^1\text{H}$  NMR ( $\text{CDCl}_3$ ,  $23\text{ }^\circ\text{C}$ ) of **1.1**



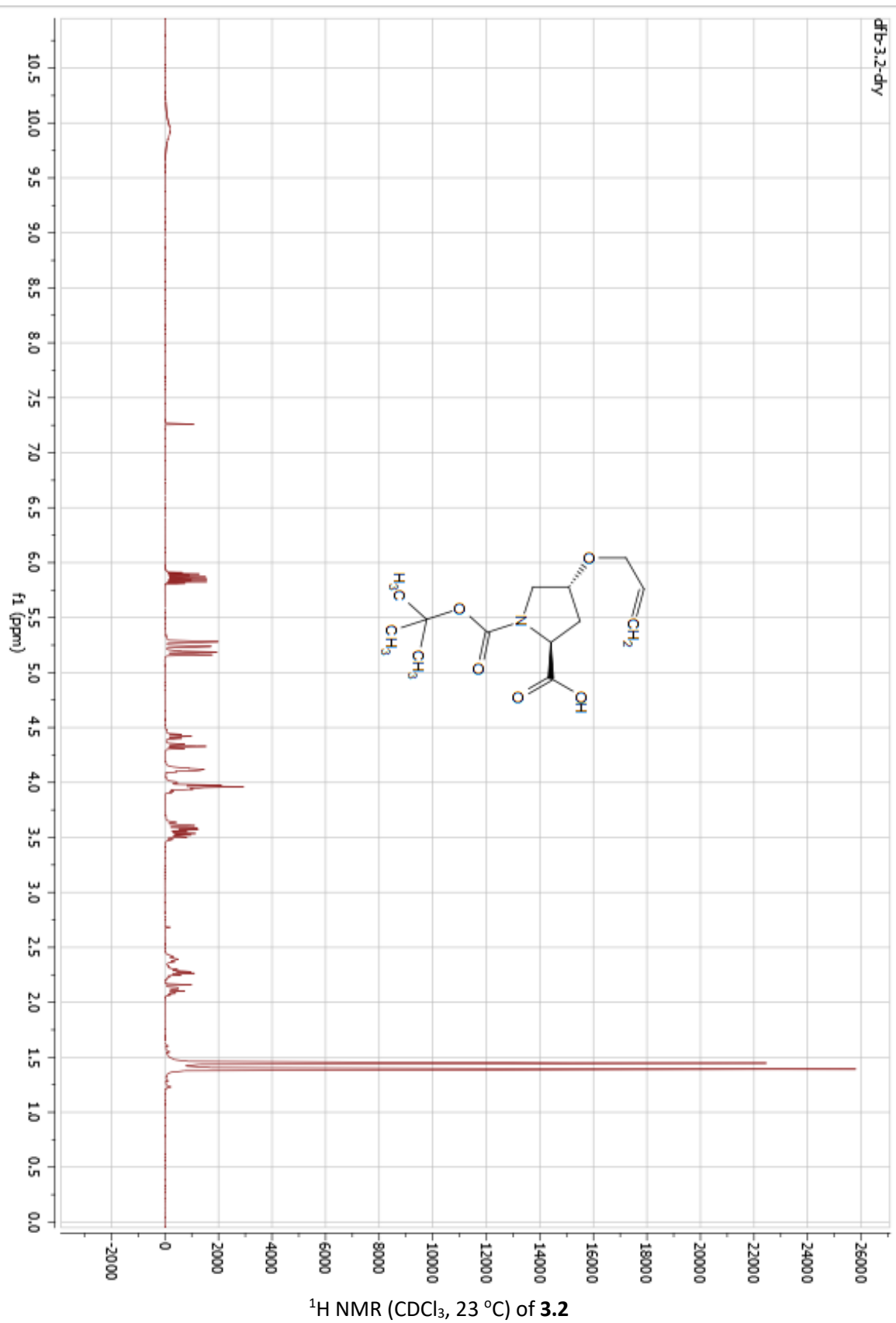


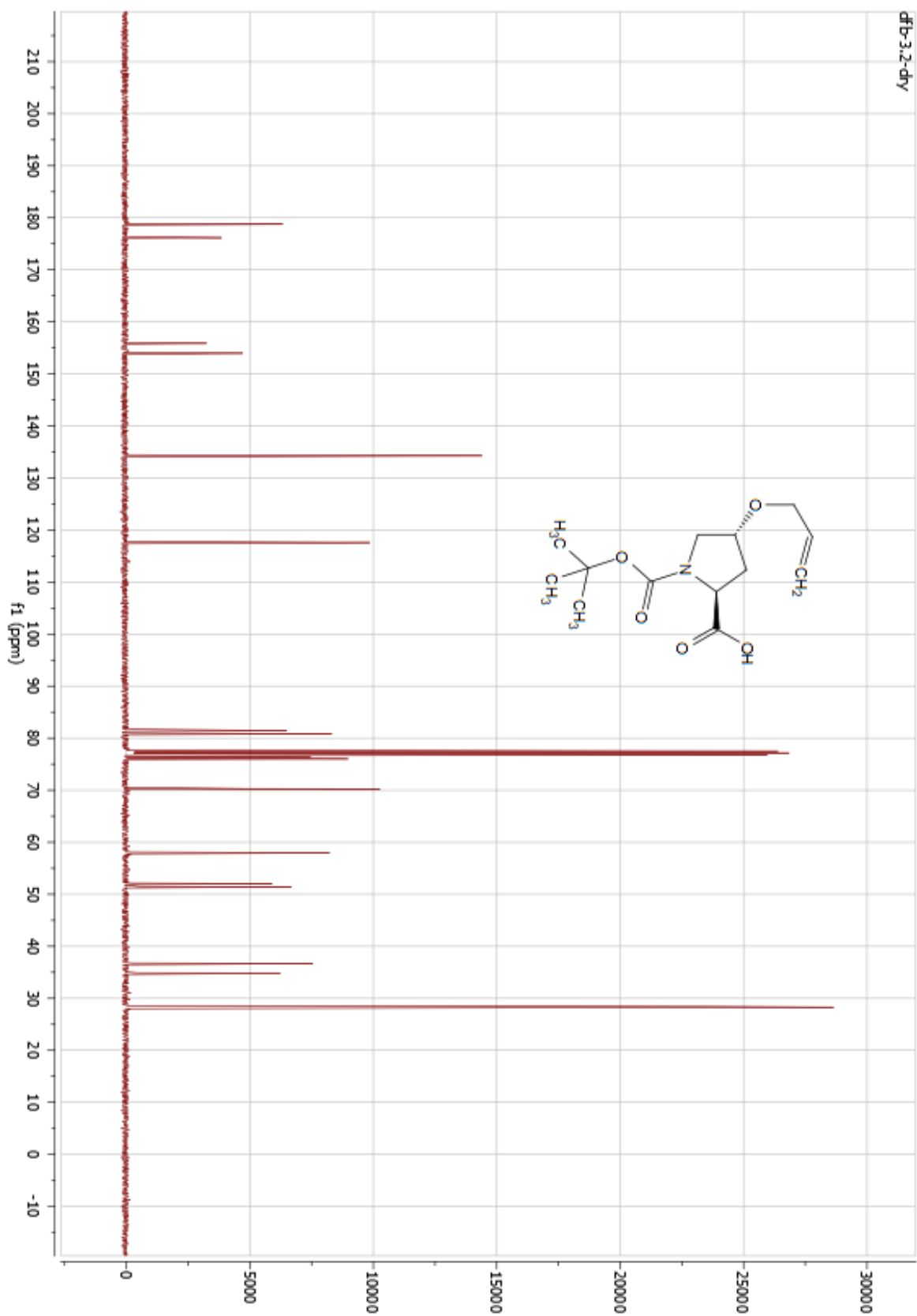


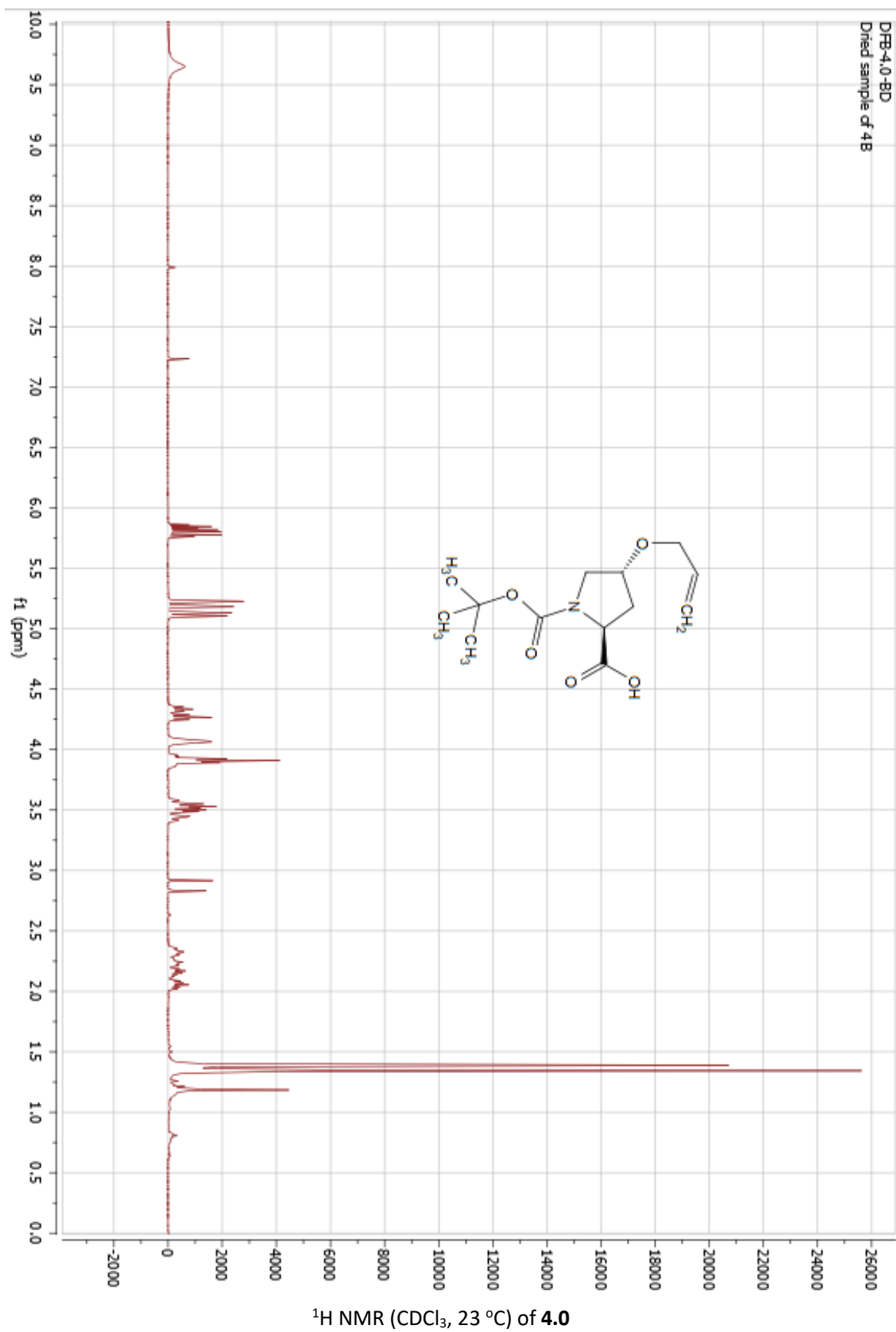


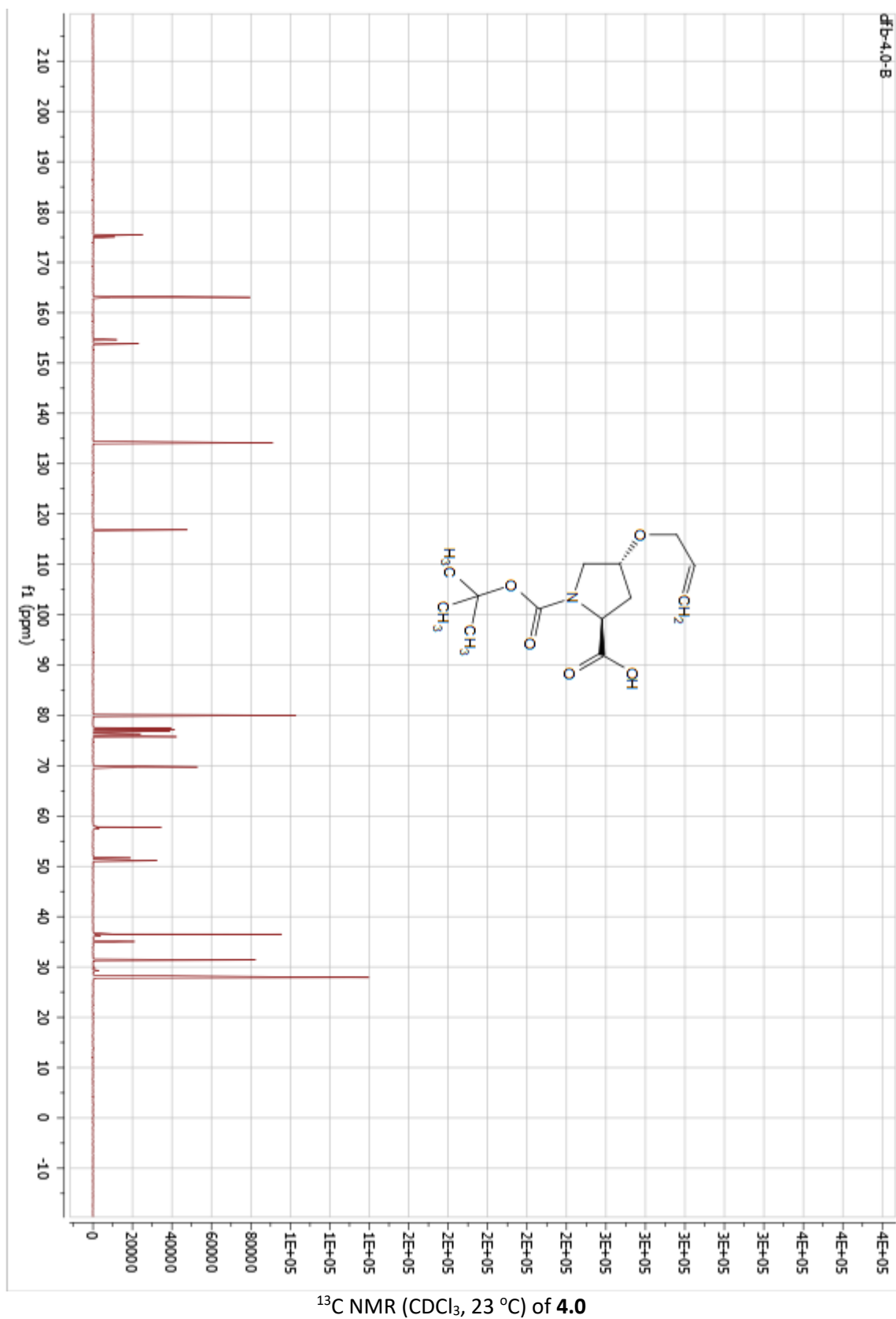


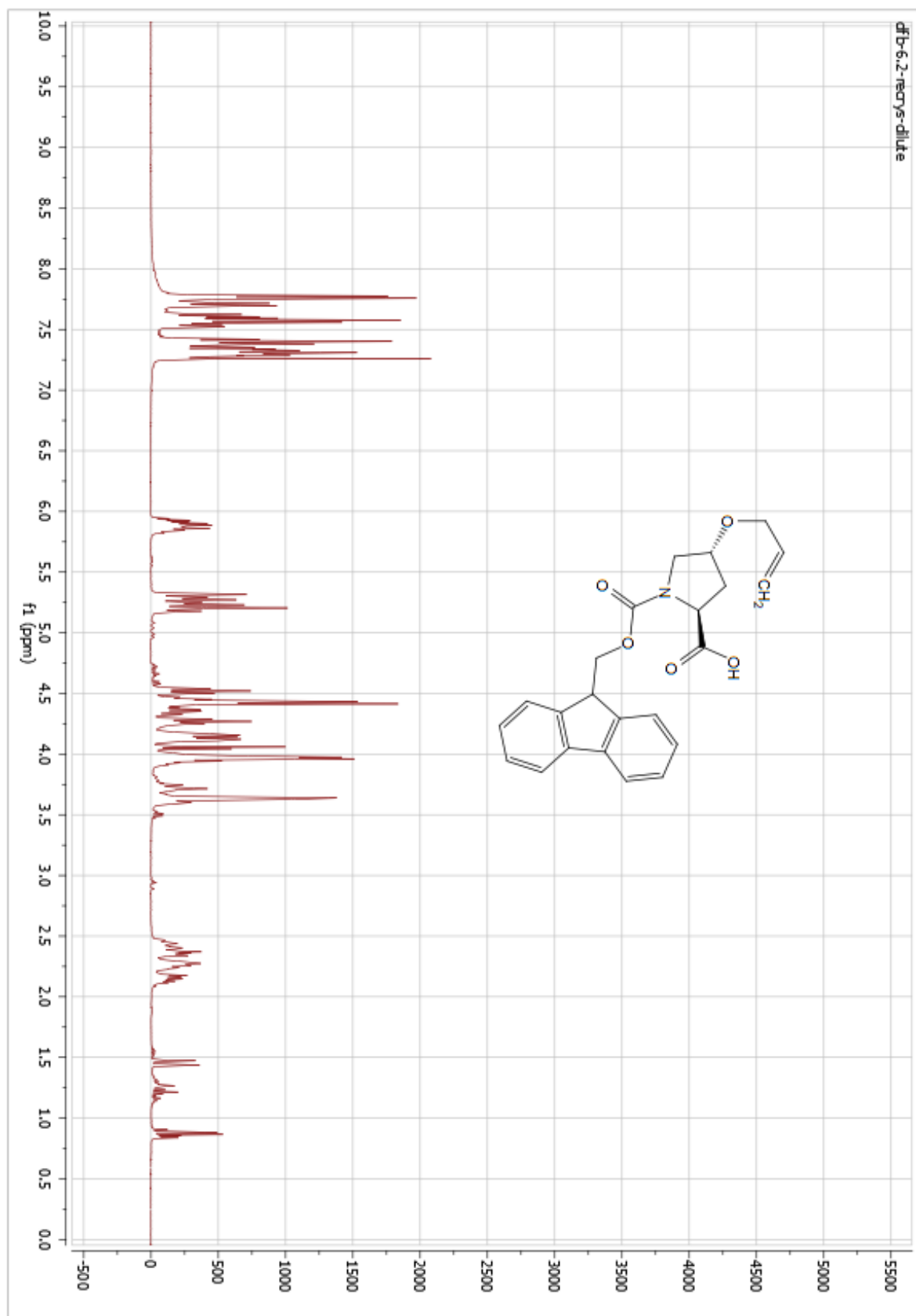
$^1\text{H}$  NMR ( $\text{CDCl}_3$ , 23 °C) of **8.0**

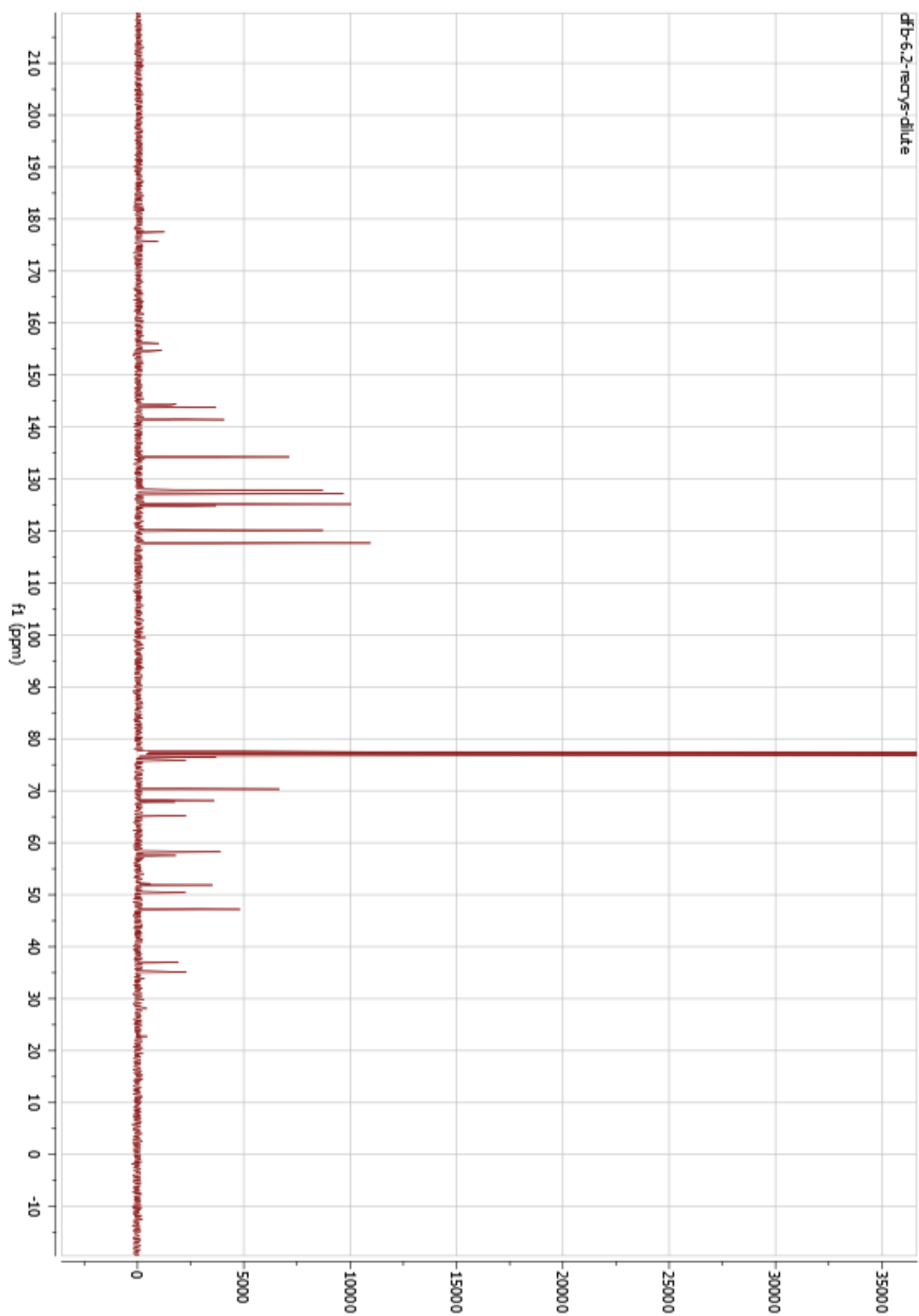


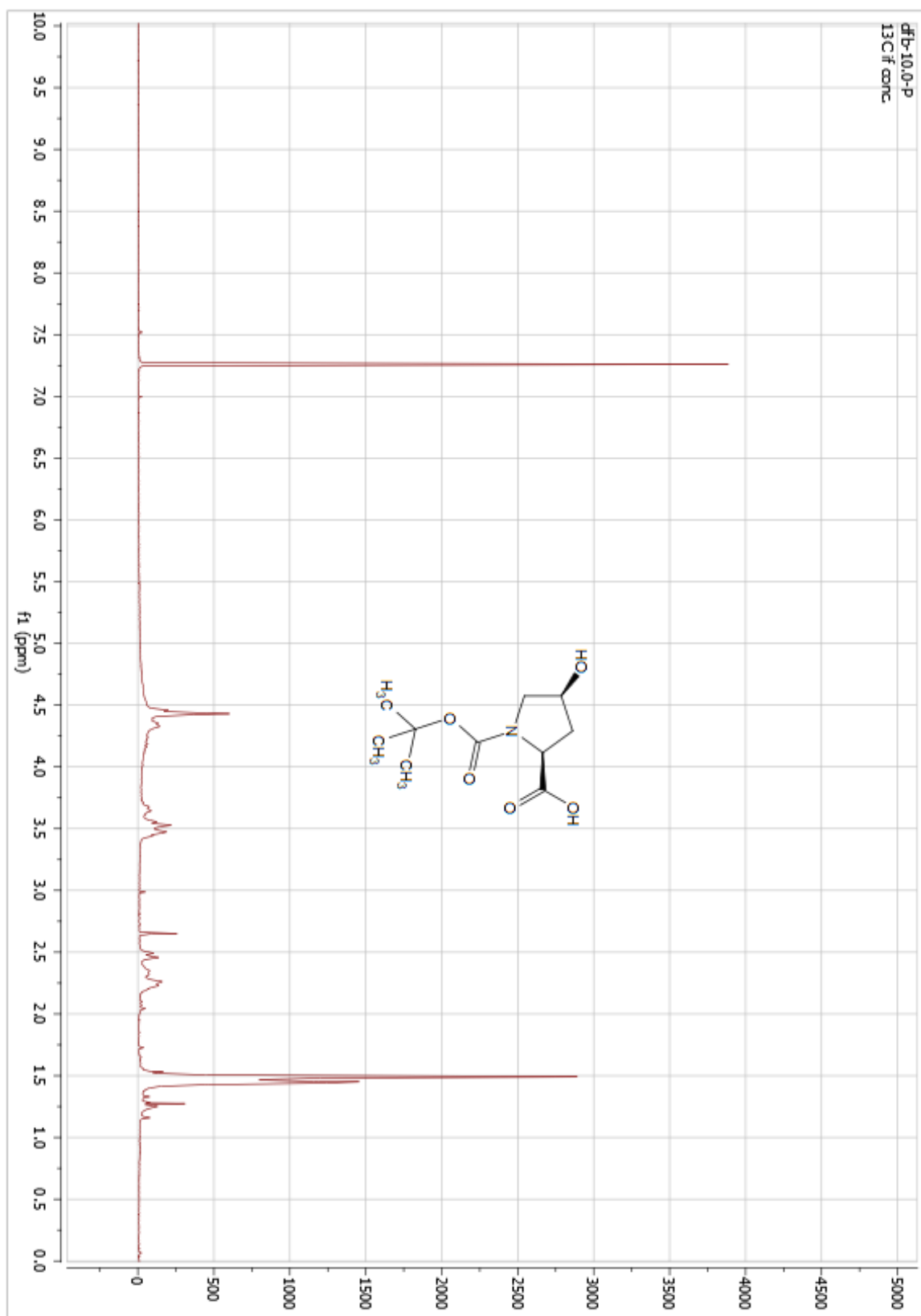




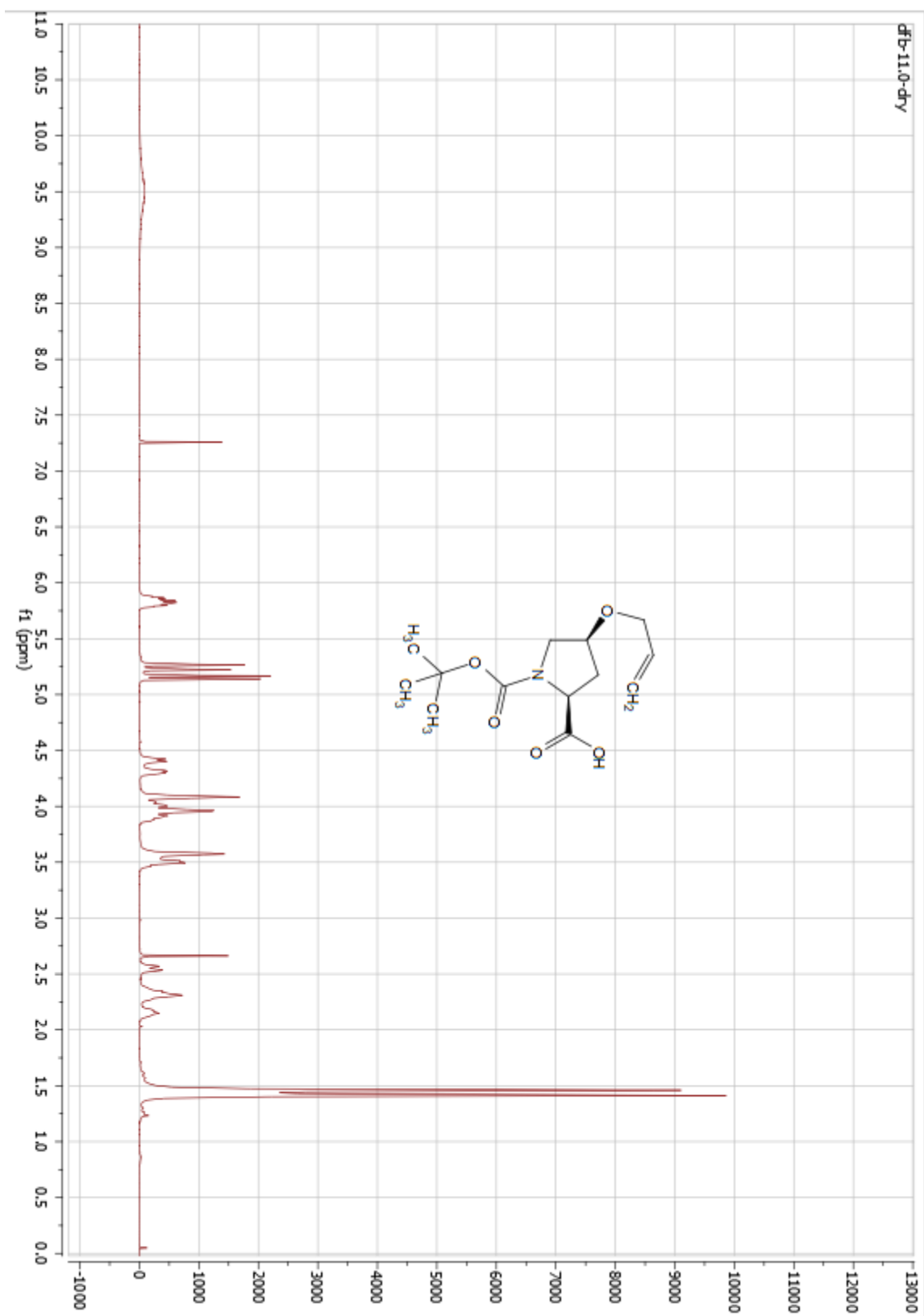


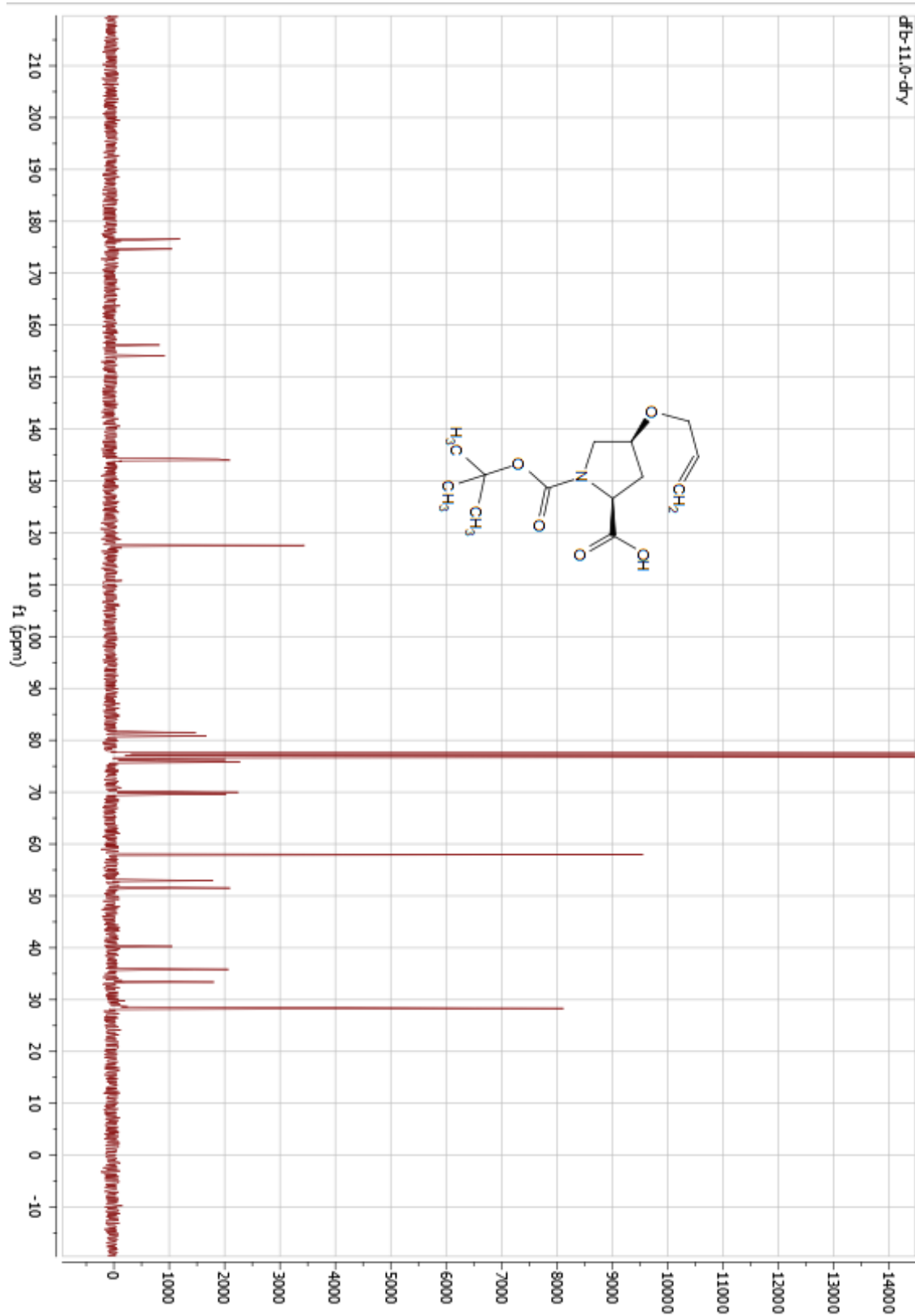


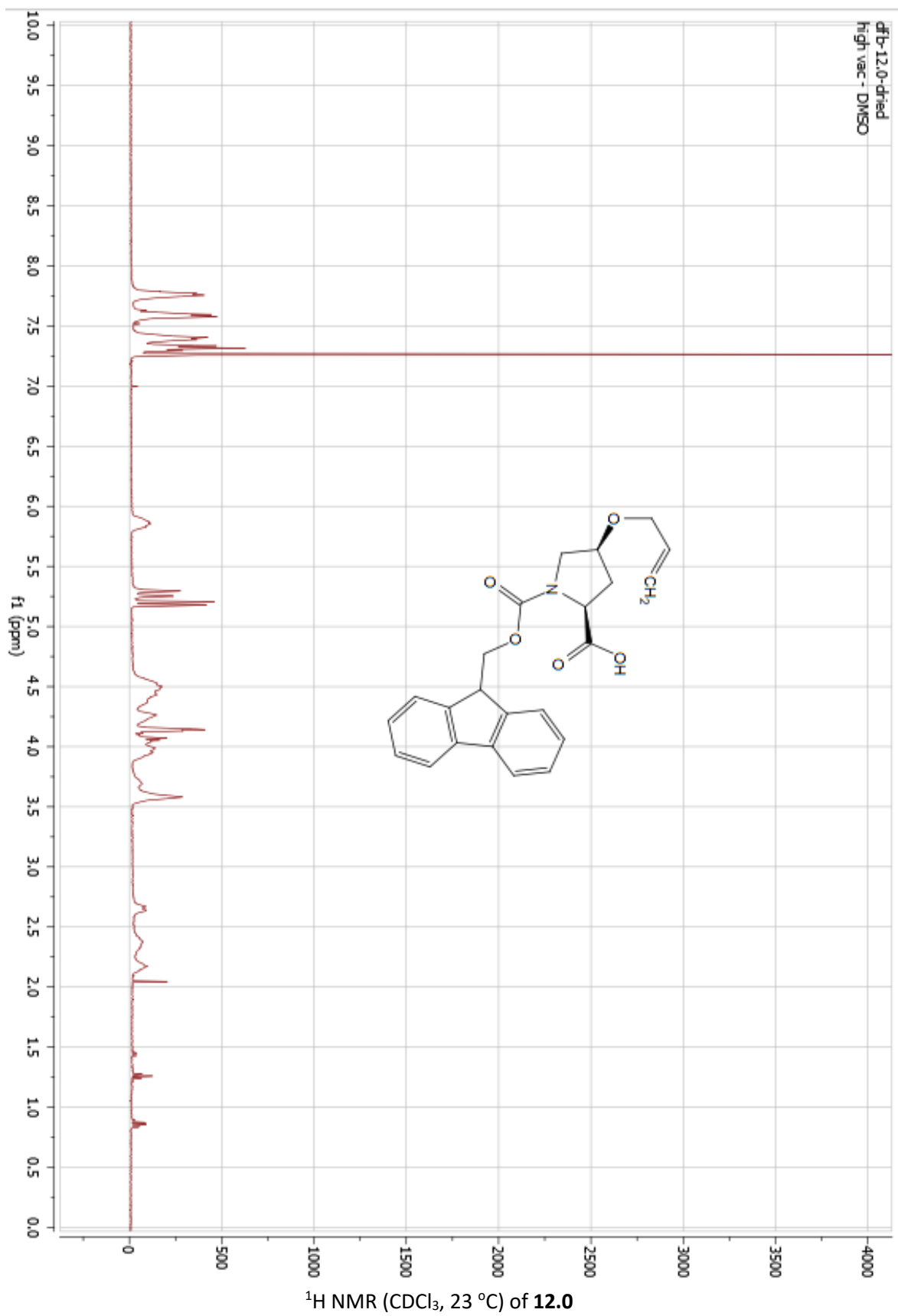


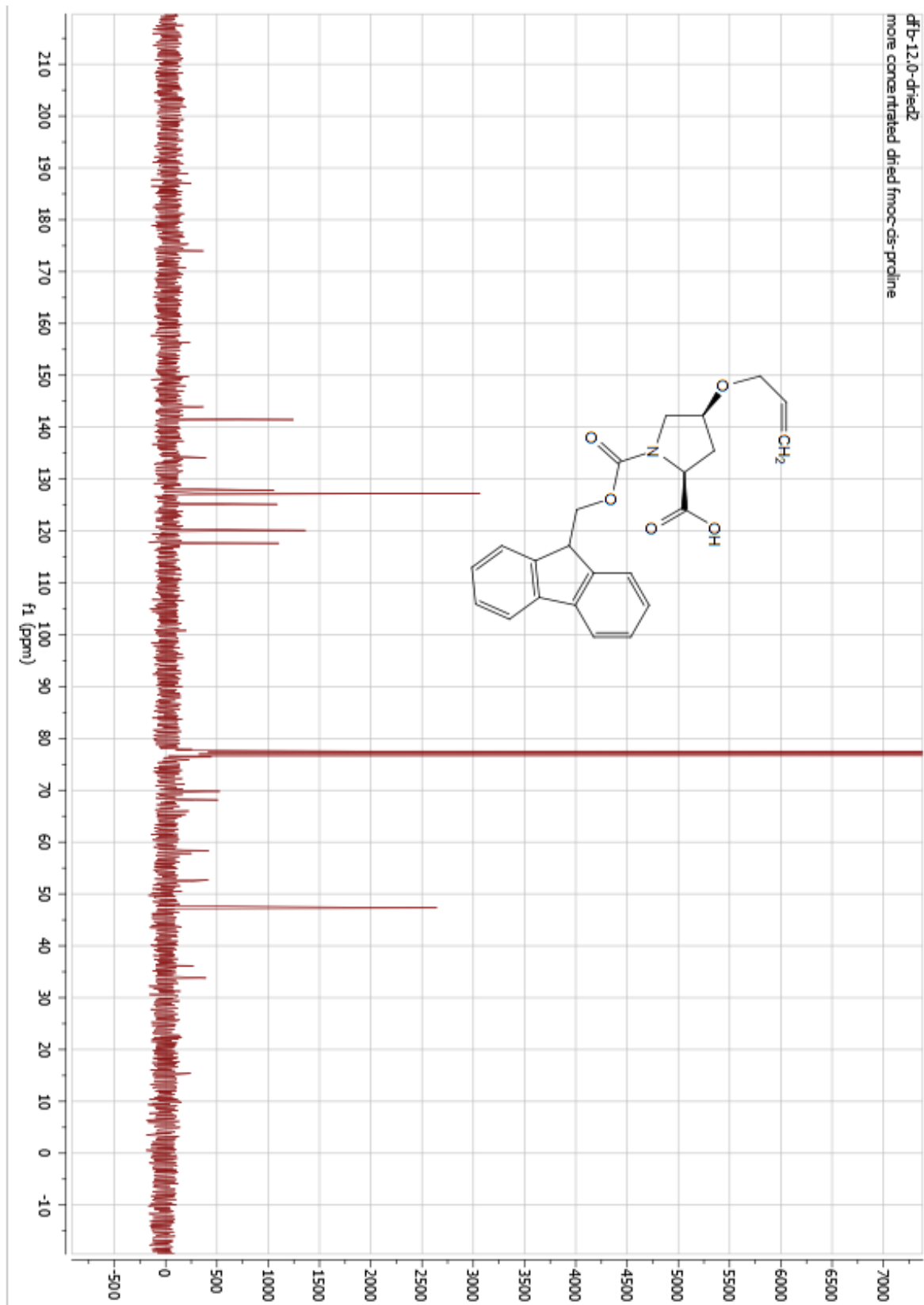


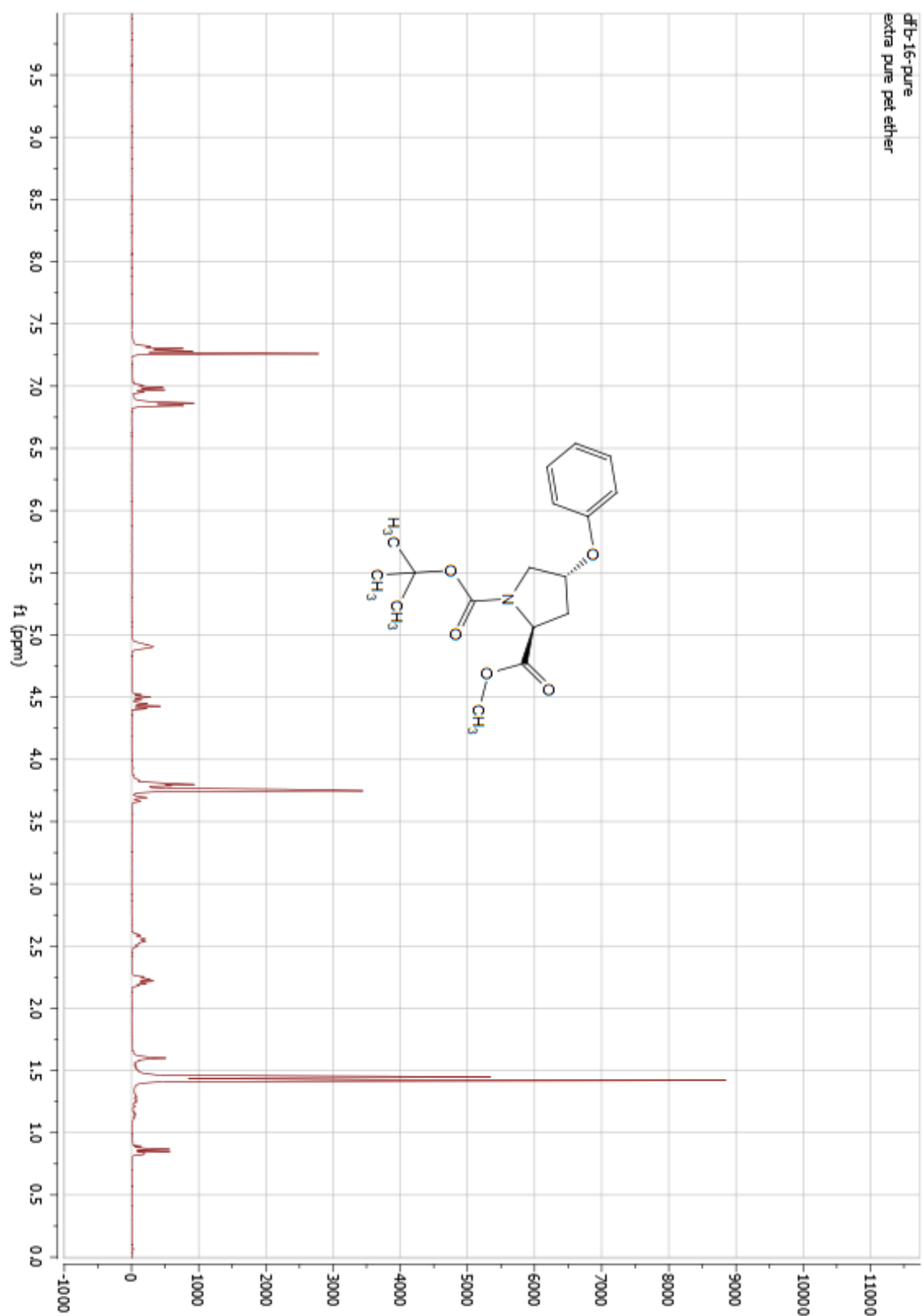
$^1\text{H}$  NMR ( $\text{CDCl}_3$ , 23 °C) of **10.0**

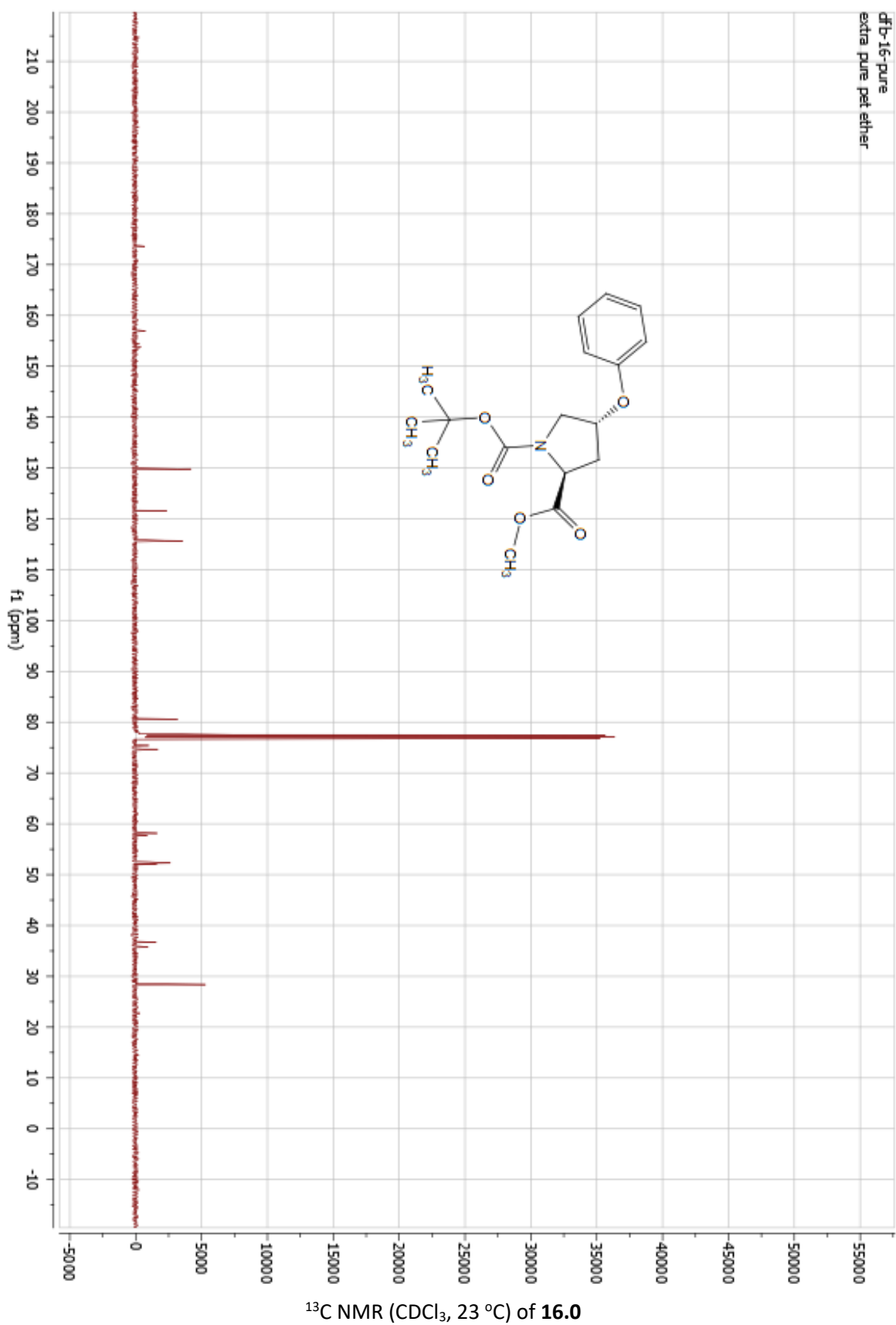


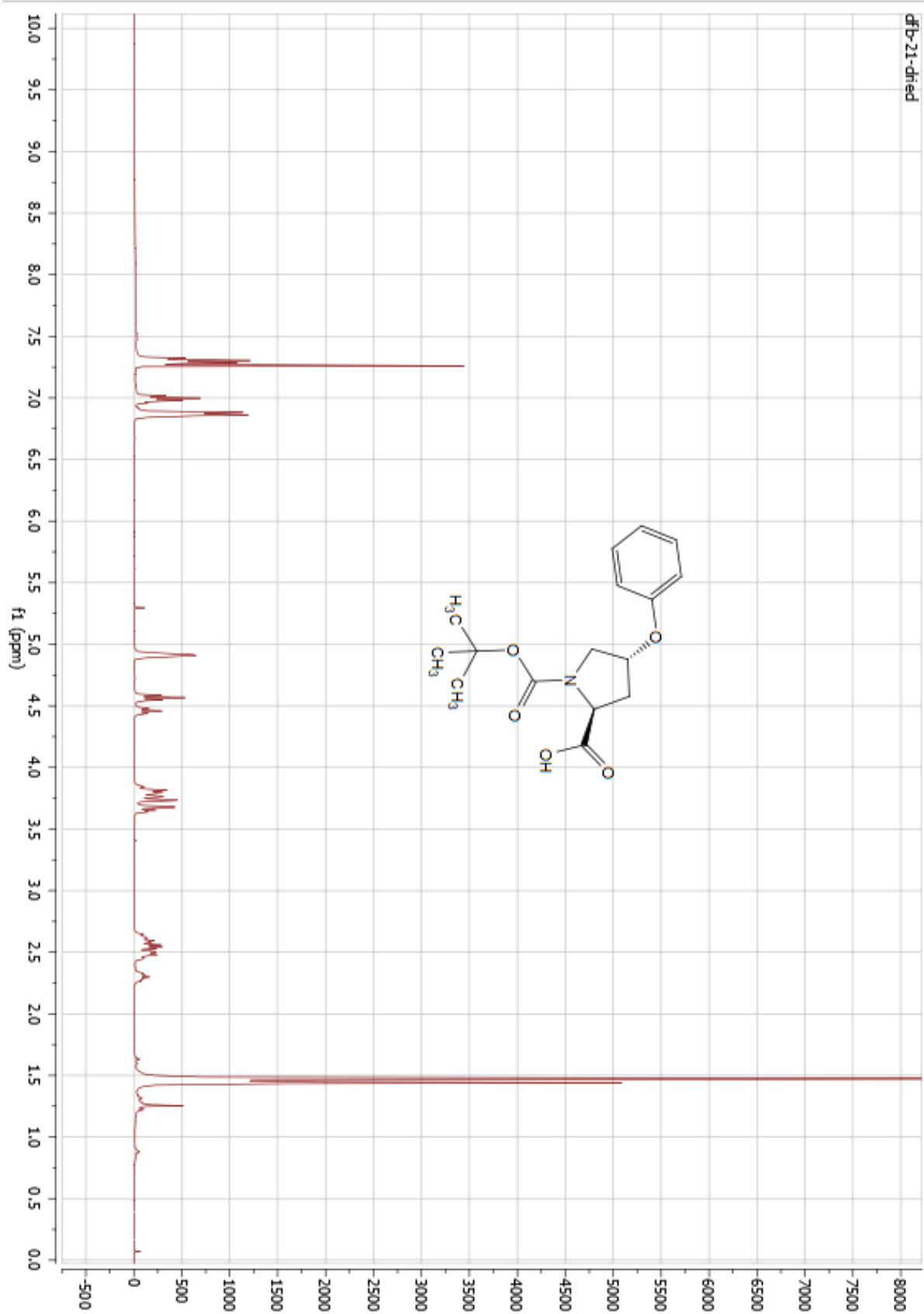




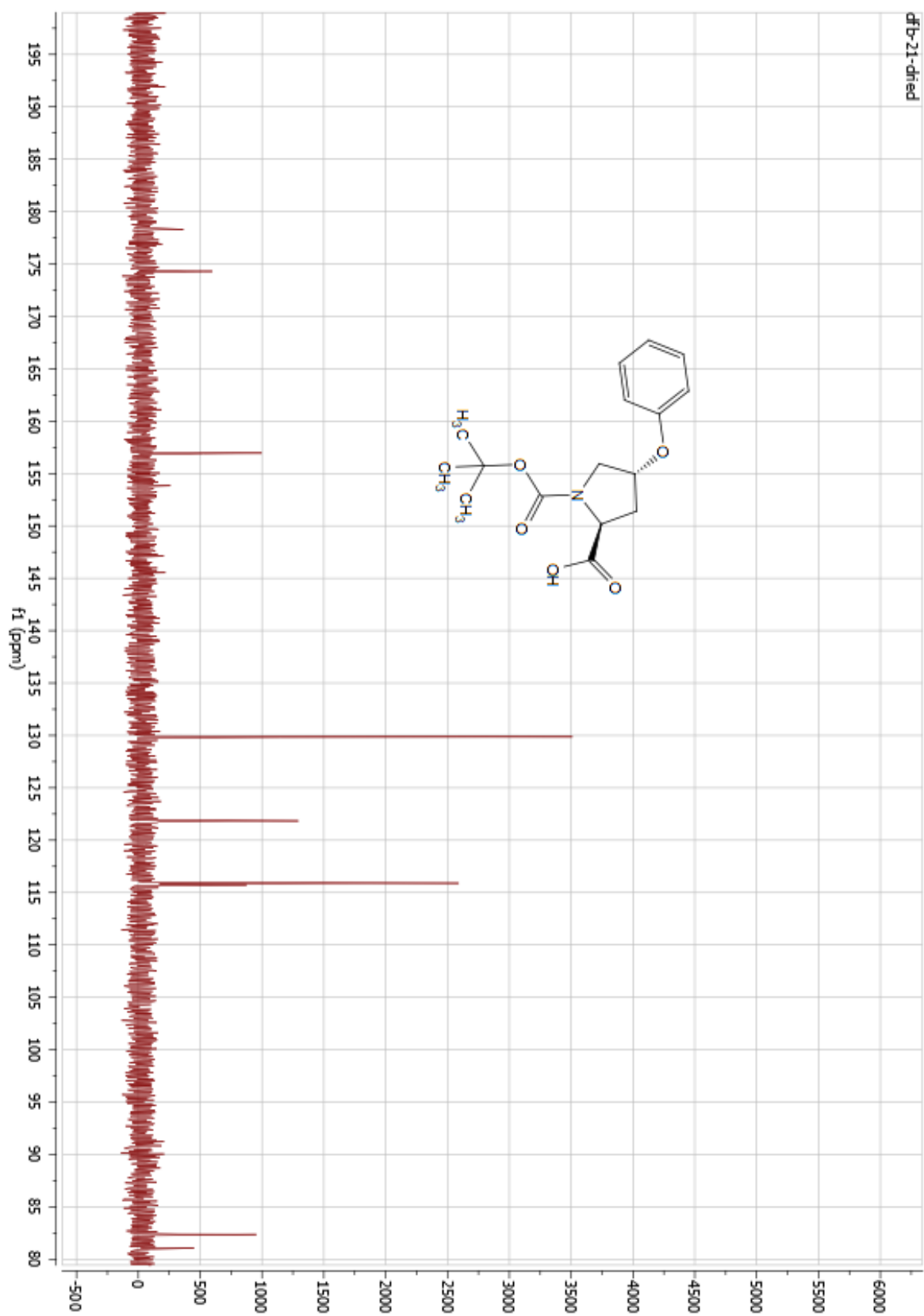


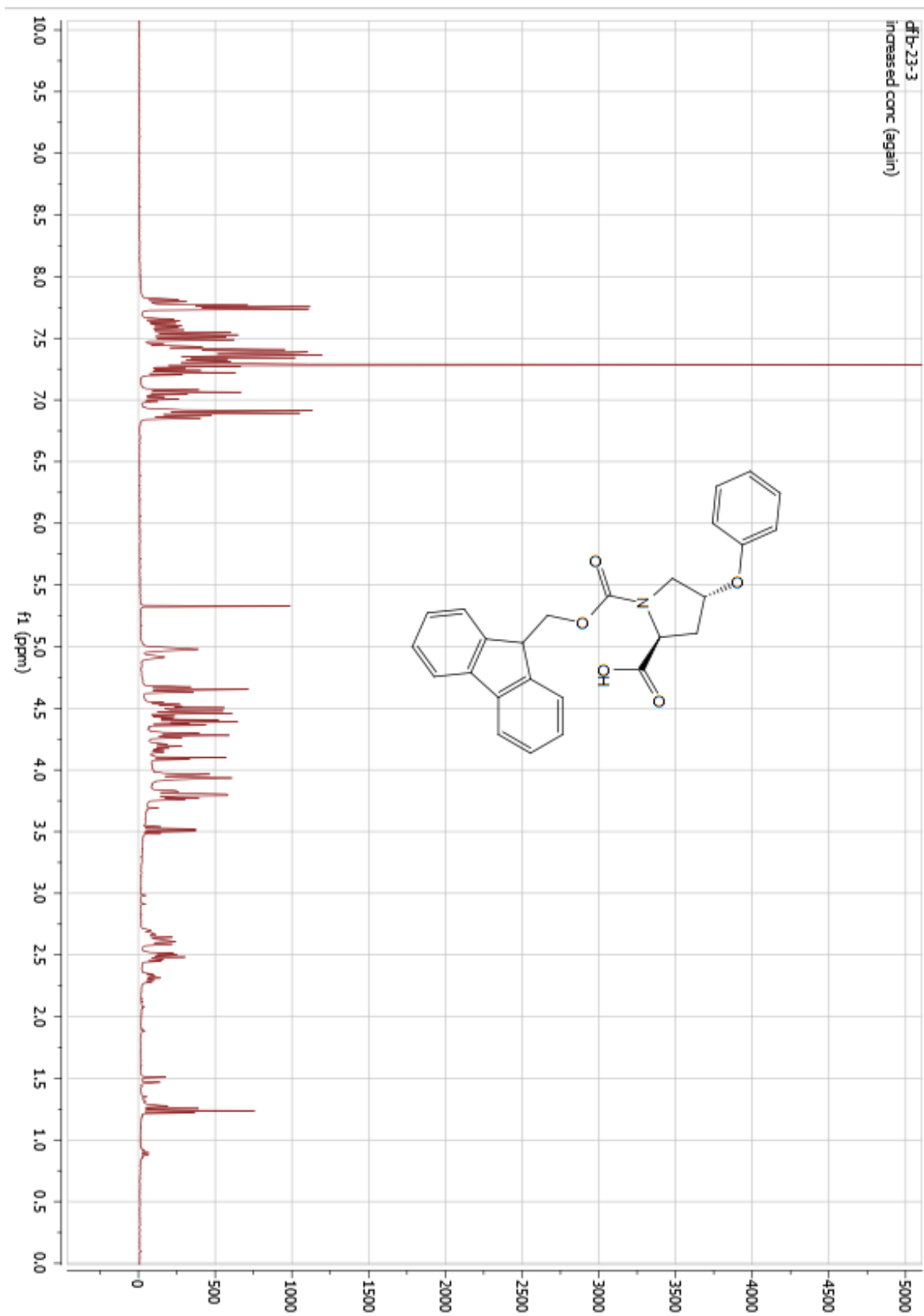


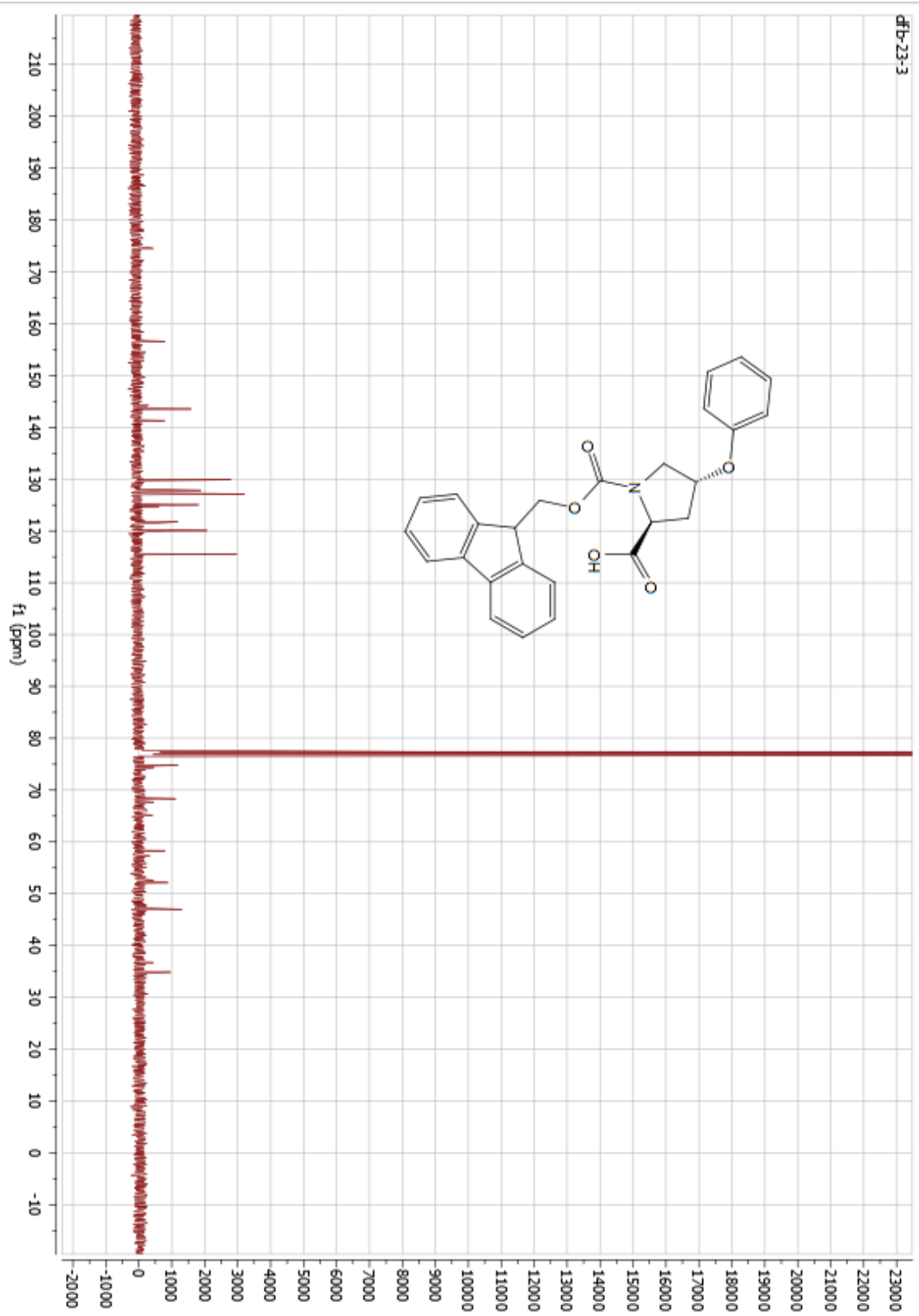


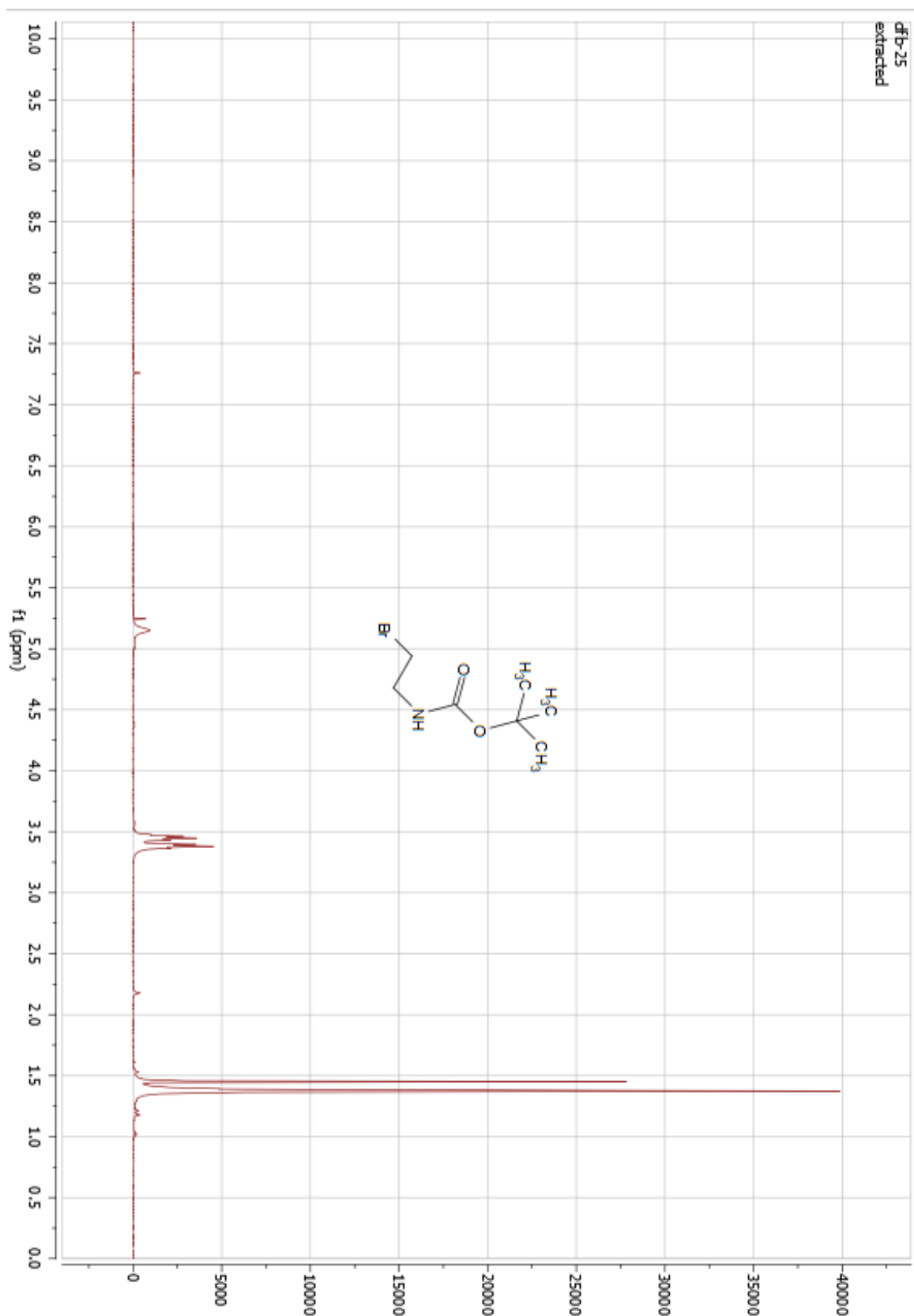


$^1\text{H}$  NMR ( $\text{CDCl}_3$ , 23 °C) of **21.0**

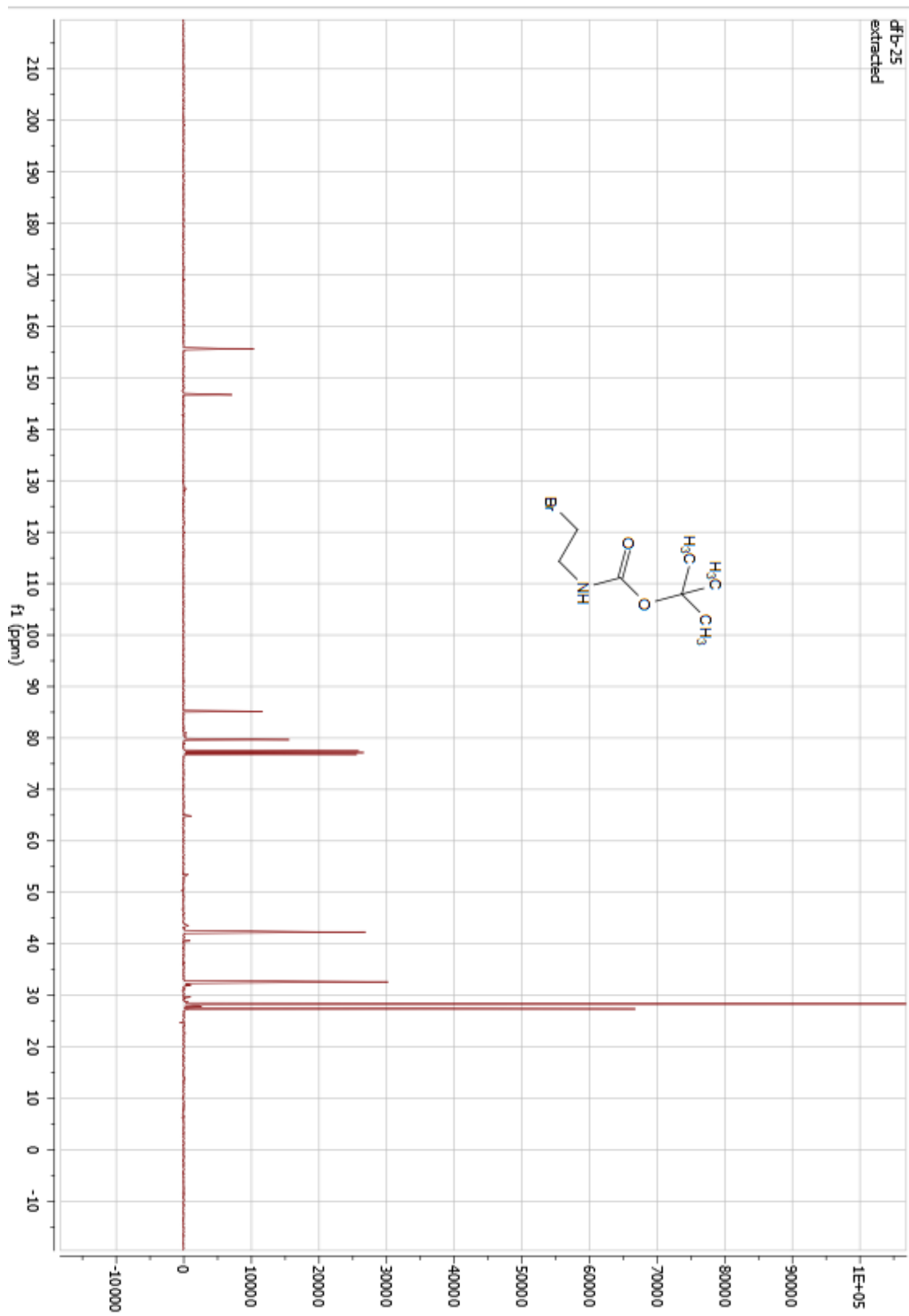


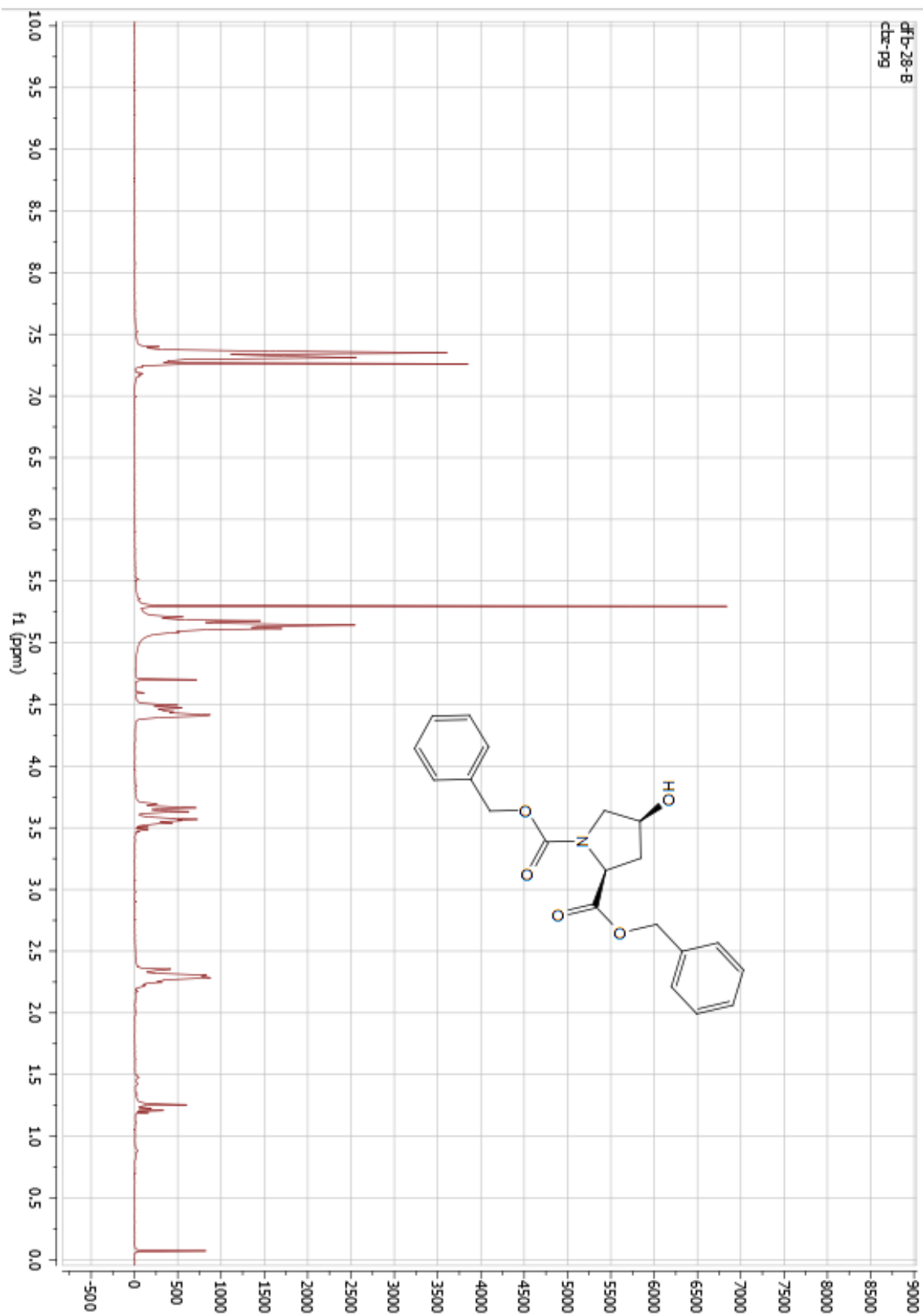




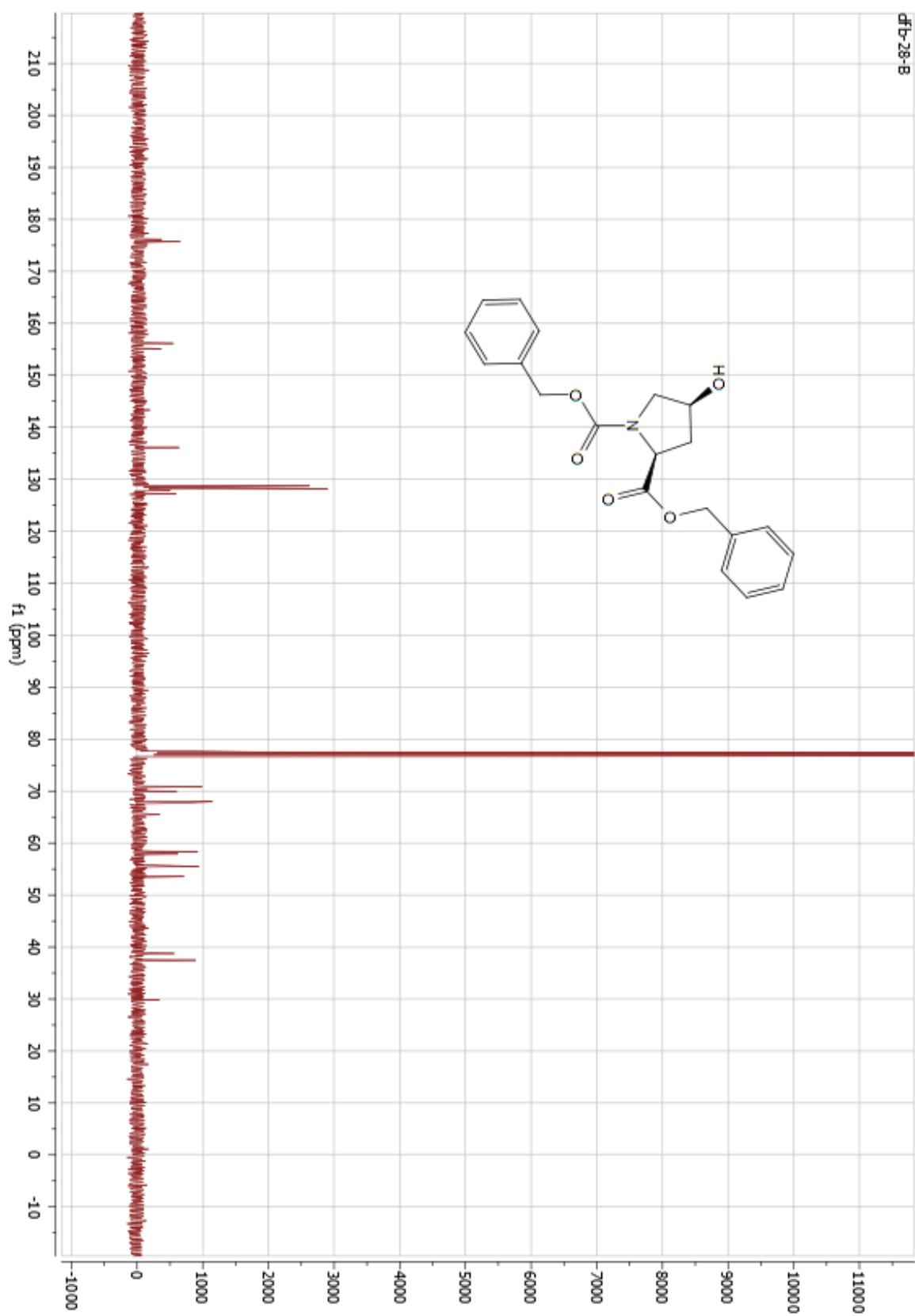


$^1\text{H}$  NMR ( $\text{CDCl}_3$ , 23 °C) of **25.0**



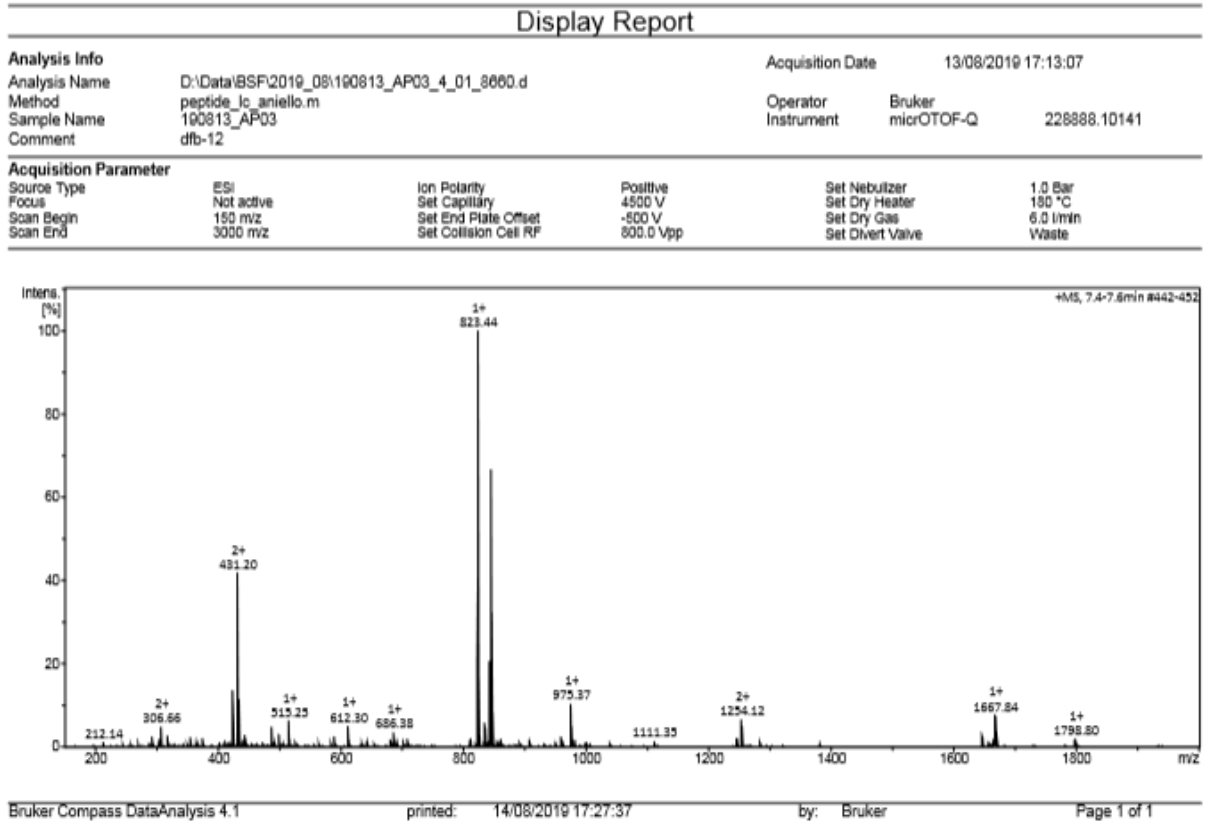
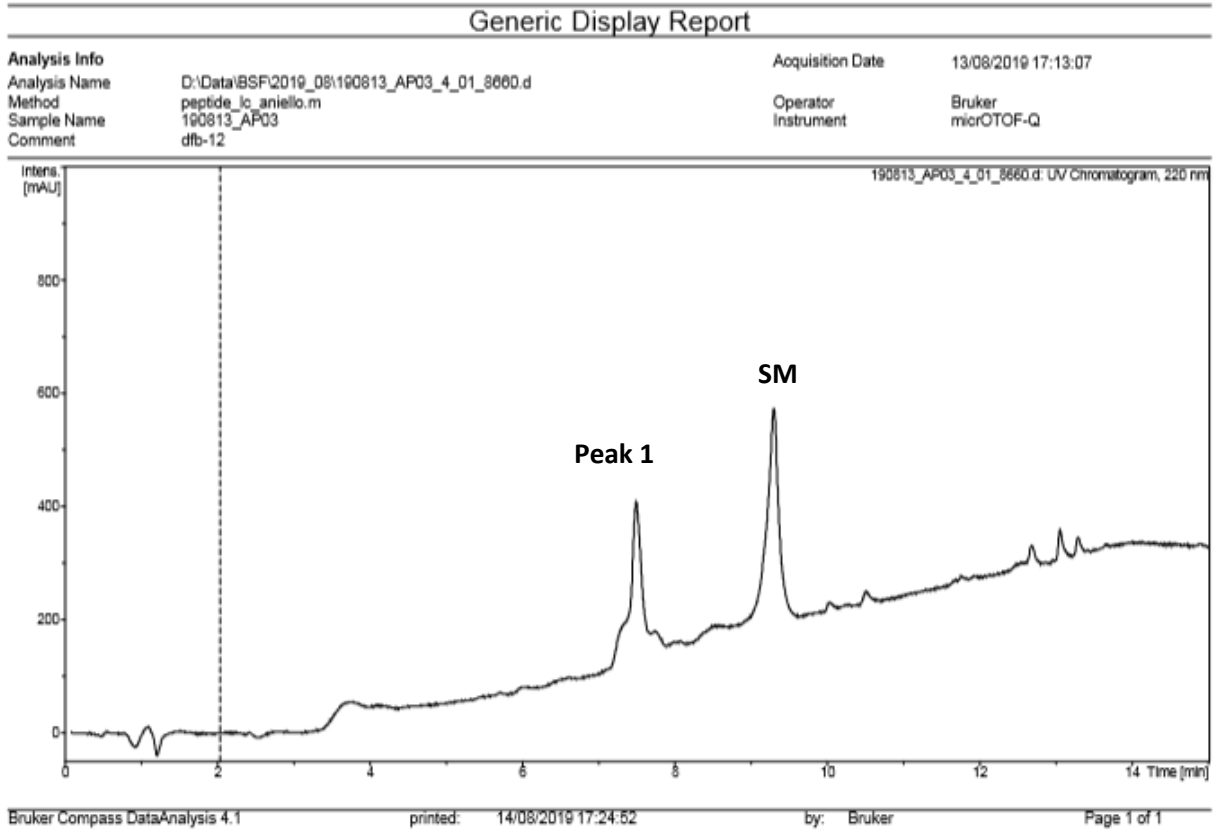


$^1\text{H}$  NMR ( $\text{CDCl}_3$ , 23 °C) of **28.0**



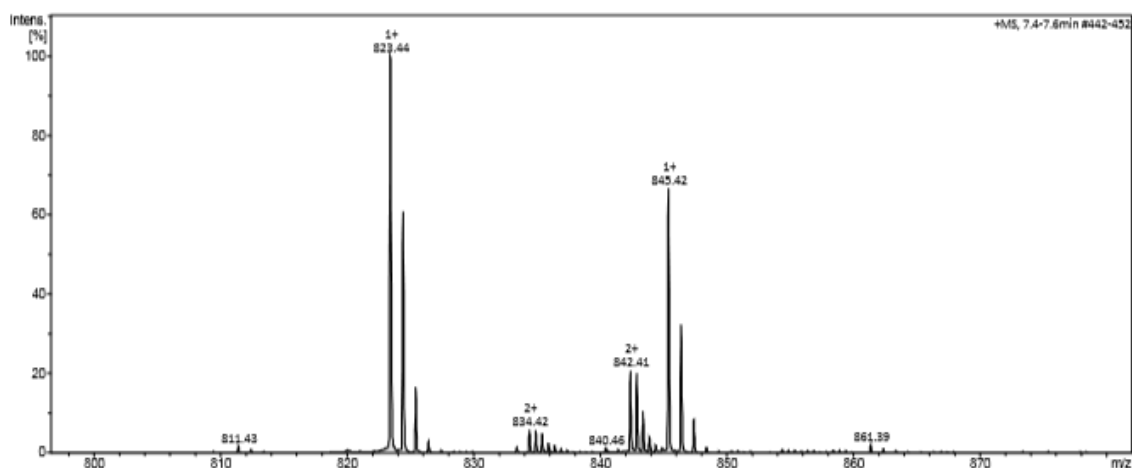
Appendix – B – Mass Spec and prep-HPLC data

ESI-MS data: peptide **17-tc**(trans-cis) RCM in THF with Hoveyda-Grubbs 2<sup>nd</sup> generation (HG), RCM products overlapping – only one major peak visible



## Display Report

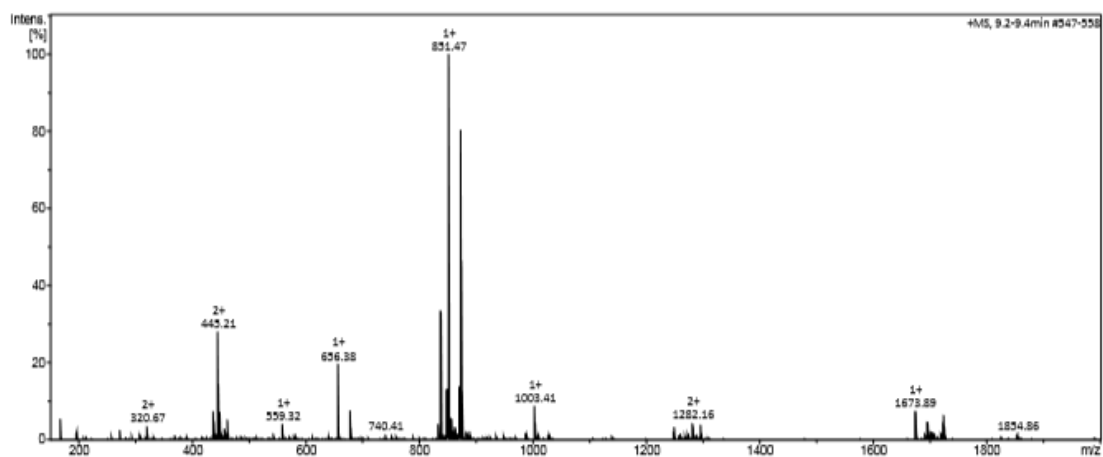
Analysis Info		Acquisition Date			
Analysis Name	D:\Data\BSF2019_08\190813_AP03_4_01_8660.d	13/08/2019 17:13:07			
Method	peptide_lc_aniello.m	Operator	Bruker		
Sample Name	190813_AP03	Instrument	micrOTOF-Q	228888.10141	
Comment	dfb-12				
Acquisition Parameter					
Source Type	ESI	Ion Polarity	Positive	Set Nebulizer	1.0 Bar
Focus	Not active	Set Capillary	4500 V	Set Dry Heater	180 °C
Scan Begin	150 m/z	Set End Plate Offset	-500 V	Set Dry Gas	6.0 l/min
Scan End	3000 m/z	Set Collision Cell RF	800.0 Vpp	Set Divert Valve	Waste



Bruker Compass DataAnalysis 4.1 printed: 14/08/2019 17:28:31 by: Bruker Page 1 of 1

## Display Report

Analysis Info		Acquisition Date			
Analysis Name	D:\Data\BSF2019_08\190813_AP03_4_01_8660.d	13/08/2019 17:13:07			
Method	peptide_lc_aniello.m	Operator	Bruker		
Sample Name	190813_AP03	Instrument	micrOTOF-Q	228888.10141	
Comment	dfb-12				
Acquisition Parameter					
Source Type	ESI	Ion Polarity	Positive	Set Nebulizer	1.0 Bar
Focus	Not active	Set Capillary	4500 V	Set Dry Heater	180 °C
Scan Begin	150 m/z	Set End Plate Offset	-500 V	Set Dry Gas	6.0 l/min
Scan End	3000 m/z	Set Collision Cell RF	800.0 Vpp	Set Divert Valve	Waste

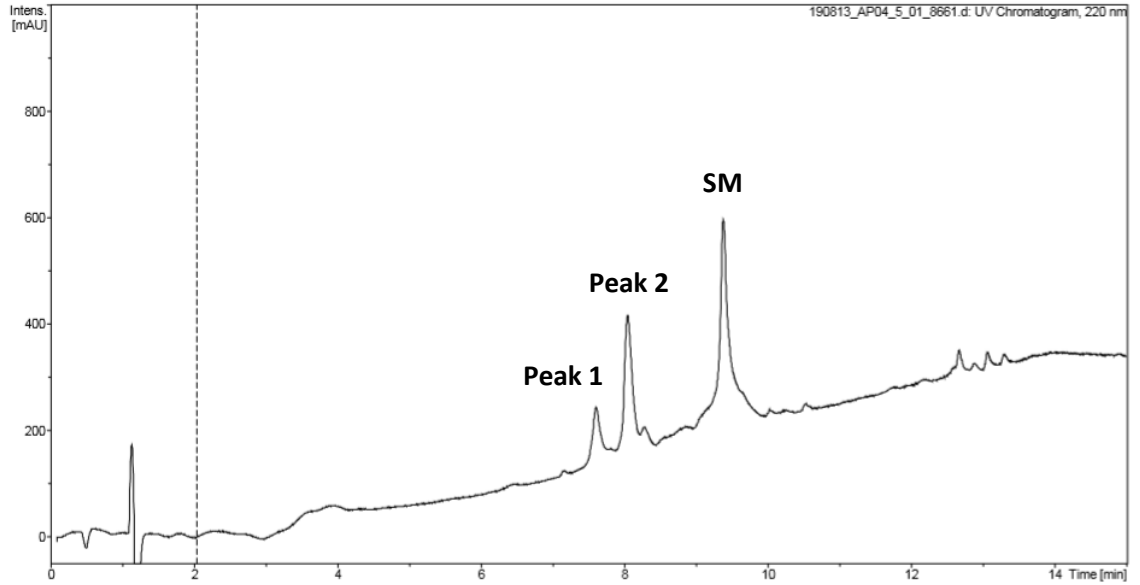


Bruker Compass DataAnalysis 4.1 printed: 14/08/2019 17:29:29 by: Bruker Page 1 of 1

ESI-MS data: peptide **13-ct**(cis-trans), RCM in **THF** with **HG** – only two major products clearly visible, two minor product peaks significantly reduced.

Generic Display Report

<b>Analysis Info</b>	D:\Data\BSF\2019_08\190813_AP04_5_01_8661.d	Acquisition Date	13/08/2019 17:44:25
Analysis Name	peptide_lc_aniello.m	Operator	Bruker
Method	190813_AP04	Instrument	micrOTOF-Q
Sample Name	dfb-13		
Comment			

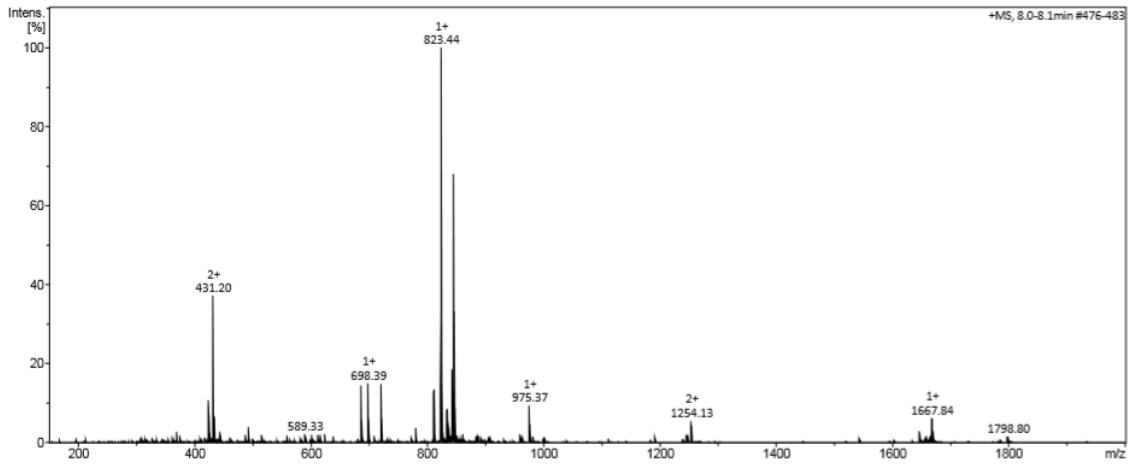


Bruker Compass DataAnalysis 4.1 printed: 14/08/2019 17:32:11 by: Bruker Page 1 of 1

Display Report

<b>Analysis Info</b>	D:\Data\BSF\2019_08\190813_AP04_5_01_8661.d	Acquisition Date	13/08/2019 17:44:25
Analysis Name	peptide_lc_aniello.m	Operator	Bruker
Method	190813_AP04	Instrument	micrOTOF-Q
Sample Name	dfb-13		228888.10141
Comment			

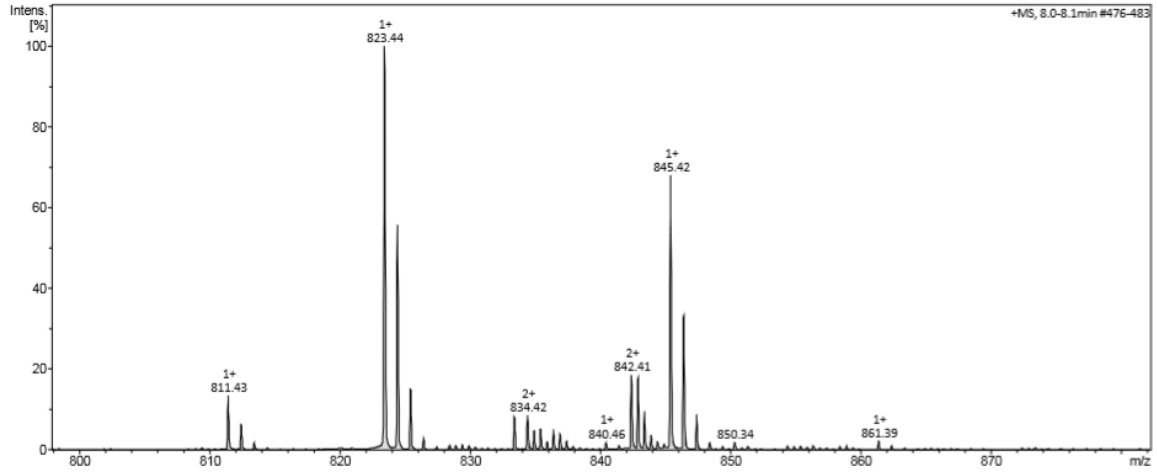
<b>Acquisition Parameter</b>	ESI	Ion Polarity	Positive	Set Nebulizer	1.0 Bar
Source Type	Not active	Set Capillary	4500 V	Set Dry Heater	180 °C
Focus	150 m/z	Set End Plate Offset	-500 V	Set Dry Gas	6.0 l/min
Scan Begin	3000 m/z	Set Collision Cell RF	800.0 Vpp	Set Divert Valve	Waste
Scan End					



Bruker Compass DataAnalysis 4.1 printed: 14/08/2019 17:33:57 by: Bruker Page 1 of 1

## Display Report

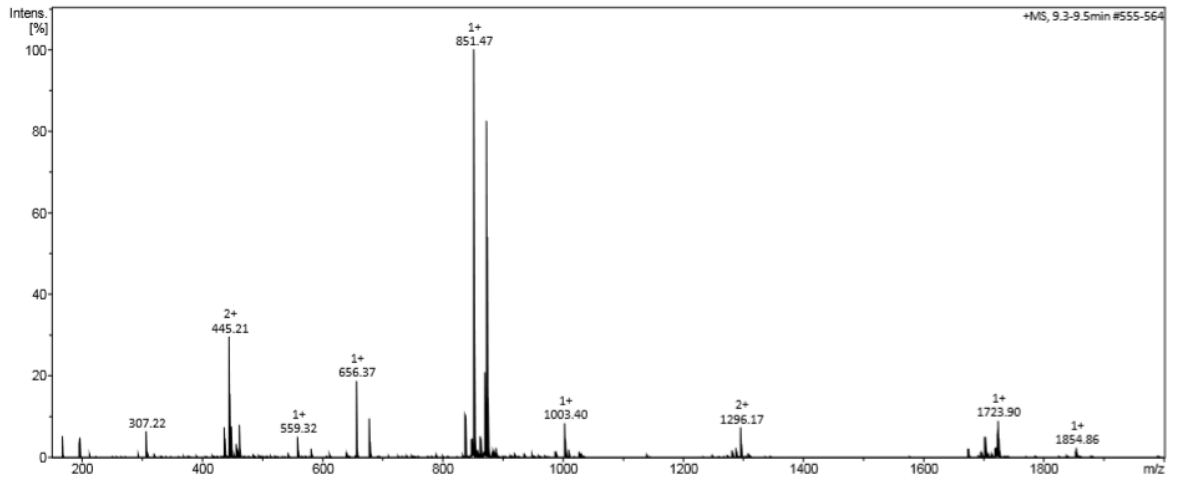
Analysis Info		Acquisition Date	
Analysis Name	D:\Data\BSF\2019_08\190813_AP04_5_01_8661.d	13/08/2019 17:44:25	
Method	peptide_lc_aniello.m	Operator	Bruker
Sample Name	190813_AP04	Instrument	microTOF-Q
Comment	dfb-13	228888.10141	
Acquisition Parameter			
Source Type	ESI	Ion Polarity	Positive
Focus	Not active	Set Capillary	4500 V
Scan Begin	150 m/z	Set End Plate Offset	-500 V
Scan End	3000 m/z	Set Collision Cell RF	800.0 Vpp
		Set Nebulizer	1.0 Bar
		Set Dry Heater	180 °C
		Set Dry Gas	6.0 l/min
		Set Divert Valve	Waste



Bruker Compass DataAnalysis 4.1 printed: 14/08/2019 17:34:55 by: Bruker Page 1 of 1

## Display Report

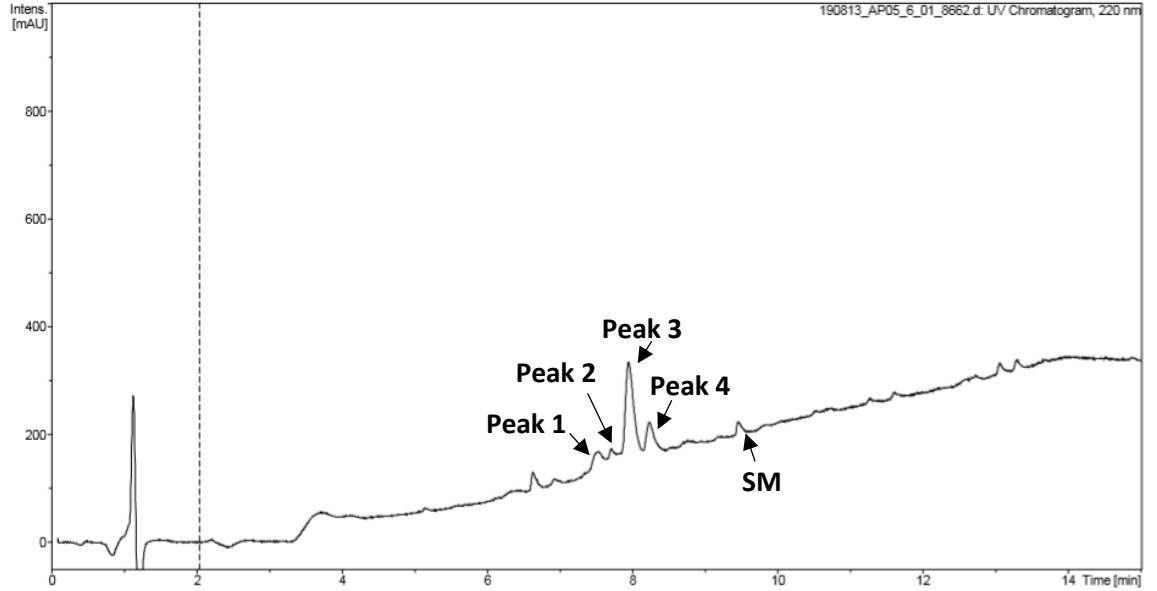
Analysis Info		Acquisition Date	
Analysis Name	D:\Data\BSF\2019_08\190813_AP04_5_01_8661.d	13/08/2019 17:44:25	
Method	peptide_lc_aniello.m	Operator	Bruker
Sample Name	190813_AP04	Instrument	microTOF-Q
Comment	dfb-13	228888.10141	
Acquisition Parameter			
Source Type	ESI	Ion Polarity	Positive
Focus	Not active	Set Capillary	4500 V
Scan Begin	150 m/z	Set End Plate Offset	-500 V
Scan End	3000 m/z	Set Collision Cell RF	800.0 Vpp
		Set Nebulizer	1.0 Bar
		Set Dry Heater	180 °C
		Set Dry Gas	6.0 l/min
		Set Divert Valve	Waste



ESI-MS data: peptide **17-tt** (trans-trans) RCM in **THF** with **HG** – Four clear RCM product peaks visible, peaks 1 and 2 isolated together.

Generic Display Report

<b>Analysis Info</b>		Acquisition Date	13/08/2019 18:15:43
Analysis Name	D:\Data\BSF\2019_08\190813_AP05_6_01_8662.d	Operator	Bruker
Method	peptide_lc_aniello.m	Instrument	micrOTOF-Q
Sample Name	190813_AP05		
Comment	dfb-17		

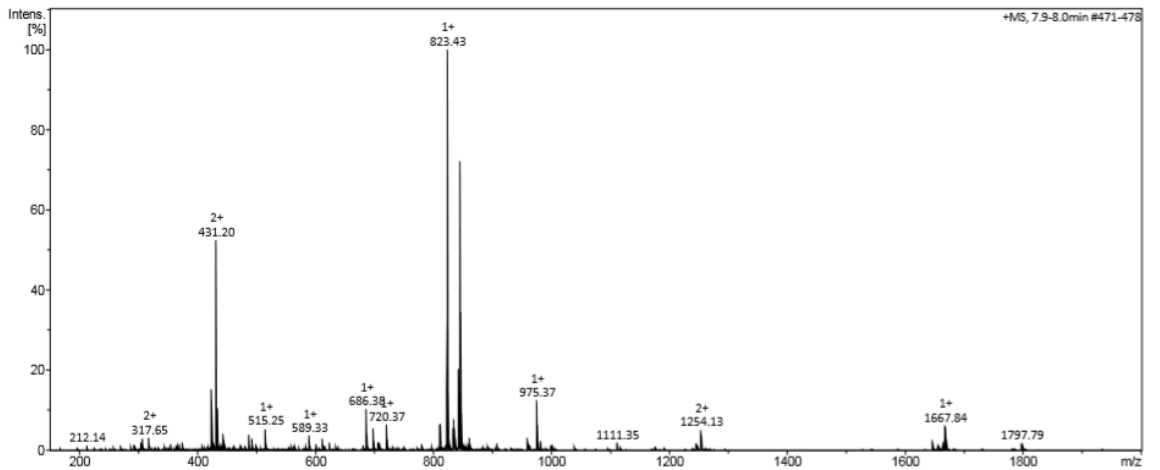


Bruker Compass DataAnalysis 4.1 printed: 14/08/2019 17:38:22 by: Bruker Page 1 of 1

Display Report

<b>Analysis Info</b>		Acquisition Date	13/08/2019 18:15:43
Analysis Name	D:\Data\BSF\2019_08\190813_AP05_6_01_8662.d	Operator	Bruker
Method	peptide_lc_aniello.m	Instrument	micrOTOF-Q
Sample Name	190813_AP05		228888.10141
Comment	dfb-17		

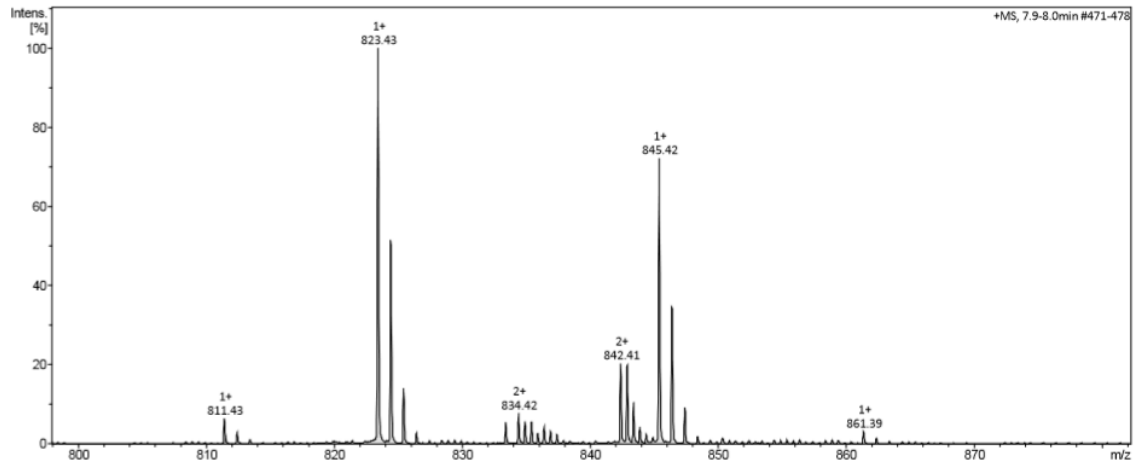
<b>Acquisition Parameter</b>			
Source Type	ESI	Ion Polarity	Positive
Focus	Not active	Set Capillary	4500 V
Scan Begin	150 m/z	Set End Plate Offset	-500 V
Scan End	3000 m/z	Set Collision Cell RF	800.0 Vpp
		Set Nebulizer	1.0 Bar
		Set Dry Heater	180 °C
		Set Dry Gas	6.0 l/min
		Set Divert Valve	Waste



Bruker Compass DataAnalysis 4.1 printed: 14/08/2019 17:39:38 by: Bruker Page 1 of 1

## Display Report

Analysis Info		Acquisition Date		13/08/2019 18:15:43	
Analysis Name	D:\Data\BSF\2019_08\190813_AP05_6_01_8662.d	Operator	Bruker		
Method	peptide_lc_aniello.m	Instrument	micrOTOF-Q	228888.10141	
Sample Name	190813_AP05				
Comment	dfb-17				
Acquisition Parameter					
Source Type	ESI	Ion Polarity	Positive	Set Nebulizer	1.0 Bar
Focus	Not active	Set Capillary	4500 V	Set Dry Heater	180 °C
Scan Begin	150 m/z	Set End Plate Offset	-500 V	Set Dry Gas	6.0 l/min
Scan End	3000 m/z	Set Collision Cell RF	800.0 V/pp	Set Divert Valve	Waste



Bruker Compass DataAnalysis 4.1

printed: 14/08/2019 17:41:11

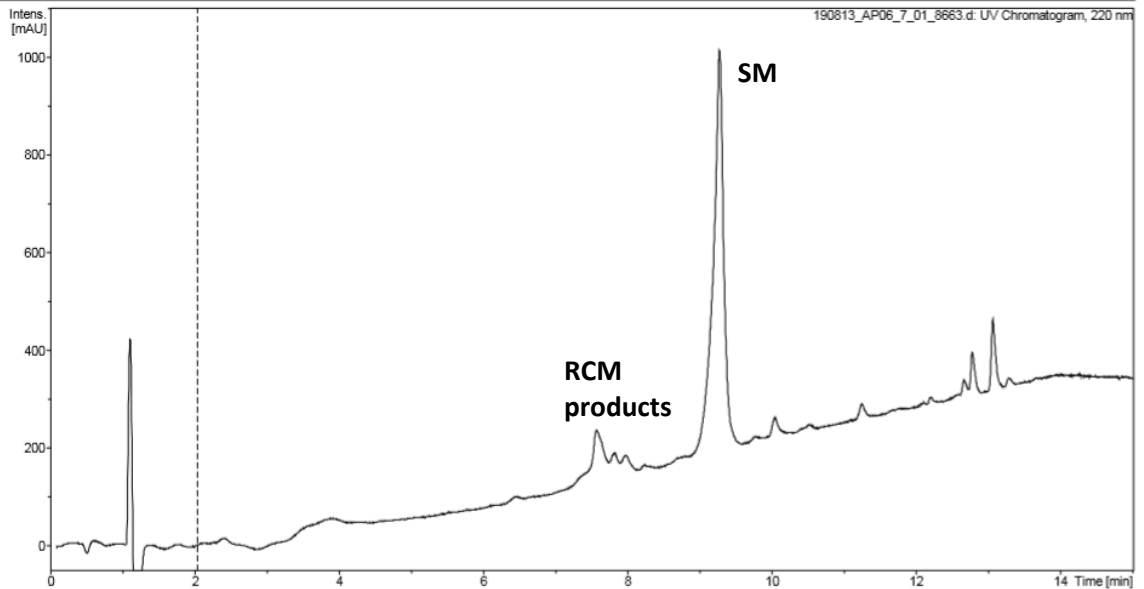
by: Bruker

Page 1 of 1

ESI-MS data: peptide **22-cc** (cis-cis), RCM in THF with HG – Minimal metathesis, product peaks not isolated.

## Generic Display Report

Analysis Info		Acquisition Date		13/08/2019 18:46:59	
Analysis Name	D:\Data\BSF\2019_08\190813_AP06_7_01_8663.d	Operator	Bruker		
Method	peptide_lc_aniello.m	Instrument	micrOTOF-Q		
Sample Name	190813_AP06				
Comment	dfb-22				



Bruker Compass DataAnalysis 4.1

printed: 14/08/2019 17:43:39

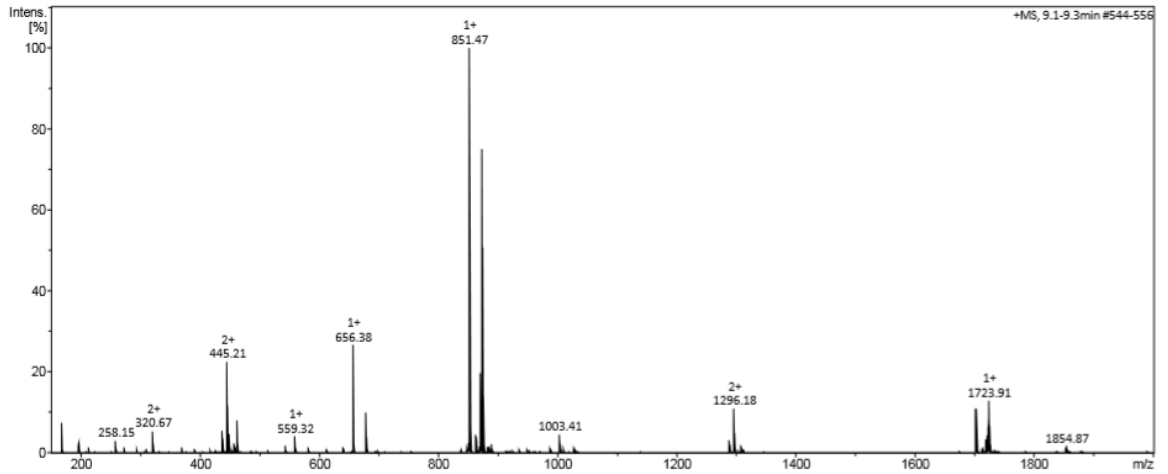
by: Bruker

Page 1 of 1

Display Report

<b>Analysis Info</b>		Acquisition Date		13/08/2019 18:46:59	
Analysis Name	D:\Data\BSF\2019_08\190813_AP06_7_01_8663.d	Operator	Bruker		
Method	peptide_lc_aniello.m	Instrument	micrOTOF-Q	228888.10141	
Sample Name	190813_AP06	Comment			
Comment	dfb-22				

<b>Acquisition Parameter</b>					
Source Type	ESI	Ion Polarity	Positive	Set Nebulizer	1.0 Bar
Focus	Not active	Set Capillary	4500 V	Set Dry Heater	180 °C
Scan Begin	150 m/z	Set End Plate Offset	-500 V	Set Dry Gas	6.0 l/min
Scan End	3000 m/z	Set Collision Cell RF	800.0 Vpp	Set Divert Valve	Waste

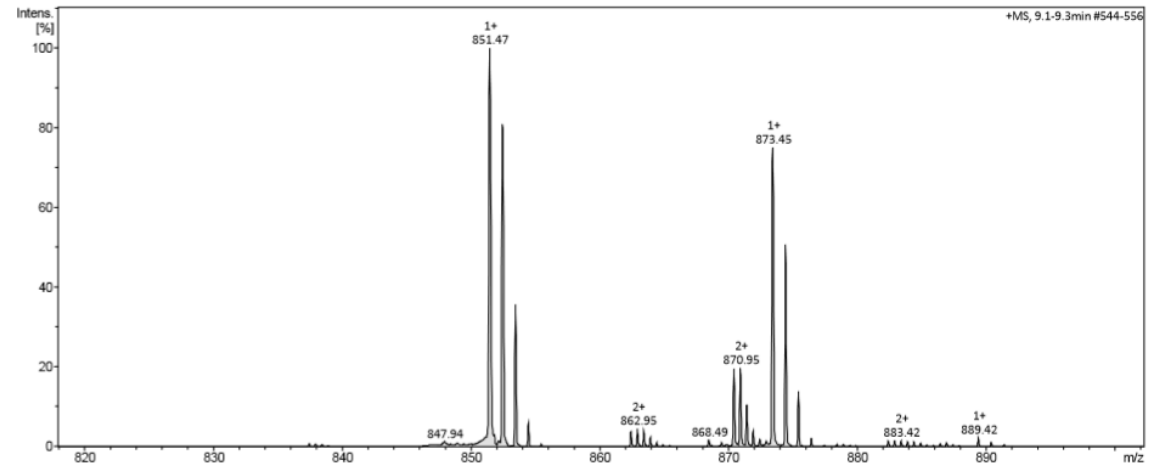


Bruker Compass DataAnalysis 4.1 printed: 14/08/2019 17:44:43 by: Bruker Page 1 of 1

Display Report

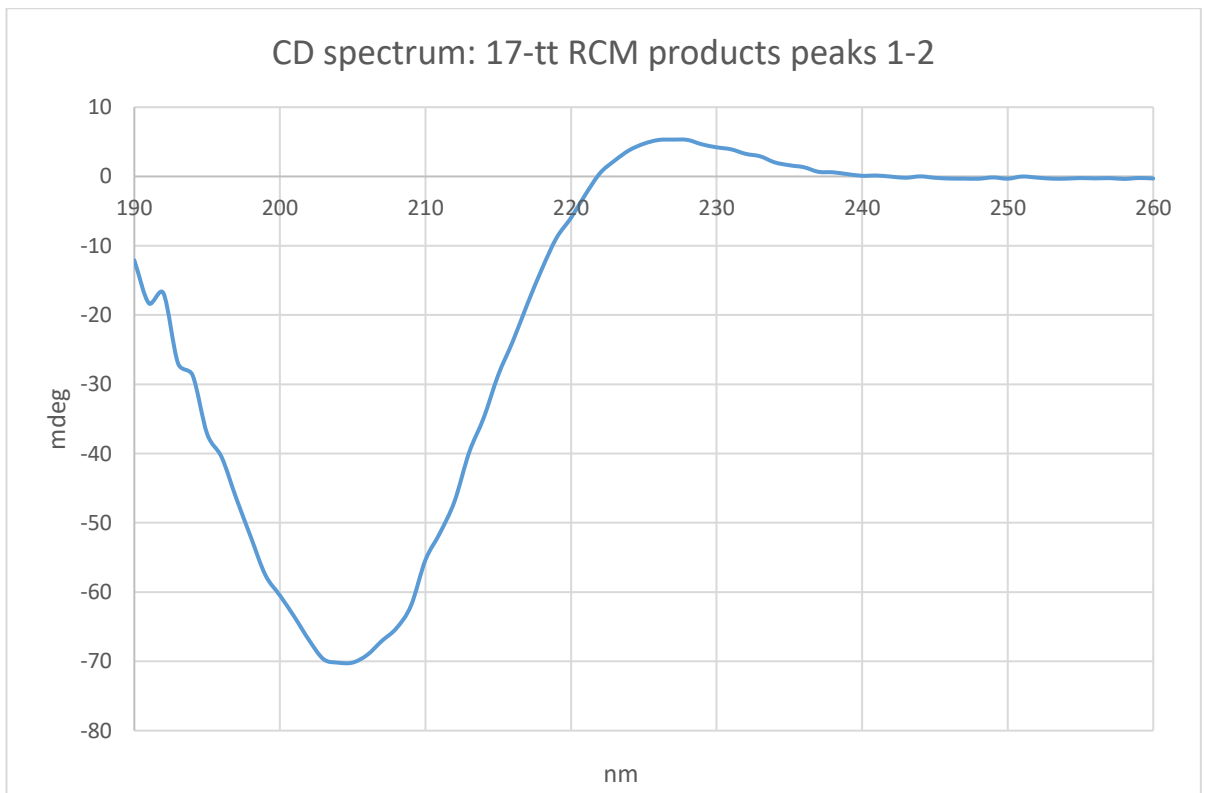
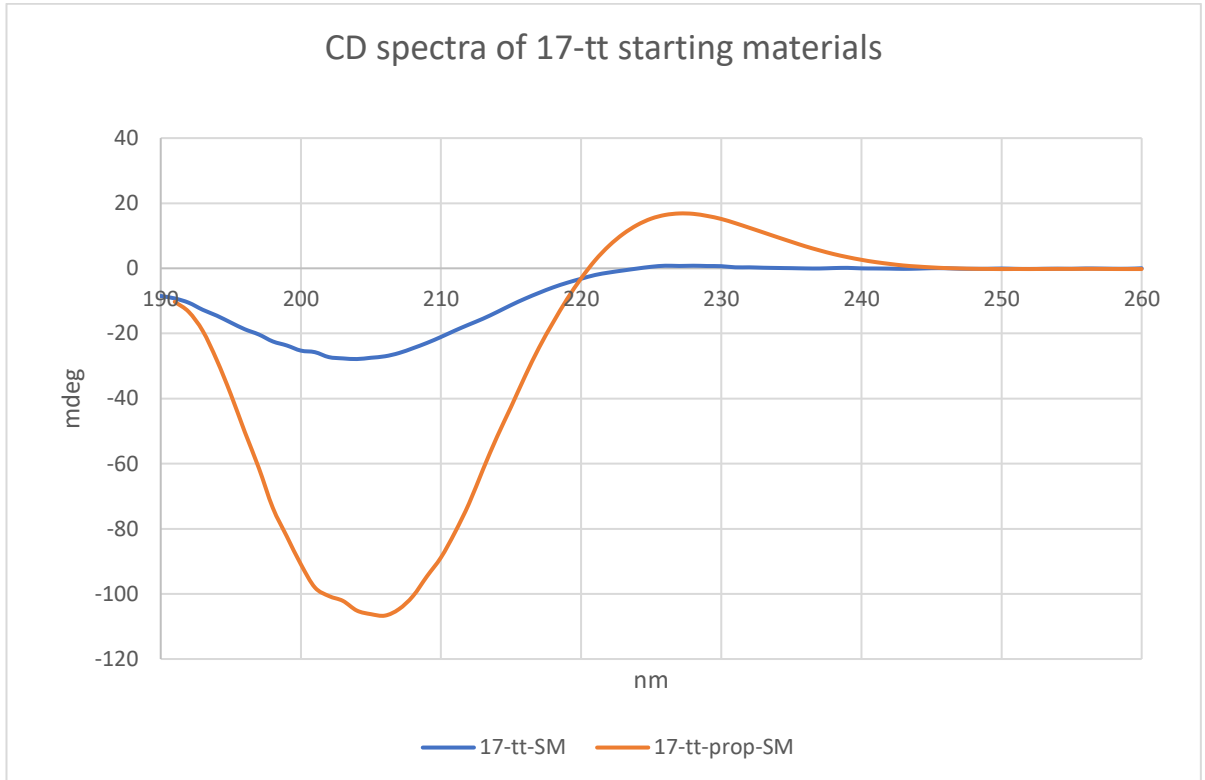
<b>Analysis Info</b>		Acquisition Date		13/08/2019 18:46:59	
Analysis Name	D:\Data\BSF\2019_08\190813_AP06_7_01_8663.d	Operator	Bruker		
Method	peptide_lc_aniello.m	Instrument	micrOTOF-Q	228888.10141	
Sample Name	190813_AP06	Comment			
Comment	dfb-22				

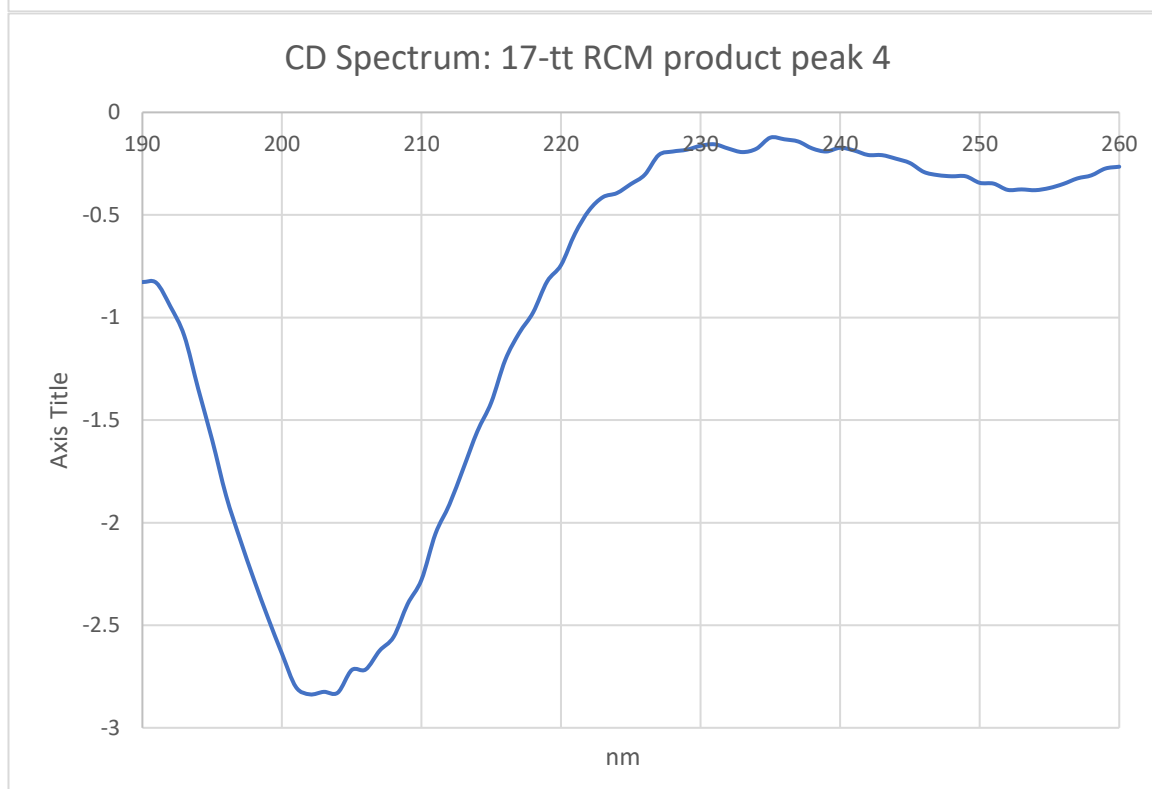
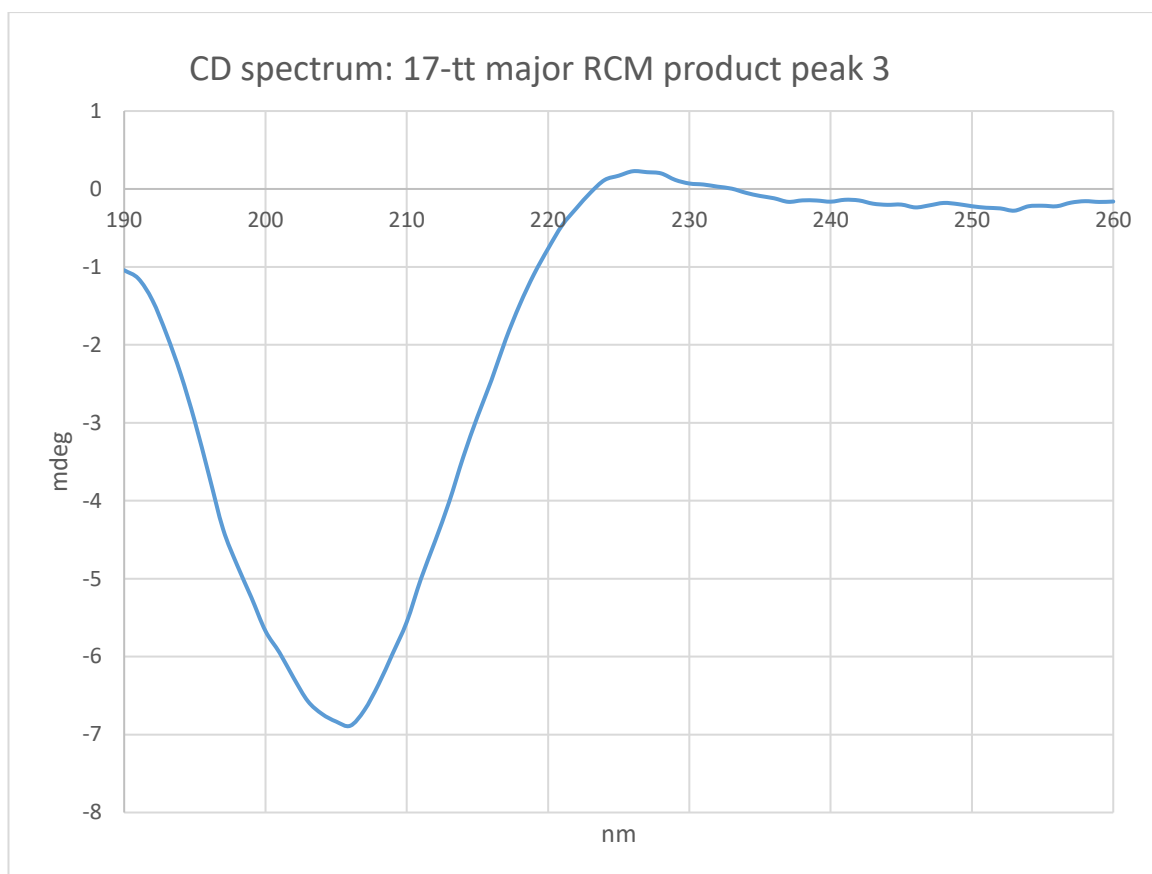
<b>Acquisition Parameter</b>					
Source Type	ESI	Ion Polarity	Positive	Set Nebulizer	1.0 Bar
Focus	Not active	Set Capillary	4500 V	Set Dry Heater	180 °C
Scan Begin	150 m/z	Set End Plate Offset	-500 V	Set Dry Gas	6.0 l/min
Scan End	3000 m/z	Set Collision Cell RF	800.0 Vpp	Set Divert Valve	Waste

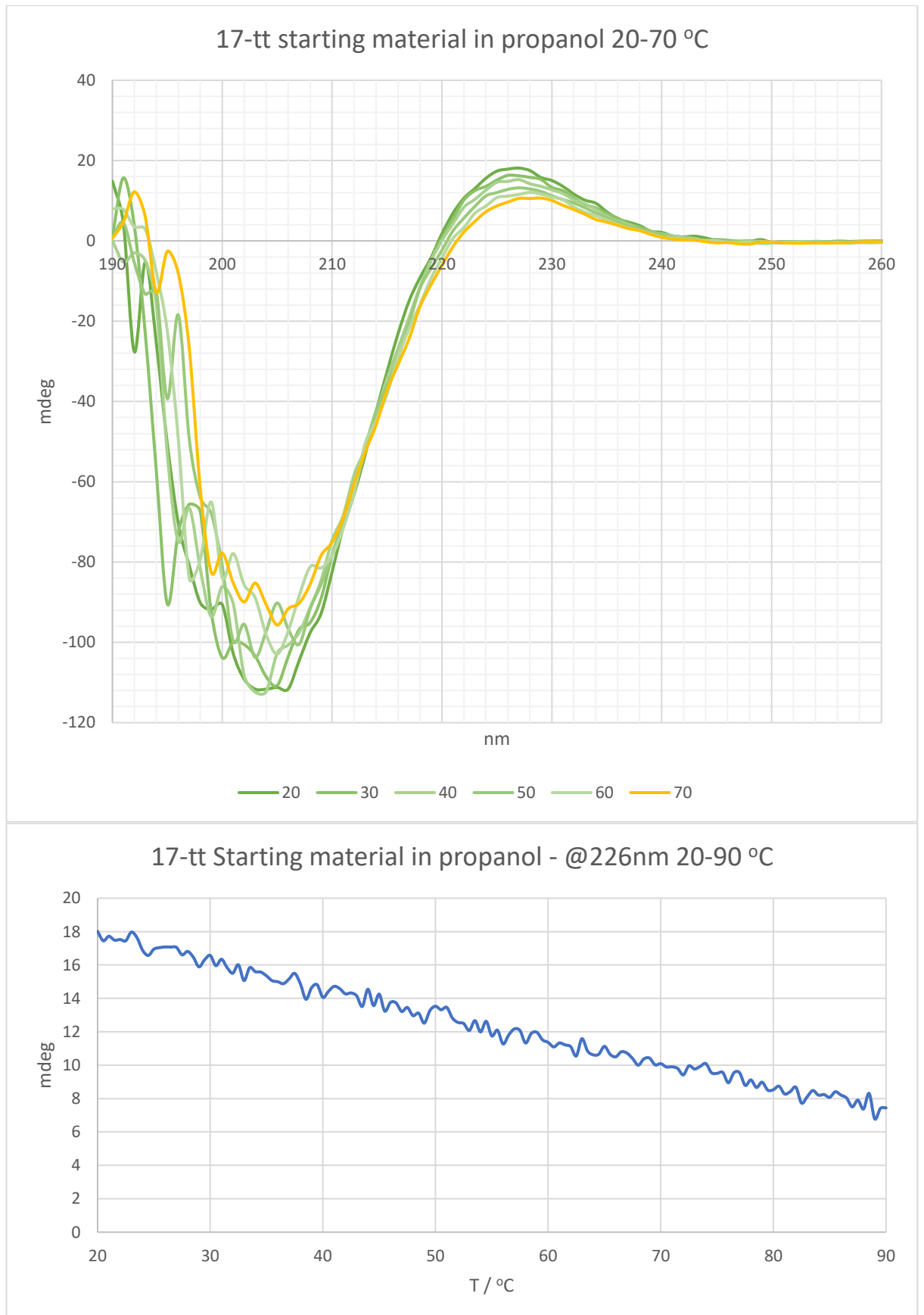


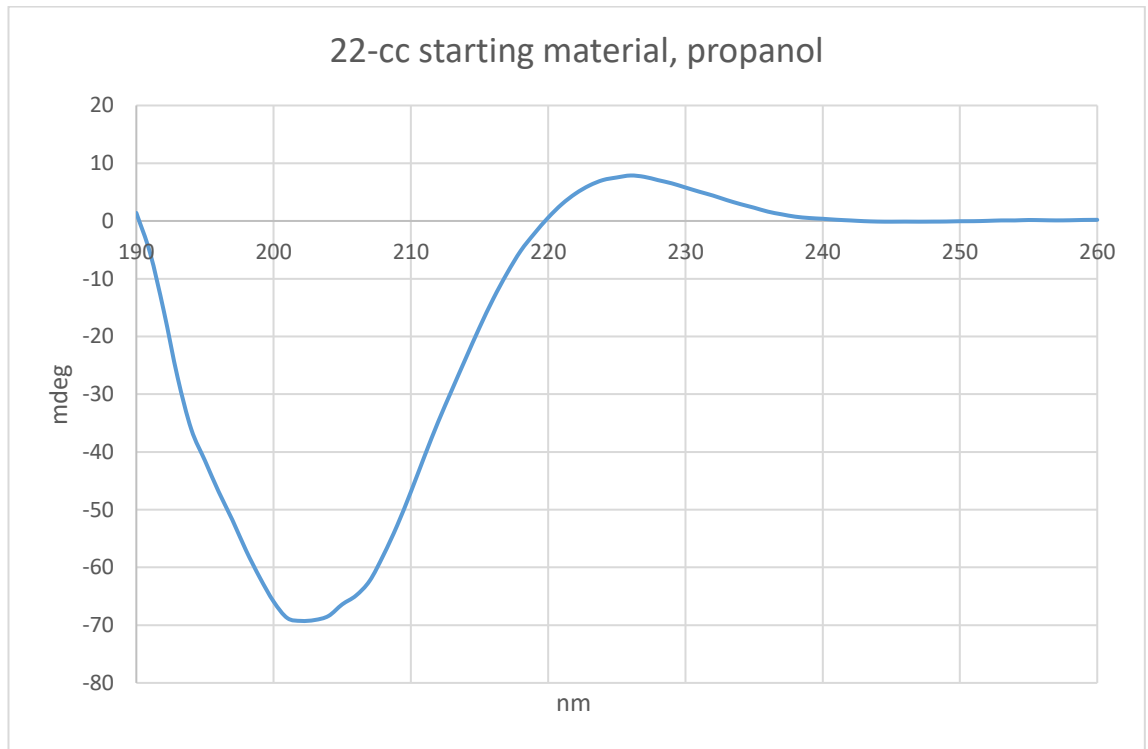
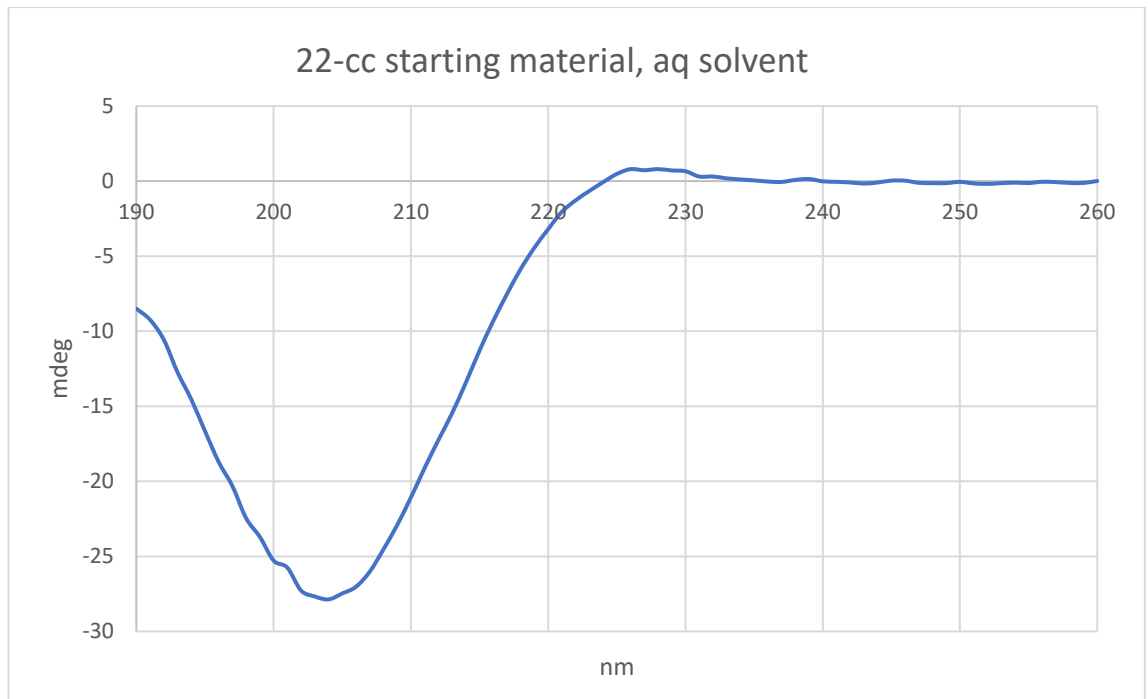
Bruker Compass DataAnalysis 4.1 printed: 14/08/2019 17:46:04 by: Bruker Page 1 of 1

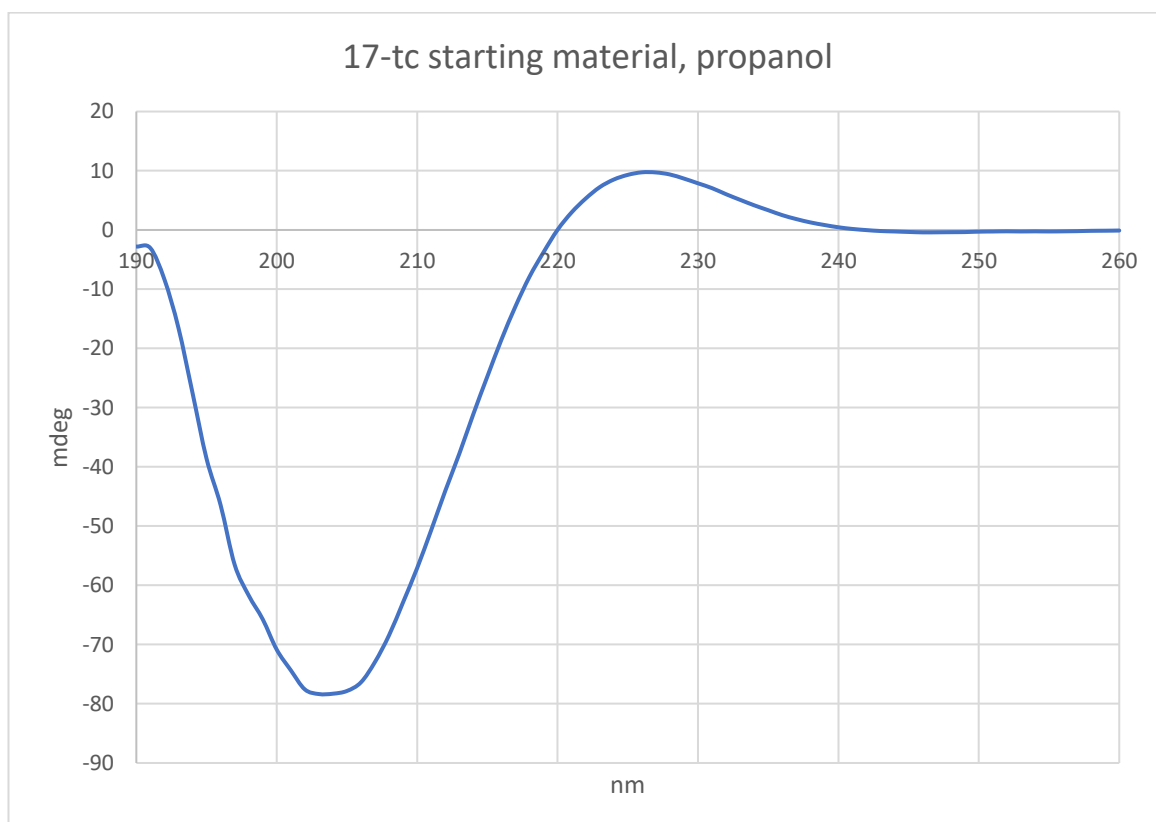
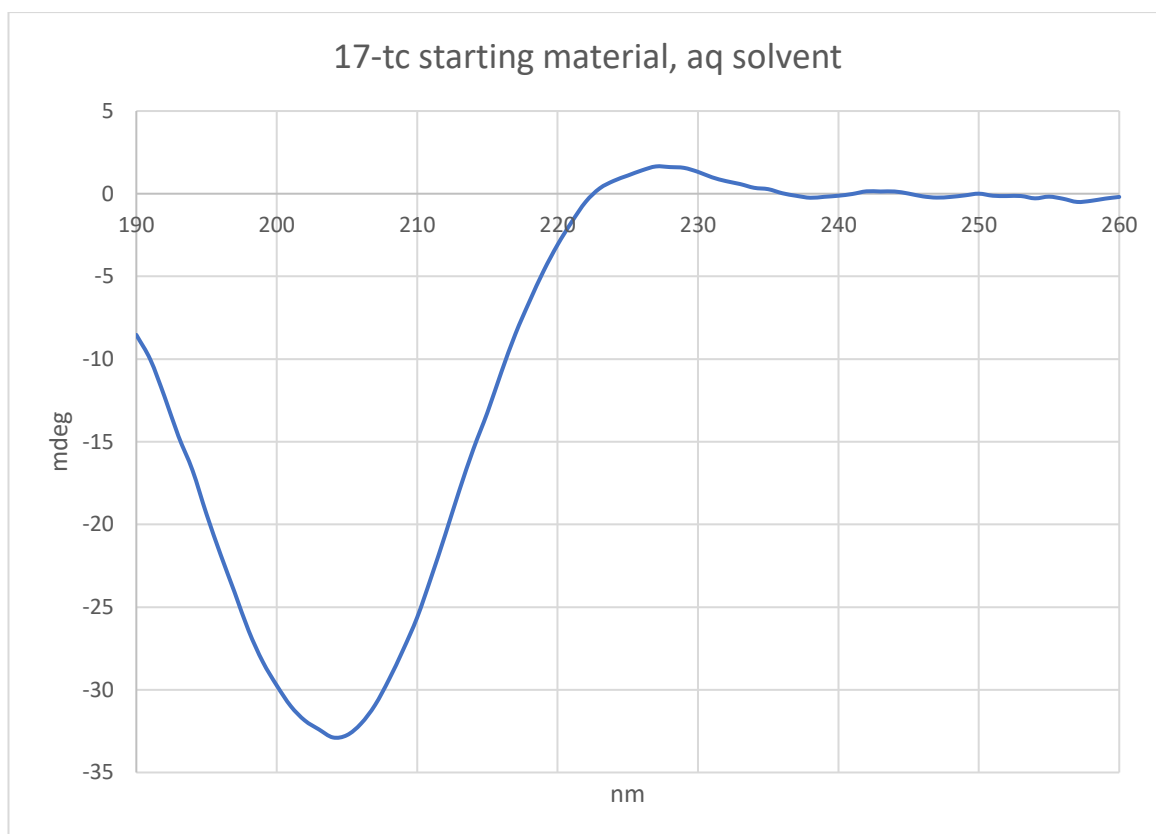
## Appendix – C – CD Spectra

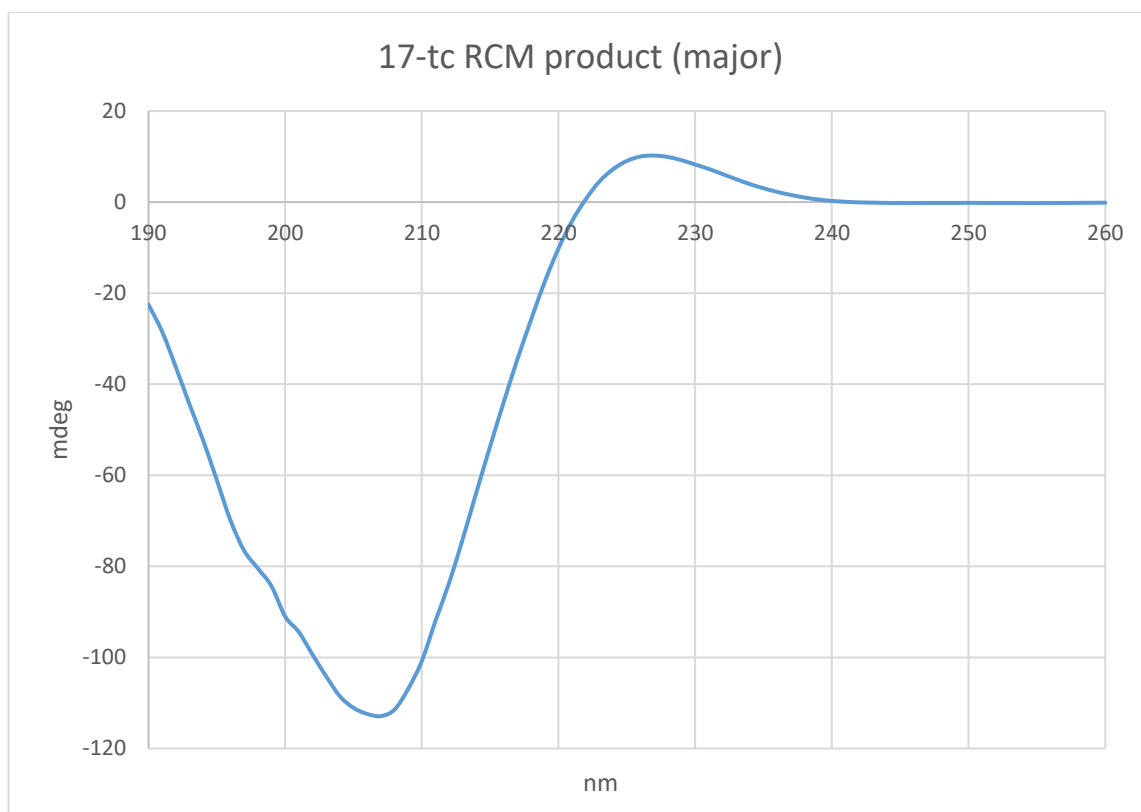


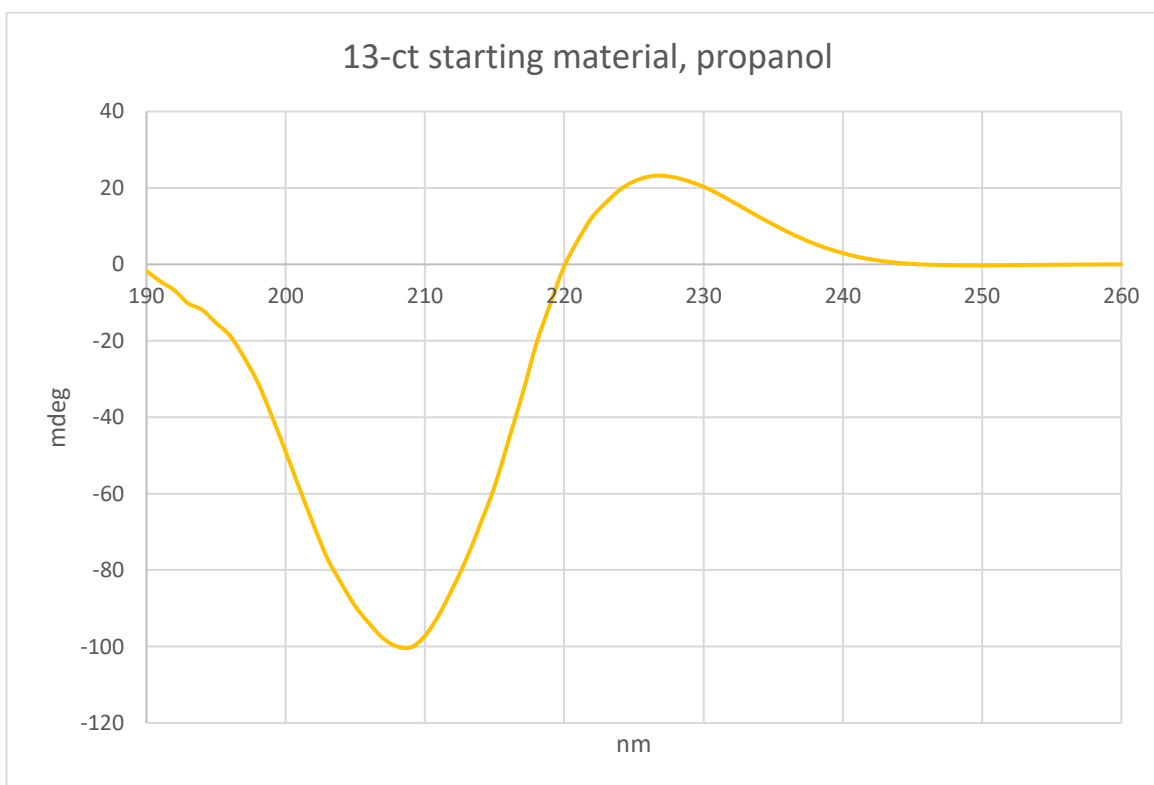
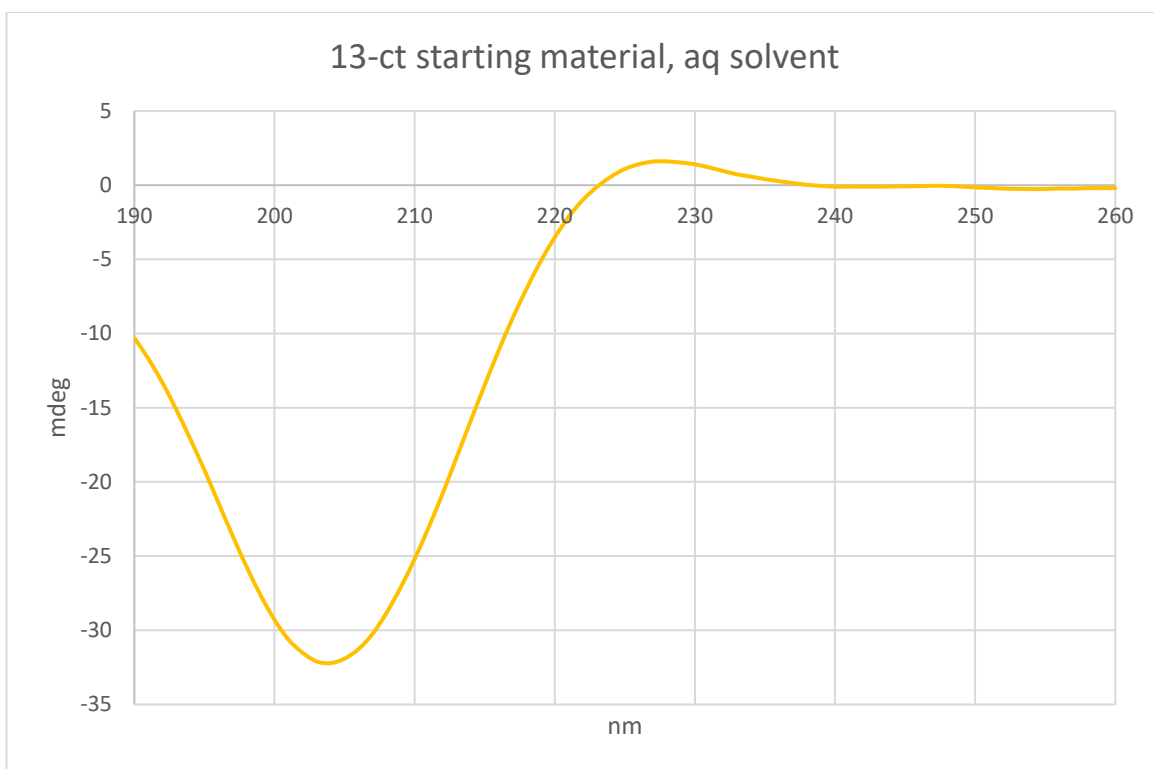


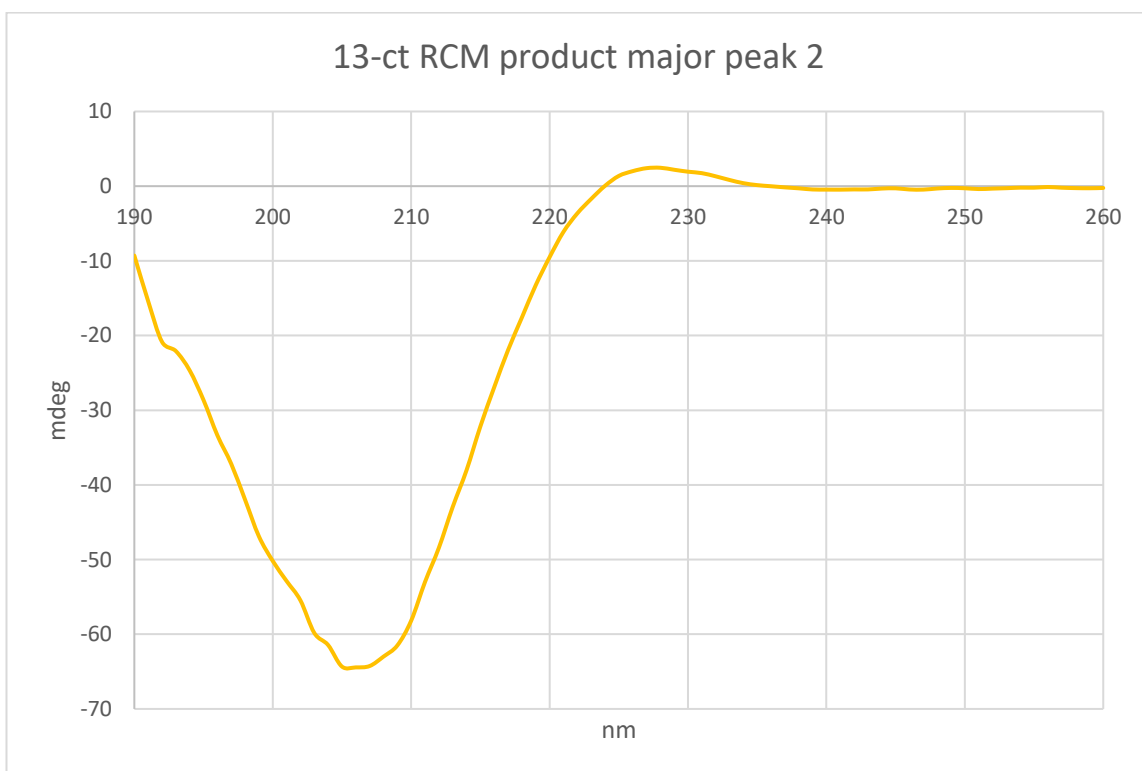
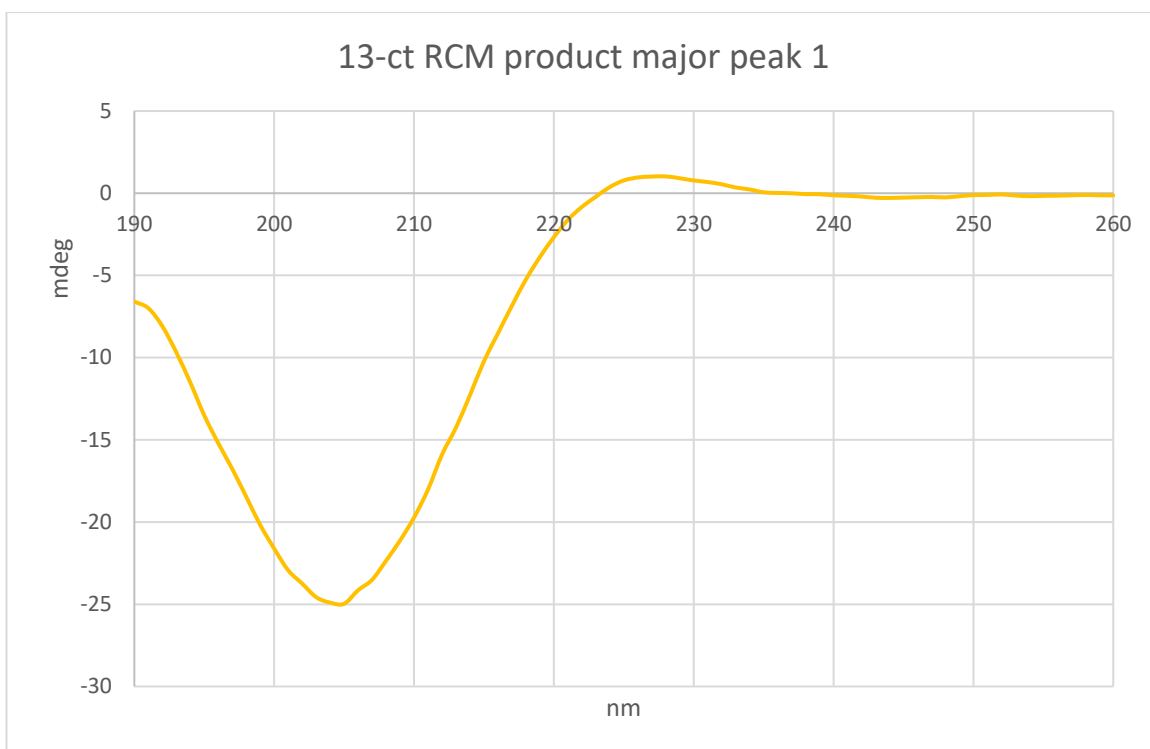












## Appendix – D – FT-IR Spectra

